

REVIEW ARTICLE

Approaches and challenges to the study of loess— Introduction to the LoessFest Special Issue

Randall J. Schaetzl^a, E. Arthur Bettis III^{b,*}, Onn Crouvi^c, Kathryn E. Fitzsimmons^d, David A. Grimley^e, Ulrich Hambach^f, Frank Lehmkühl^g, Slobodan B. Marković^{h,i}, Joseph A. Mason^j, Piotr Owczarek^k, Helen M. Roberts^l, Denis-Didier Rousseau^{m,n}, Thomas Stevens^o, Jef Vandenberghe^p, Marcelo Zárate^q, Daniel Veres^{r,s}, Shiling Yang^t, Michael Zech^{u,v}, Jessica L. Conroy^w, Aditi K. Dave^d, Dominik Faust^u, Qingzhen Hao^x, Igor Obreht^{g,y}, Charlotte Prud'homme^d, Ian Smalley^z, Alfonsina Tripaldi^{aa}, Christian Zeeden^{g,bb}, Roland Zech^{cc}

^aDepartment of Geography, Environment, and Spatial Sciences, 673 Auditorium Rd., Michigan State University, East Lansing, Michigan 48824-1117, USA

^bDepartment of Earth and Environmental Sciences, IIHR—Hydroscience and Engineering, University of Iowa, Iowa City, Iowa 52242, USA

^cGeological Survey of Israel, Jerusalem 9550161, Israel

^dResearch Group for Terrestrial Palaeoclimates, Max Planck Institute for Chemistry, Hahn-Meitner-Weg 1, 55128 Mainz, Germany

^eIllinois State Geological Survey, University of Illinois at Urbana-Champaign, Champaign, Illinois 61820, USA

^fBayCEER and Chair of Geomorphology, University of Bayreuth, 95447 Bayreuth, Germany

^gDepartment of Geography, RWTH Aachen University, Templergraben 55, 52066 Aachen, Germany

^hFaculty of Sciences, University of Novi Sad, Trg Dositeja Obradovića 3, 21000 Novi Sad, Serbia

ⁱSerbian Academy of Sciences and Arts Knez Mihajlova 35, 11000 Belgrade, Serbia

^jDepartment of Geography, University of Wisconsin-Madison, 550 N. Park St., Madison, Wisconsin 53706, USA

^kInstitute of Geography and Regional Development, Faculty of Earth Sciences and Environmental Management, University of Wrocław, Pl. Uniwersytecki 1, 50-137 Wrocław, Poland

^lDepartment of Geography and Earth Sciences, Aberystwyth University, Aberystwyth SY23 3DB, United Kingdom

^mEcole Normale Supérieure, UMR CNRS 8539, Laboratoire de Météorologie Dynamique, and CERES-ERTI, 24 rue Lhomond, 75231 Paris CEDEX 5, France

ⁿLamont-Doherty Earth Observatory of Columbia University, Palisades, New York 10964, USA

^oPhysical Geography, Program for Air, Water and Landscape Sciences, Department of Earth Sciences, Uppsala University, Villav. 16, SE-751 05 Uppsala, Sweden

^pDepartment of Earth Sciences, Vrije Universiteit Amsterdam, De Boelelaan 1085, 1081 HV Amsterdam, The Netherlands

^qInstituto de Ciencias de la Tierra y Ambientales de la Pampa (CONICET-UNLPam), Avenida Uruguay 151, 6300 La Pampa Argentina

^rInstitute of Speleology, Romanian Academy, 050711 Bucharest, Romania

^sInterdisciplinary Research Institute on Bio-Nano-Science of Babes-Bolyai University, Cluj-Napoca 400084, Romania

^tInstitute of Geology and Geophysics, Chinese Academy of Sciences, 19 BeiTuChengXi Road, Beijing 100029, China

^uInstitute of Geography, Technical University of Dresden, Helmholtzstrasse 10, D-01062 Dresden, Germany

^vDepartment of Terrestrial Biogeochemistry, Martin-Luther University Halle-Wittenberg, Weidenplan 14, D-06120 Halle, Germany

^wDepartments of Geology and Plant Biology, University of Illinois at Urbana-Champaign, Champaign, Illinois 61820, USA

^xKey Laboratory of Cenozoic Geology and Environment, Institute of Geology and Geophysics, Chinese Academy of Sciences, and College of Earth Science, University of Chinese Academy of Sciences, 100029, Beijing, China

^yOrganic Geochemistry Group, MARUM-Center for Marine Environmental Sciences and Department of Geosciences, University of Bremen, 28359 Bremen, Germany

^zSchool of Geology, Geography and the Environment, University of Leicester, Leicester LE1 7RH, United Kingdom

^{aa}IGEB-CONICET-Universidad de Buenos Aires Pabellón 2, Primer piso, Oficina 3, Ciudad Universitaria C1428EHA, Buenos Aires, Argentina

^{bb}IMCCE, Observatoire de Paris, PSL Research Université, CNRS, Sorbonne Universités, UPMC Université Paris 06, Université Lille, 75014 Paris, France

^{cc}Institute of Geography, Friedrich-Schiller University Jena, Löbdegraben 32, D-07743 Jena, Germany

(RECEIVED December 21, 2017; ACCEPTED February 19, 2018)

Abstract

In September 2016, the annual meeting of the International Union for Quaternary Research's Loess and Pedostratigraphy Focus Group, traditionally referred to as a LoessFest, met in Eau Claire, Wisconsin, USA. The 2016 LoessFest focused on "thin" loess deposits and loess transportation surfaces. This LoessFest included 75 registered participants from 10 countries. Almost half of the participants were from outside the United States, and 18 of the participants were students. This review is the introduction to the special issue for *Quaternary Research* that originated from presentations and discussions at the 2016 LoessFest. This introduction highlights current understanding and ongoing work on loess in various regions of the world and provides brief summaries of some of the current approaches/strategies used to study loess deposits.

Keywords: Loess

* Corresponding author at: Department of Earth and Environmental Sciences, IIHR—Hydroscience and Engineering, University of Iowa, Iowa City, Iowa 52242, USA. E-mail address: art-bettis@uiowa.edu (E.A. Bettis III).

INTRODUCTION

In September 2016, the annual meeting of the International Union for Quaternary Research's (INQUA) Loess and Pedostratigraphy Focus Group met in western Wisconsin, USA. This focus group is part of INQUA's Commission on Stratigraphy and Chronology (<https://www.inqua.org/commissions/sacom>). Meetings of this group have traditionally been referred to as LoessFests. The 2016 LoessFest focused on "thin" loess deposits and loess transportation surfaces. Held in Eau Claire, Wisconsin, from September 22 to 25, this LoessFest included 75 registered participants from 10 countries. Almost half of the participants were from outside the United States, and 18 of the participants were students. In all, 29 oral papers and 14 posters were presented during the first two days. Kathleen Goff (University of Iowa) won the award for the best student poster, and Rastko Marković (University of Novi Sad, Serbia) won the award for the best student oral paper. The last two days of the conference involved field trips to sites in western Wisconsin. The trips included 13 stops, most of which were exposures or backhoe pits in loess or related sediments (Fig. 1).

After the meeting, the conference organizers were approached by *Quaternary Research* and *Aeolian Research* about developing special issues for these journals, dedicated to topics focusing on loess. This review represents the introduction to the special issue for *Quaternary Research*. The goals of this introduction are to (1) provide brief summaries of some of the current approaches/strategies used to study loess deposits and, in so doing, (2) highlight some of the ongoing work on loess in various regions of the world. Numerous examples from, and reviews of, some of the world's major loess deposits are discussed first to provide context. We hope that these summaries, written by a selection of the world's most prominent loess researchers, will not only highlight the fascinating world of loess research, but also draw attention to loess-related questions, approaches, and methods that may form the basis of future research.



Figure 1. (color online) Participants taking turns examining thin loess in a soil pit at one of the several field trip stops at the 2016 LoessFest in western Wisconsin, USA. Photo by R. Schaetzl.

(MOST OF) THE WORLD'S MAJOR LOESS DEPOSITS

Loess in China

By Shiling Yang

Loess deposits in China are widely distributed across the Chinese Loess Plateau (Fig. 2), where they attain thicknesses ranging from several tens of meters to >300 m, across an area of ~273,000 km² (Liu, 1985). The thickest and most complete loess sequences occur mainly in the central and southern parts of the plateau, where they range from 130 to 200 m thick and consist of as many as 34 loess-paleosol couplets (Fig. 3; Yang and Ding, 2010). As per standard nomenclature, loess horizons are labeled L_i and the intercalated paleosols S_i. Several loess and paleosol units are usually used as stratigraphic markers across the Chinese Loess Plateau, including thick and coarse-grained loess units L₉, L₁₅, L₂₄, L₂₇, and L₃₂, and strongly developed paleosols S₅ and S₂₆ (Ding et al., 1993, 2002a). The alternation of loess and paleosols reflects large-scale oscillations between glacial conditions, when loess accumulates, and interglacial conditions, when loess deposition wanes and soils form.

The modern climate of the Chinese Loess Plateau is characterized by the seasonal alternation of summer and winter monsoons. During winter, the northwesterly monsoonal winds driven by the Siberian High dominate the Chinese Loess Plateau and lead to cold and dry weather, whereas in summer, the southeasterly monsoonal winds bring heat and moisture from the low-latitude oceans, leading to warm and humid weather. Meteorologic data indicate that ~60–80% of annual precipitation is concentrated in the summer season (Yang et al., 2012, 2015).

Loess material in northern China is likely to have first formed through glacial abrasion and erosion by other geomorphic processes in mountainous areas (Sun, 2002b; Smalley et al., 2014), then was transported by fluvial and eolian processes into deserts, which act as silt and clay storage regions, rather than places where particles are formed. The eolian dust that constitutes the loess is mainly transported from these deserts by the winter monsoon, whereas the postdepositional alteration of dust deposits is closely related to the precipitation provided by the summer monsoon (Liu, 1985; Liu and Ding, 1998). Therefore, Chinese loess deposits provide a unique opportunity to investigate the evolution of the East Asian monsoon over the past 2.8 Ma (Yang and Ding, 2010) and the complex interactions of Earth surface-climate systems (Sun, 2002a; Smalley et al., 2014).

Studies of Chinese loess have shown that various proxy records in the loess column can reveal abundant information on regional climatic and environmental changes. The most common paleoenvironmental proxies used here are magnetic susceptibility (Kukla et al., 1988; An et al., 1991a), grain size (An et al., 1991b; Ding et al., 1994), chemical weathering indexes (Gallet et al., 1996; Chen et al., 1999; Yang et al., 2006), isotopic ratios (Liu et al., 2011; Yang et al., 2012), soil

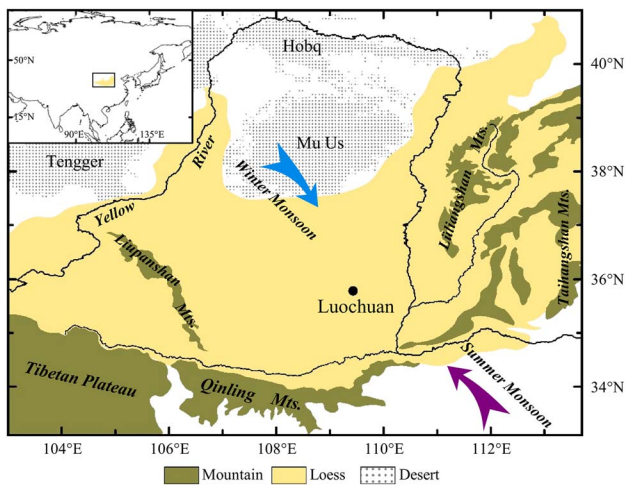


Figure 2. Map of loess deposits (yellow) on the Chinese Loess Plateau. Arrows indicate the direction of the East Asian winter and summer monsoonal winds. Inset shows the location of the Chinese Loess Plateau in Eurasia. After Yang et al. (2015). (For interpretation of the references to color in this figure legend, the reader is referred to the web version of this article.)

micromorphology (Bronger and Heinkele, 1989; Rutter and Ding, 1993), biomarkers (Peterse et al., 2014; Li et al., 2016b; Thomas et al., 2016), and pollen, snail, and opal phytolith assemblages (Lu et al., 2007; Rousseau et al., 2009; Jiang et al., 2013, 2014). In the last few decades, many studies have focused on the evolution of the East Asian monsoon and regional tectonic uplift (e.g., Liu and Ding, 1998 and references therein; Maher, 2016 and references therein), using mainly proxy data from loess deposits. The East Asian monsoon varies over tectonic to millennial time scales but is mostly driven by Northern Hemisphere glacial cyclicity (Ding et al., 2002a, 2005; Yang and Ding, 2014). On tectonic (i.e., the longest) time scales, since the mid-Pliocene there appears to have been a stepwise weakening of the East Asian summer monsoon at 2.6, 1.2, 0.7, and 0.2 Ma (Ding et al., 2005). On orbital time scales, the East Asian



Figure 3. (color online) Photograph of the eolian deposits at Luochuan (Fig. 1), in the central Chinese Loess Plateau, with loess (L)–soil (S) couplets for the L₁–L₆ portion indicated. For details on stratigraphic nomenclature of Chinese loess, see Rutter et al. (1991) and Ding et al. (1993). Photo by Shiling Yang.

summer (winter) monsoon weakened (strengthened) during glacial periods, and vice versa during interglacial periods, leading to a 200 to 300 km advance-retreat of the desert boundary (Yang and Ding, 2008) and its associated vegetation changes (Jiang et al., 2013, 2014; Yang et al., 2015) in northern China. As for the millennial-scale climate variability, high-resolution grain-size data from the Chinese loess deposits show that millennial-scale climatic events are superimposed onto a prominent long-term cooling trend, during both the last and penultimate glaciations (Yang and Ding, 2014). However, millennial-scale ecological reconstructions of the Chinese Loess Plateau remain to be investigated.

Although the foundational work on Chinese loess, such as the major stratigraphic, chronological, sedimentologic, and paleoclimatic frameworks, has already been established (Liu and Ding, 1998; Ding et al., 2002a), there remains a great deal of work to be done. First, accurate quantitative reconstructions of temperature and precipitation are needed to improve existing ones, and there is a need to develop new methods and approaches for quantitative paleoenvironmental and paleoclimatic reconstructions. These reconstructions are challenging. Second, it is crucial to investigate whether the exceptionally coarse-grained units (e.g., L₉, L₁₅, and L₃₃) in the Chinese loess deposits are the products of enhanced erosion produced by tectonic uplift of mountains in Asia (Sun and Liu, 2000; Wu and Wu, 2011) or of extreme regional climatic events (Ding et al., 2002a). Third, the provenance of Chinese loess remains a highly debated topic (Sun, 2002a; Pullen et al., 2011; Che and Li, 2013; Stevens et al., 2013b; Nie et al., 2015), mainly because of varying interpretations of geochemical proxies used for determining the main source areas. The controversy centers on whether the loess deposits come from the deserts to the west or to the north of the Loess Plateau. A possible solution in this regard would be to combine geochemical data with the data on the spatiotemporal changes in sedimentologic characteristics of Chinese loess to gain a better insight into past loess source areas (Liu, 1966; Yang and Ding, 2008). Finally, modeling studies of dust production, transport, and deposition are required to fully understand the processes responsible for the formation of the loess deposits across the Chinese Loess Plateau.

Loess in central Asia

By Kathryn E. Fitzsimmons, Charlotte Prud'homme, and Ariti K. Dave

Central Asia is characterized by comparatively patchy piedmont deposits of loess of varying thickness, in contrast to other regions of the world. The widespread riverine loess steppe of the Russian Plain has a distinctly different character and is therefore not included in our definition. We define the central Asian piedmont deposits as extending from the foothills of the north Iranian Alborz/Elbruz Mountains at their westernmost extent (Kehl et al., 2005; Vlamincq et al., 2016), eastward to the Pamir and Alai ranges (Dodonov and

Baiguzina, 1995; Dodonov, 2002), the Tien Shan (Youn et al., 2014; Fitzsimmons et al., 2016, 2017), and north along the Altai (Zykina and Zykin, 2012; Zykin and Zykina, 2015) and Mongolian Hangay (Lehmkuhl and Haselein, 2000; Lehmkuhl et al., 2011) mountain margins. The loess deposits around the Tarim basin rim may also be considered part of the central Asian piedmont loess because of their geographic similarities (Zheng et al., 2002, 2003). Figure 4 shows the general distribution of loess deposits across the core of this region (after Dodonov, 1991).

The active uplift of the central Asian high mountains (Campbell et al., 2015; Grützner et al., 2017) results in steep, rugged terrain, effectively preventing wide-scale accumulation and development of loess plateaus. This central Asian piedmont, set in the rain shadow of the Asian high mountains, generally experiences a semiarid continental climate. Climatic parameters vary more specifically with altitude, latitude, orographic effects, and the relative influences of the major Northern Hemisphere climate subsystems. The dominant climatic influences are the midlatitude westerlies, northerly polar fronts, the Siberian high pressure system, and East Asian and Indian monsoon systems (Dettman et al., 2001; Vandenberghe et al., 2006; Machalett et al., 2008).

The thickest sections of central Asian piedmont loess extend beyond the Brunhes-Matuyama paleomagnetic reversal (Dodonov and Baiguzina, 1995; Shackleton et al., 1995; Ding et al., 2002b; Wang et al., 2016). As such, they represent long sediment archives that may provide a wealth of potential paleoclimatic information (Vandenberghe et al., 2006; Yang and Ding, 2006; Machalett et al., 2008). Despite the location of these deposits in a sensitive transitional climatic zone, however, relatively little is known about the past environmental history of this region, in part because of political history and logistical challenges.

Loess formation in central Asia was generally assumed to be genetically linked to sediments generated by glaciers and rivers in the mountains, which flow into the desert basins to

the north and from which fine-grained dust is transported back onto the piedmonts (Aubekerov, 1993; Smalley, 1995; Smalley et al., 2006, 2009). Because numerical chronologies for loess and glaciation in this region were lacking until recently, scholars assumed that periods of peak loess flux corresponded to cold glacial phases, and pedogenesis corresponded with interglacial periods (Ding et al., 2002; Vandenberghe et al., 2006; Machalett et al., 2008). This assumption implied an overwhelming and continuous influence of the North Atlantic westerlies on the region and has been recently challenged. Direct dating of glacial moraines showed that some central Asian glaciers expanded during warmer, wetter phases such as Marine Oxygen Isotope Stage (MIS) 3 (Koppes et al., 2008), and that the timing of glacial expansion varied across the Asian high mountains (Owen and Dortch, 2014). Subsequent dating of piedmont loess deposits also showed variable timing and rates of accumulation (Song et al., 2015; Fitzsimmons et al., 2016, 2017; Li et al., 2016a). Proxy data relating to paleoenvironmental conditions relating to temperature, precipitation, influence of specific climate subsystems, and geomorphic stability are so far limited. Data are limited either through lack of direct chronological information (Vandenberghe et al., 2006; Yang and Ding, 2006; Yang et al., 2006; Machalett et al., 2008) or because of insufficient chronological depth of the available paleoenvironmental proxies (Dodonov et al., 2006; Feng et al., 2011; Fitzsimmons et al., 2016; Ghafarpour et al., 2016).

The current state of knowledge for the region indicates variable influence of the different climate subsystems over the region and through time. One recent hypothesis suggests that loess accumulation in the central Asian piedmont peaks under two scenarios (Fitzsimmons et al., 2016). Under the first scenario, loess flux increases because of the increased sediment availability facilitated by glacial expansion—resulting from increased mountain precipitation attributable to northward monsoon migration—combined with compression of

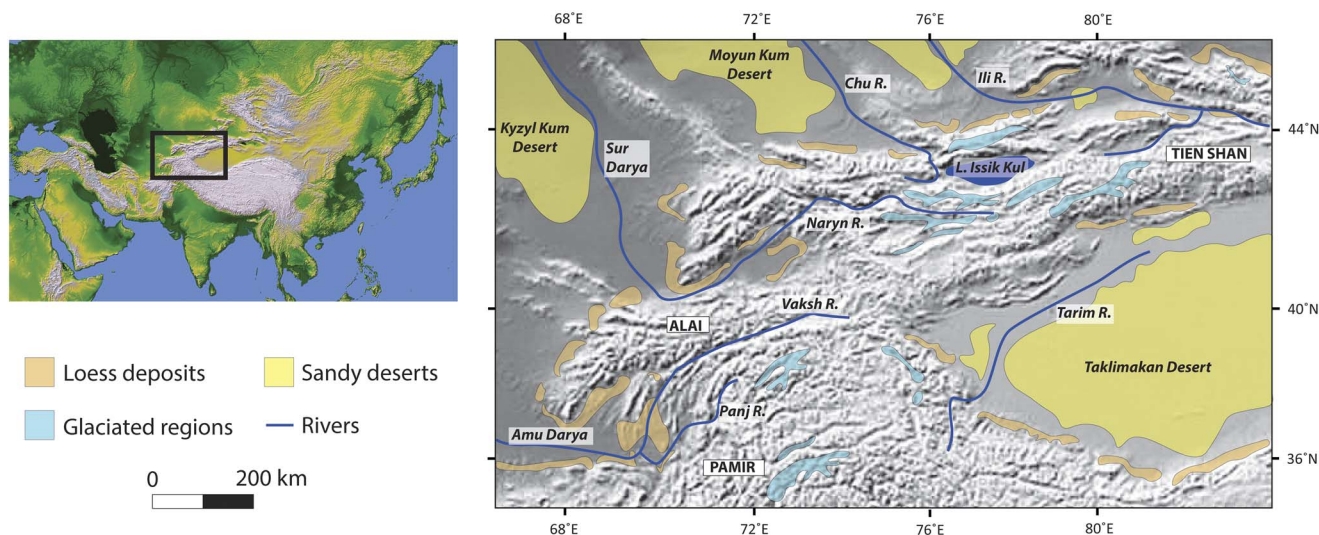


Figure 4. (color online) Loess distribution along the core central Asian piedmonts in the rain shadow of the Asian high mountains, showing geographic associations of loess deposits to glaciated regions, major rivers and deserts, as well as key regions and localities. After Dodonov (1991).

the midlatitude westerlies against the glaciated mountains and increasing wind strength (e.g., during MIS 3). Under the second scenario, loess deposition increases under cold, dry glacial conditions with reduced but sustained ice volume and persistent westerly winds (e.g., the last glacial maximum). So far, the climate mechanisms driving this hypothesis remain unidentified.

Elucidating climatic patterns from loess across central Asia through time will require targeted investigations covering the entire piedmont and applying methods that provide meaningful information addressing gaps in our understanding. Robust, long-term chronological frameworks—for example, exploiting new luminescence dating protocols (e.g., Pickering et al., 2013; Ankjærgaard et al., 2016; Liu et al., 2016; Wintle and Adamiec, 2017)—are required to place proxy paleoclimatic data in context. Meaningful proxies that quantify climatic parameters, such as temperature, precipitation, and seasonality (e.g., Peterse et al., 2014; Prud'Homme et al., 2015), are important future tools for clarifying the influence of climatic subsystems on the region through time. These should always be combined with classical measures of physical characteristics collected at high resolution (e.g., Vandenberghe et al., 2006; Zeeden et al., 2016a) and measures of loess sediment provenance facilitating wind regime reconstruction (e.g., Újvári et al., 2012; Stevens et al., 2013a, 2013b; Li et al., 2016a). These approaches herald a new direction for loess research in this poorly understood region that may be the key to global paleoclimate reconstruction.

Loess in Europe

By Frank Lehmkuhl, Dominik Faust, Ulrich Hambach, Slobodan B. Marković, Igor Obreht, Denis-Didier Rousseau, and Jef Vandenberghe

Loess is one of the most extensively distributed terrestrial Pleistocene deposits in Europe. The thickness of loess varies between a few decimeters to several tens of meters, depending on its proximity to the source area and the geomorphological setting. Because of its wide distribution, loess is often studied in thick stratigraphic sequences interbedded with paleosols (loess-paleosol sequences [LPSs]). LPSs are the most intensively and extensively studied terrestrial archives for the reconstruction of environmental and climatic changes of glaciations in Europe, since the 1950s. This work has continued onward in the context of the International Union for Quaternary Research's Loess Commission (e.g., Gullentops, 1954; Fink, 1956; Pécsi, 1966; Fink and Kukla, 1977; Kukla, 1977; Lautridou, 1981). Often these studies focused on stratigraphic subdivisions and correlations (e.g., Paepe, 1966) and were based on field data from sites that have given their name to classical lithostratigraphic horizons (e.g., Rocourt, Kesselt).

Maps of loess in Europe were first presented by Grahmann (1932) and later by Fink et al. (1977); the most recent compilations were published by Haase et al. (2007) and Bertan et al. (2016). In Europe, loess is distributed across several main regions (Fig. 5): (1) the northern European loess belt, south of

the Weichselian (Marine Oxygen Isotope Stage [MIS] 2) ice margin in the north, extending to the uplands in the south (e.g., Ardennes, Rhenish shield, Harz Mountains, Ore Mountains, Karkonosze Mountains, and northern Carpathians [Tatra]); (2) eastern Europe (east of the Carpathians), including eastern Romania, Moldova, southeastern Poland, Ukraine, western Kazakhstan, and Russia; (3) the Upper Rhine Valley and the basins of the mountainous areas in central and southwestern Germany, including Bohemia and Moravia in Česká; and (4) along the Danube River, from Bavaria toward Austria, Hungary, Slovakia, Croatia, Serbia, Romania, and northern Bulgaria. Small patches of loess also occur in southern and Mediterranean parts of Europe, mainly in Spain and along the Rhone River in southern France. Minor, although paleoclimatically important loess deposits, also occur in the Po plain of Italy and along the northern Adriatic coast (Cremaschi et al., 2015; Wacha et al., 2017).

According to various authors, the trapping of dust (loess) is mostly related to vegetation cover (e.g., Tsoar and Pye, 1987; Danin and Ganor, 1991; Hatté et al., 1998, 2013; Svirčev et al., 2013). Therefore, the northern border of the loess distribution probably coincides with the northern fringe of past vegetation systems. Almost no loess accumulated south of the northern timberline during the last glacial maximum, as the accumulation of loess was mostly related to both tundra and steppe environments. Erosion, transport, deposition, and preservation/loessification of dust follows completely different flows of processes in the periglacial areas compared with the steppe regions.

The northern European loess belt, extending from France to Germany, Poland, and northern Ukraine, was strongly influenced by periglacial environments, with its fluctuating boundaries of continuous and discontinuous permafrost (Vandenberghe et al., 2012, 2014a). As a consequence, and because of the North Atlantic influence, loess in northern Europe has a complex stratigraphy that is generally similar from Brittany through to Ukraine (Rousseau, 1987; Antoine et al., 2009, 2013; Buggle et al., 2009; Lehmkuhl et al., 2016; Rousseau et al., 2017a; Fig. 5). Loess in the northern European loess belt is situated mainly at the northern front of the central European mountains, in basins below 200 to 300 m and partly below 400 to 500 m in southern Germany (Lehmkuhl et al., 2016). Environmental conditions during periods of loess deposition were likely highly variable, with erosive processes (slopewash and deflation) playing important roles, implying that loess was not continuously deposited here or completely preserved during glacial periods. Thus, erosional unconformities are typical features of central European LPSs, which often make stratigraphic interpretations and correlations challenging (Zöller and Semmel, 2001). The distribution of eolian sediments was also influenced by sediment availability (e.g., proximity to larger river systems and the ice sheet itself) and prevailing wind directions. As a result, the temporal resolution and thickness of LPSs can vary locally as well as between different loess regions. Despite the growing focus on the impact of source areas and geomorphological position on loess deposits (Lehmkuhl et al., 2016), there is still a search for

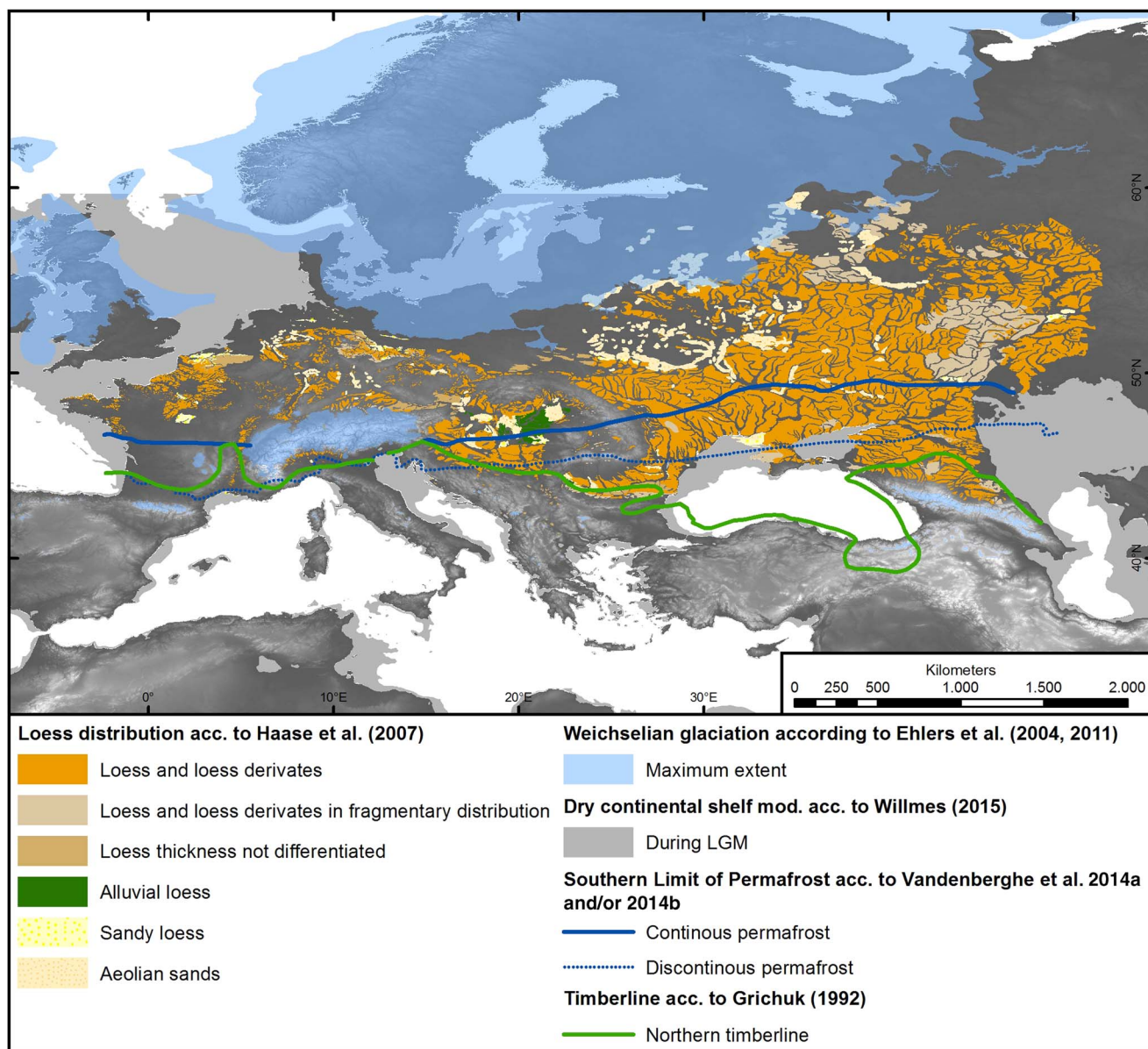


Figure 5. (color online) Loess distribution map (Haase et al., 2007) including last glacial maximum (LGM) maximum extent (Ehlers et al., 2004, 2011), dry continental shelf (Willmes, 2015), LGM permafrost distribution (Vandenberghe et al., 2014a), and northern LGM timberline (Grichuk, 1992).

(litho-) stratigraphic correlations (e.g., Haesaerts et al., 2016; Schirmer, 2016). More recently, research has been focusing on the impact of rapid climatic oscillations on European continental environments, by comparing biological, geochemical, and sedimentologic proxy data from LPSs with variations in Greenland ice core data (e.g., Rousseau et al., 2002, 2007, 2013, 2014, 2017a, 2017b; Antoine et al., 2003, 2009, 2013; Moine, 2014; Schirmer, 2016).

Loess in southeastern Europe is mostly found on large, broad loess plateaus, mainly in the Danube basin (Fitzsimmons et al., 2012), indicating the Danube River and its tributaries were important source areas (Smalley and Leach, 1978; Buggle et al., 2008; Újvári et al., 2008; Bokhorst et al., 2011). The Danube basin represents the largest European loess region west of the Russian/Ukrainian

Plain, preserving a paleoenvironmental record extending to the Early Pleistocene (Marković et al., 2011). Because of its plateau setting and the absence of periglacial influences (Fig. 5), Danube LPSs are some of the most complete, representing one of the thickest (up to >40 m), longest (since Early/Mid-Pleistocene), and most widespread terrestrial Quaternary paleoclimate archives in Europe (Fink and Kukla, 1977; Buggle et al., 2013; Marković et al., 2015). In the southern Pannonian/Carpathian basin (Hungary and Serbia) and in the lower Danube basin (Romania and Bulgaria) core data point to loess thicknesses >100 m (Pfannenstiel, 1950; Pécsi, 1985; Koloszar, 2010; Jipa, 2014). Unlike central and western Europe, loess here is characterized by a generally straightforward stratigraphy (Fig. 6), where stronger soil formation is related to warmer phases (usually associated



Figure 6. (color online) A Middle Pleistocene loess-paleosol sequence from Mircea Voda (Dobrogea, Romania). The approximately 25-m-high sequence represents the dry steppe loess facies of the lower Danube basin. Note the characteristic uppermost double paleosol (S2) that corresponds to Marine Oxygen Isotope Stage (MIS) 7, while the lowermost strongly developed paleosol (S6) represents MIS 17 (Bugge et al., 2009). Photo by Ulrich Hambach.

with odd-numbered MISs), and loess deposition occurs mainly during colder stages (Fig. 7) (Marković et al., 2015). Despite the wide distribution of the Danube loess, the southern limit of the European loess belt interior of the Balkan Peninsula is characterized by many isolated loess

deposits that originate from local sources rather than from the Danube proper. These smaller loess deposits exhibit unique geophysical and geochemical properties (Basarin et al., 2011; Obrecht et al., 2014, 2016).

Loess in eastern Europe forms a blanket that covers an area exceeding 1 million km². This loess was derived from the alluvial and lacustrine plains that formed in front of the advancing and retreating Pleistocene ice sheets (Velichko, 1990). This huge loess belt covers different bioclimatic zones, from the boreal southern taiga to the sub-Mediterranean, Black, and Azov Sea coasts, and also farther east to the Caspian Sea. Loess thickness here generally increases to the south, indicating glacial sources but also including material from local and other origins within a mixed zone in the south. Most comprehensive studies of LPSs in eastern Europe have been performed in the southern part of the East European Plain (Tsatskin et al., 1998; Rousseau et al., 2001, 2013; Haesaerts et al. 2003; Velichko et al., 2009; Liang et al., 2016).

Loess in southwestern Europe is almost entirely concentrated in the Ebro valley and central Spain (e.g., Bertran et al., 2016). This loess does not reach the thicknesses of loess in central and eastern Europe and is mostly preserved as relocated loess derivatives. Boixadera et al. (2015) reported about loess deposits that are generally 3–4 m thick and consist of well-sorted fine sands and silts (i.e., coarser than typical loess). Loess in central Spain is distributed along the Tajo River, covering fluvial terraces and depressions nearby.

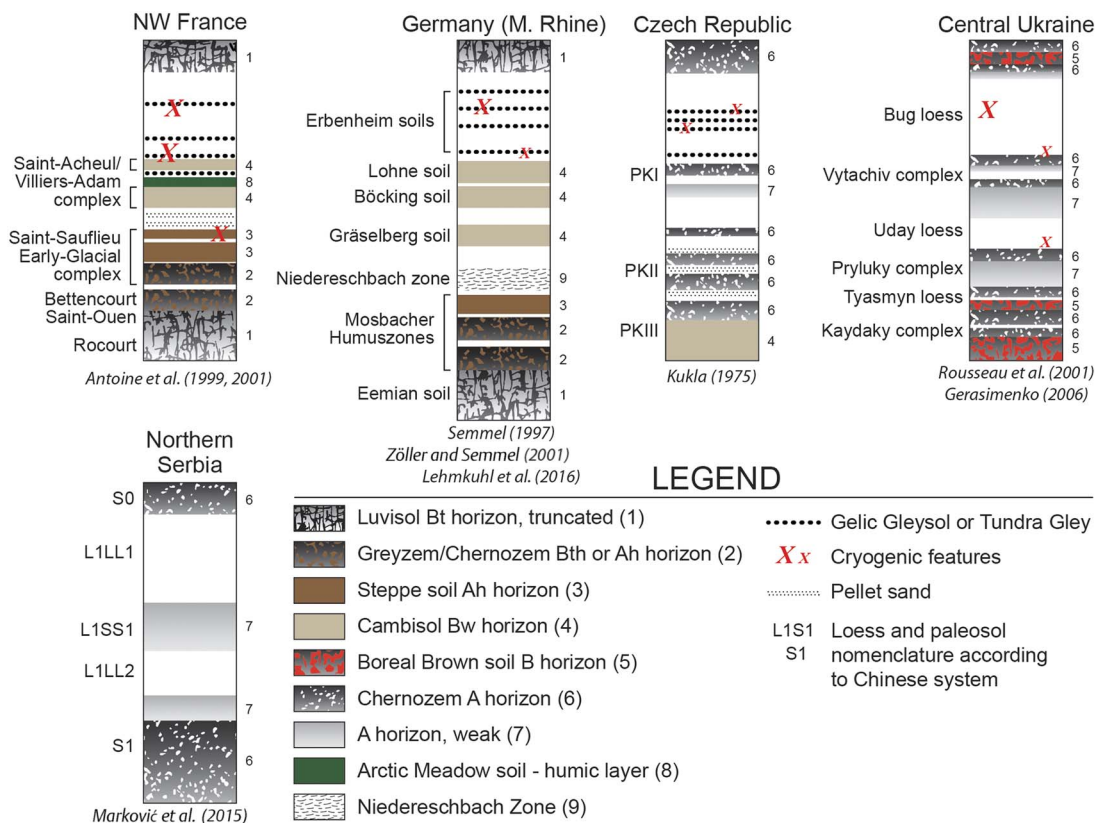


Figure 7. (color online) Principal stratigraphic subdivisions and important paleosols within the lithologic/loess record for the last 130 ka, for five main sites throughout Europe. Vertical scales on the diagrams are not uniform. In order to better match the graphics to the legend, each soil has been numbered, and the numbers have placed next to the stratigraphic profiles. After Marković et al. (2008).

Loess in midcontinent North America

By Joseph A. Mason

Some of the most important issues that still challenge loess researchers in the Central Lowlands and Great Plains of North America were already apparent in the classic map of eolian deposits of the United States, Alaska, and parts of Canada by Thorp and Smith (1952). Drawing on extensive observations by soil surveyors and geologists, Thorp and Smith (1952) mapped thick loess bordering the Mississippi, Missouri, Illinois, Wabash, and Ohio Rivers, all of which had drained the ice sheet of the last glaciation. Loess deposits exhibited well-defined thinning trends away from each river valley. A much broader swath of thick loess extended across the central Great Plains, from eastern Colorado to the Missouri River, thinning toward the southeast but with no obvious relationship to possible river valley sources (for an updated map, see Bettis et al., 2003). Thorp and Smith (1952) also accurately mapped many areas of thin loess across the Central Lowlands and Great Plains and provided a separate map of the Illinoian (Marine Oxygen Isotope Stage [MIS] 6) Loveland Loess, but their work emphasized the great thickness and extensive distribution of Late Pleistocene (MIS 2) Peoria Loess.

Today, interpretations of Peoria Loess, its sources and their paleoenvironmental controls, and its episodic and often very rapid accumulation rates, remain a central issue in midcontinent loess research. Provenance studies have revealed that much of the Peoria Loess of the central Great Plains was derived from Cenozoic rocks cropping out in unglaciated landscapes to the northwest (Aleinikoff et al., 1999, 2008; Muhs et al., 2008b). The paleoenvironments and processes involved in this enormous amount of nonglacial dust production remain poorly understood. In contrast, much of the Peoria Loess farther east is closely linked to glacial sediments carried by the Mississippi and other rivers during MIS 2, with changing sediment availability linked to ice lobe advance and retreat (Follmer, 1996; Grimley, 2000; Bettis et al., 2003). Peoria Loess deposits record some of the highest mass accumulation rates known worldwide, and just as interesting, improved age control—most recently through ^{14}C dating of gastropod shells—has confirmed large changes in accumulation rate over time (Roberts et al., 2003; Muhs et al., 2013a; Pigati et al., 2013; Nash et al., 2017). At present, it appears that these changes were not synchronous across the Central Lowlands or Great Plains and thus may be related to local variations in sediment supply, or changing source areas (e.g., Nash et al., 2017) rather than broader climatic change, not surprising given the complexity of Peoria Loess sources. Geomorphic evidence also exists for large-scale deflation of coarse, source-proximal Peoria Loess, and experimental evidence suggests that there is a high potential for eolian reentrainment in the absence of vegetation cover or cohesive crusts (Sweeney and Mason, 2013). These processes could also be responsible for abrupt local changes in grain size or accumulation rate.

The stratigraphy of loess, both older and younger than the Peoria Loess, emphasizes the unique nature of the loess system during MIS 2 (Mason et al., 2007) but also raises

many other questions. Parts of the White River (Late Eocene-Oligocene) and Arikaree (Oligocene-Miocene) groups in western Nebraska are interpreted as volcanoclastic loess (Swinehart et al., 1985; Hunt, 1990; LaGarry, 1998), helping to explain why large volumes of these rocks were later reworked into Peoria Loess (Aleinikoff et al., 1999, 2008; Yang et al., 2017). Loesslike silt predating the Matuyama-Brunhes (M-B) boundary at 780 ka has been identified in Illinois (Grimley and Oches, 2015); however, continuous loess sequences in the midcontinent apparently all postdate the M-B boundary and/or the Lava Creek B tephra (~630 ka; Matthews et al., 2015). The relative scarcity of Early Pleistocene loess must in part reflect poor preservation, but other factors should also be explored. For example, if Early Pleistocene ice sheets extended farther south but had lower profiles (Clark and Pollard, 1998), the resulting glacial atmospheric circulation might not have favored dryland dust production from potential sources on the Great Plains.

The loess sequence in eastern and central Nebraska (Fig. 8) is broadly representative of the stratigraphy of thick loess at localities across the midcontinent where preservation is high. The oldest part of this sequence includes multiple thin depositional units of the Middle Pleistocene Kennard Formation (Mason et al., 2007). The stratigraphy, chronology, provenance, and paleoenvironmental record of the Kennard Formation remain largely unstudied, as have possible correlations with pre-Loveland Loess units reported from scattered localities along the Mississippi River valley (Porter and Bishop, 1990; Jacobs and Knox, 1994; Leigh and Knox, 1994; Grimley, 1996; Rutledge et al., 1996; Markewich et al., 1998). A variety of evidence indicates the overlying Loveland Loess was deposited during the MIS 6 glacial period, although luminescence ages at some sites suggest the uppermost part may be younger (Forman et al., 1992; Maat and Johnson, 1996; Rodbell et al., 1997; Markewich et al., 1998; Forman and Pierson, 2002; Grimley and Oches, 2015). An intriguing characteristic of thick Loveland Loess is the presence of a lower, darker-colored zone, which may contain multiple weak paleosols, suggestive of slow and/or intermittent deposition (Grimley, 1996; Mason et al., 2007). Above the prominent Sangamon Soil, which caps the Loveland Loess and developed through MIS 5 and 4, is an MIS 3 loess unit variously known as the Roxana Silt (Mississippi valley), Pisgah Loess (Iowa), or Gilman Canyon Formation (Great Plains). It has characteristics similar to the lower Loveland Loess; ^{14}C and luminescence dating confirms its slow accumulation rate (Leigh, 1994; Follmer, 1996; Markewich et al., 1998; Bettis et al., 2003; Johnson et al., 2007; Muhs et al., 2013a). This similarity suggests the lower zone of Loveland Loess on the Great Plains could preserve an isotopic record of shifting dominance by C_3 and C_4 grassland, as does the Gilman Canyon Formation (Johnson et al., 2007). Above the MIS 3 loess, Peoria Loess accumulated between about 28 ka and 13 ka (MIS 2) across the midcontinent, with the exact time span varying regionally and possibly locally (Bettis et al., 2003; Muhs et al., 2013a; Pigati et al., 2013; Nash et al., 2017). On the

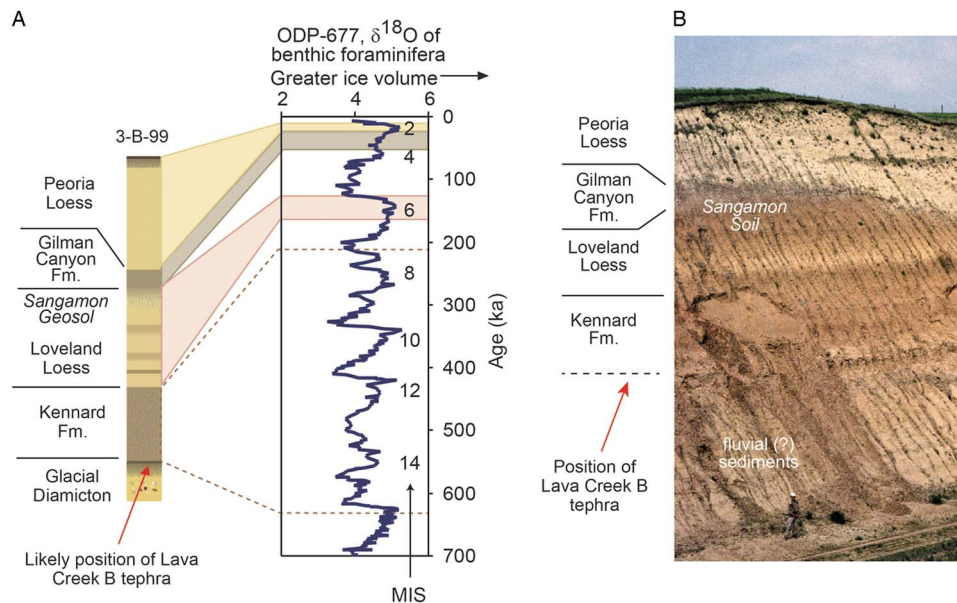


Figure 8. (color online) (A) The general loess stratigraphy found in eastern Nebraska, USA, as represented by core 3-B-99 (41°29'N, 96°13'W) (Mason et al., 2007). Peoria Loess, Gilman Canyon Formation, and Loveland Loess are correlated with specific parts of marine isotope record based on numerical dating. Ages assigned to Loveland Loess are based on luminescence dating at the paratype locality in western Iowa (Forman and Pierson, 2002); ages assigned to Kennard Formation are based on its stratigraphic position between Loveland Loess and Lava Creek B tephra, supported by burial dating of Balco et al. (2005). MIS, Marine Oxygen Isotope Stage. (B) Loess stratigraphy in the Elba Cut section of central Nebraska (41°18'N, 98°31'W), interpreted by J. Mason by comparison with eastern Nebraska sections (Mason et al., 2007). Note person at base of section for scale. The tephra present in this section (to left of area shown here) is the Lava Creek B (E.A. Bettis III, personal communication 2006).

central Great Plains and along the Missouri River valley in North and South Dakota, the loess record continues into the Holocene. The Brady Soil, formed during a period of limited dust accumulation between about 14 and 10 ka, is sometimes found in the upper Peoria Loess, when Bignell Loess overlies it. Where the latter is thick, it represents a high-resolution record of Holocene dust deposition (Johnson and Willey, 2000; Mason et al., 2003, 2008). The specific geomorphic mechanisms of Holocene dust production, downwind dispersal, and patchy retention in the landscape, and their connections to changing climate and vegetation, are worthy of additional study because of their potential relevance to the environmental changes associated with a warmer and drier future climate.

Loess in Alaska

By E. Arthur Bettis III

Loess associated with glacial valley-train sources is extensive over much of Alaska and adjacent parts of adjacent Yukon Territory in Canada (Fig. 9). In some parts of central Alaska, loess can be as much as several tens of meters thick and, based on a combined tephra and paleomagnetic record, may date back as far as the onset of North American glaciation, ~3 Ma (Westgate et al., 1990). It was not until the mid-1950s that the extensive deposits of silt on the Alaskan landscape were properly recognized as loess. Prior to that time, some researchers regarded them as the result of frost

shattering or other processes (Taber, 1943, 1953, 1958). It was Péwé (1955), however, who finally brought together several converging lines of evidence—geomorphic, stratigraphic, and mineralogical—that established that these silt bodies in Alaska are loess. Loess is now recognized over many parts of the region, including a broad area of the coastal plain north of the Brooks Range, over parts of the Seward Peninsula (Hopkins, 1963), in the Yukon River basin (Williams, 1962; Begét et al., 1991; Jensen et al., 2013), in the Tanana River valley and along the Delta River valley of central Alaska (Péwé, 1955, 1975; Muhs et al., 2003b), in southern Alaska in the Matanuska Valley (Muhs et al., 2004, 2016), on the Kenai Peninsula (Reger et al., 1996), and along the Copper River valley in Wrangell–St. Elias National Park (Muhs et al., 2013b; Pigati et al., 2013).

Loess deposits in Alaska that have been securely dated to the last glacial period are elusive or are very thin. On the Seward Peninsula, less than a meter of loess blankets a land surface with fossil tundra vegetation that dates to the last glacial period (Höfle and Ping, 1996; Höfle et al., 2000). In the Fox Permafrost Tunnel near Fairbanks, loess that is bracketed by a radiocarbon age of ~9.5 ka above and ~34 ka below could date to the last glacial period (Hamilton et al., 1988), as is the case for very thin loess dated between ~12 ka and ~36 ka nearby in an upland locality (Muhs et al., 2003b). In neither of these two cases, however, is loess dated directly to the last glacial period. Attempts to date other last-glacial central Alaskan loess deposits have been frustrated by a lack

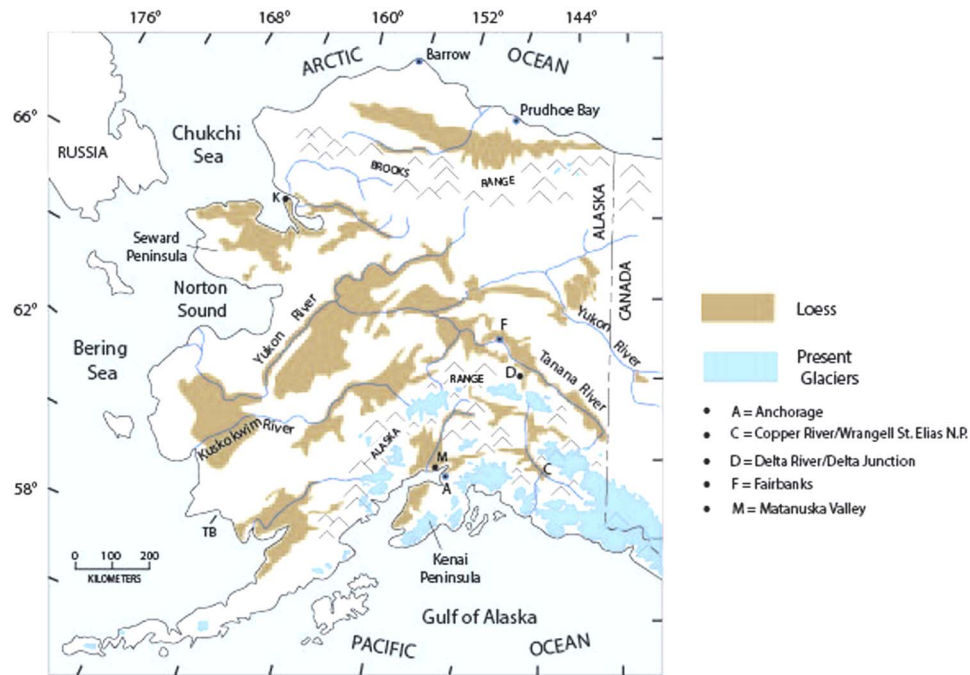


Figure 9. (color online) Map of Alaska showing the distribution of Quaternary loess deposits and the distribution of modern glaciers. Lettered dots refer to localities discussed in the text. After Muhs et al. (2003b).

of materials suitable for radiocarbon analyses or uncertainties in luminescence geochronology (Oches et al., 1998; Berger, 2003; Muhs et al., 2003a; Auclair et al., 2007). However, recent identification of the Dawson tephra (~30 ka) in the upper part of loess deposits near Fairbanks permits an interpretation of as much as ~3 m of accumulation since the time of tephra deposition (Jensen et al., 2016). Nevertheless, it is not known how much of this sediment is of last-glacial age and how much may be of Holocene age.

Older, pre-last-glacial loesses are well documented in Alaska. The chronology of these older loesses has been aided immeasurably by detailed studies of tephras that are interbedded with the eolian silts (Westgate et al., 1990; Begét et al., 1991; Preece et al., 1999; Jensen et al., 2013, 2016). Jensen et al. (2016) described evidence for significant pre-last-glacial loess accumulation in central Alaska during Marine Isotope Stages 4 and 6, with accumulation rates greatest during transitions between isotope stages. Furthermore, these investigators noted that in the middle and early Pleistocene, glaciations were much more extensive in Alaska than during the last glacial period (Kaufman et al., 2004), which likely enhanced the supply of glaciogenic silt available for loess accumulation.

Whereas loess dated to the last glacial period has been elusive in Alaska, there are abundant loess bodies that date to the Holocene, and deposition continues today in many parts of the region. In the Delta Junction area of central Alaska, only Holocene loess has been documented (Péwé, 1975; Muhs et al., 2003b). On the Kenai Peninsula of southern Alaska, the Lethe tephra dating to ~19 ka to ~15 ka is found below, or in the lower part of loess, but as on the Seward Peninsula, this eolian silt is less than a meter thick (Reger

et al., 1996). Elsewhere in southern Alaska, near Anchorage, loess of the Matanuska Valley all dates to the Holocene (Muhs et al., 2004, 2016), as does loess of the Copper River valley in Wrangell–St. Elias National Park, to the east (Muhs et al., 2013b; Pigati et al., 2013).

Paleosols intercalated in loess sequences have long been the focus of study, for stratigraphy, geochronology, and paleoenvironmental interpretation in most loess regions. In Alaska, however, little mention of paleosols in the loess sequence was made by geologists until relatively recently. Indeed, some researchers even doubted their existence (Péwé et al., 1997). Begét and his colleagues at the University of Alaska were the first to bring the geologic community's attention to the rich record of paleosols in Alaskan loess in a landmark series of papers (Begét and Hawkins, 1989; Begét, 1990; Begét et al., 1990). Paleosol research in Alaska and adjacent Yukon Territory since the time of these pioneering studies has provided new insights into the paleoenvironment during periods of reduced loess accumulation (Sanborn et al., 2006; Muhs et al., 2008a).

Loess in Argentina, South America

By Marcello Zárata and Alfonsina Tripaldi

The loess deposits of southern South America cover broad areas of the eastern Pampean plain of Argentina, southern Brazil, and Uruguay, as well as several areas of the Chaco region, and mountain valleys of the northwestern Pampean ranges (Fig. 10). The focus of this overview is on the loess deposits in Argentina. In the Pampean region of Argentina, loess and loesslike deposits range in age from the

late Miocene through the Quaternary; in some Pampean areas, loess accumulation even continued until the early–mid-Holocene. Luminescence chronology carried out in the extensive apron of the last-glacial loess suggests regional variation in depositional rates over this interval, with relatively high accumulation rates during the last glacial maximum and the late glacial intervals. The average thickness of the last-glacial Pampean loess is ~1.5–2 m, with up to 3–4 m in the mountains surrounding the Pampean plain (i.e., the Tandilia and Ventania ranges and the Pampean ranges of Córdoba-San Luis). Sandy eolian deposits (dune fields, sand sheets) dominate in the western-southwestern Pampean plain and grade into loess mantles downwind (Zárate and Tripaldi, 2012). The loess deposits also show a gradual grain-size decrease from silty fine sands to silty deposits in the eastern Pampean plain (González Bonorino, 1966). The mineralogical assemblage of the Pampean loess is dominantly composed of plagioclase, volcanic shards (both fresh and weathered), quartz, K-feldspars, and fragments of basalt, andesite, and rhyolite. Magnetite, amphibole, and pyroxene, among others, are the most common heavy minerals. The direct input of Andean volcanic eruptions in the loess deposits is documented by fresh volcanic shards, whereas most of the loess grains were derived from the erosion and fluvial transportation of extensive volcanoclastic units (*sensu* Fisher, 1961) exposed in the Andes Cordillera and its piedmont. These volcanoclastic units comprise late Miocene to Quaternary fine-grained pyroclastic deposits, and volcanic rocks (basalts, andesites), as well as lower Mesozoic acid volcanic rocks (González Bonorino, 1966). The origin of the volcanoclastic sedimentary sand and silt particles has been attributed to explosive volcanism (Zárate and Blasi, 1993) and physical weathering (Iriondo, 1990). Secondary loess sources, including the Brazilian plateau, the Tandilia and

Ventania ranges, and the Pampean ranges surrounding the Pampean plain, have also been documented and show variable contributions, according to the area considered (Zárate and Tripaldi, 2012). The eolian sand and silt particles are thought to have been deflated by west–southwest winds from the fluvial system of (1) the Bermejo-Desaguadero-Salado-Curacó (BDSC) River (Iriondo, 1990), a wide depositional system at the distal eastern piedmont of the Andes, and (2) the Colorado-Negro Rivers (Zárate and Blasi, 1993), where volcanoclastic sediments are abundant. Northeast–southeast winds prevailed along the northern extent of the BDSC system, between the Diamante and San Juan Rivers, and the western Pampas near the San Luis ranges (Fig. 10), where eolian sandy sediments document a mixed provenance, including volcanoclastic, metamorphic, and igneous rocks from the surrounding Pampean ranges (Zárate and Tripaldi, 2012). In order to improve our understanding of Quaternary eolian systems, most current research has focused on two main topics related to the loess here: (1) investigation of the sedimentary environments of the source area represented by the BDSC fluvial system and (2) Quaternary loess deposits of the northwestern mountain valleys.

Studies in progress suggest that the BDSC fluvial system is a complex sedimentary setting consisting of major alluvial fans generated by its main tributaries (i.e., the San Juan, Mendoza, Tunuyán, Atuel, and Diamante Rivers), all of which drain eastward, out of the Andes Mountains. General paleoclimatological and paleoenvironmental reconstructions suggest that arid and arid-semiarid conditions dominated here during the accumulation of the alluvial deposits (i.e., from the late Pleistocene to the present; Mancini et al., 2005). The San Juan, Mendoza, Tunuyán, Atuel, and Diamante drainage basins have a seasonal precipitation regime, with winter snowfalls generated by the Pacific cyclones, in their upper basins. These areas were also glaciated (Espizúa, 2004), promoting increased seasonal discharges during the Pleistocene. Sedimentologic analysis focused on the lower basins of the Atuel and Diamante Rivers has documented a large alluvial fan (200 km long and 100 km wide) dominated by fine sand/coarse silt deposits. Diverse sedimentary settings, including numerous channels and their associated floodplains, as well as shallow saline lakes, are reported for this system, along with extensive eolian deposits (dunes and sand sheets) covering large parts of the alluvial deposits (Lorenzo et al., 2017; Tripaldi and Zárate, 2017). Farther north, in Catamarca Province, loess deposits have been recently explored in a valley situated ~100 km southwest of the Tafi del Valle loess locality of Tucumán (Stiglitz et al., 2006). The loess deposits here are up to 40 m thick and include interlayered fluvial sediments and paleosols. Loess has also been reported nearby, covering the planation surface of the Ancasti Pampean range (Sayago, 1983). Immediately west of the Catamarca valley are large intermountain tectonic basins (e.g., the Salar de Pipanaco, Campo del Arenal) that contain fine alluvial sands and silts from rivers that drain the Andes and the Puna region and their associated dune fields.

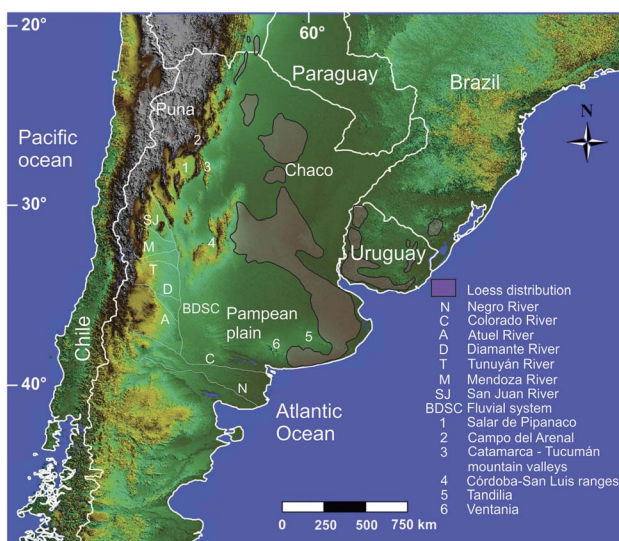


Figure 10. (color online) DEM (Digital Elevation Model) image of southern South America with general location of the Pampean plain, Chaco, Puna, and other areas discussed in the text. Localities referred to in the text are keyed to the legend in the lower right of the figure.

Although several areas still remain unexplored and/or poorly investigated, current studies allow for a reinterpretation of the BDSC fluvial system as a large bajada resulting from the north–south coalescence of several major alluvial fans generated by rivers with highly seasonal flow regimes from winter snowfalls and glaciers, under generally arid-semiarid conditions. This depositional environment has abundant sand and silt, derived from the erosion of late Cenozoic volcanic rocks and pyroclastic deposits, and older volcanic and volcanoclastic units exposed in the Andes and the eastern piedmont, as well as metamorphic and igneous rocks from the surrounding Pampean ranges. These sediments were subject to entrainment by prevailing west–southwest winds in the southern part of the BDSC fluvial system, and northeast–southeast winds in the northern part.

Two important questions remain regarding the source area of the northwestern mountain valley loess of Catamarca: (1) What were the prevailing wind directions? (2) Has this loess been deflated from the tectonic basins located to the west-northwest, or did it originate via high suspension from more distal environments (i.e., the Puna plateau)? Future research should include a more detailed analysis of the late Quaternary eolian deposits in the northern BDSC system that may show a mixed provenance, and that may have been derived from northeast–southeast winds, as well as the loess deposits of the northwestern mountain valleys. These studies may help discern the role played by regional and/or local factors during the eolian accumulation phases in this region.

Loess at desert margins

By Onn Crouvi

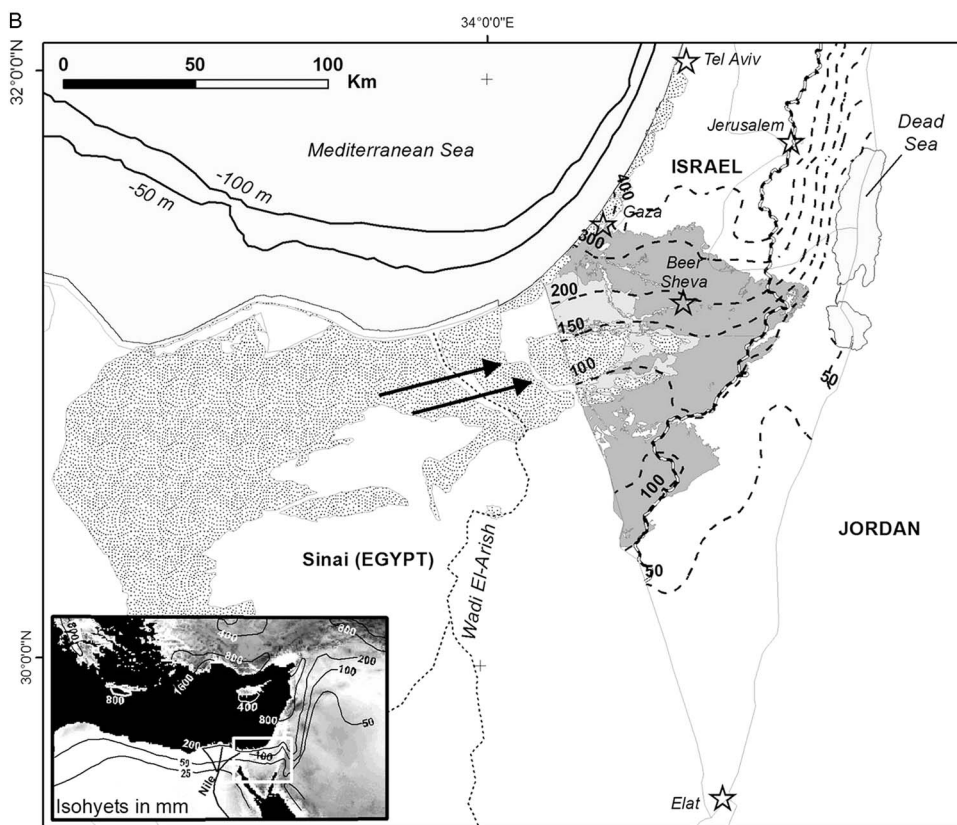
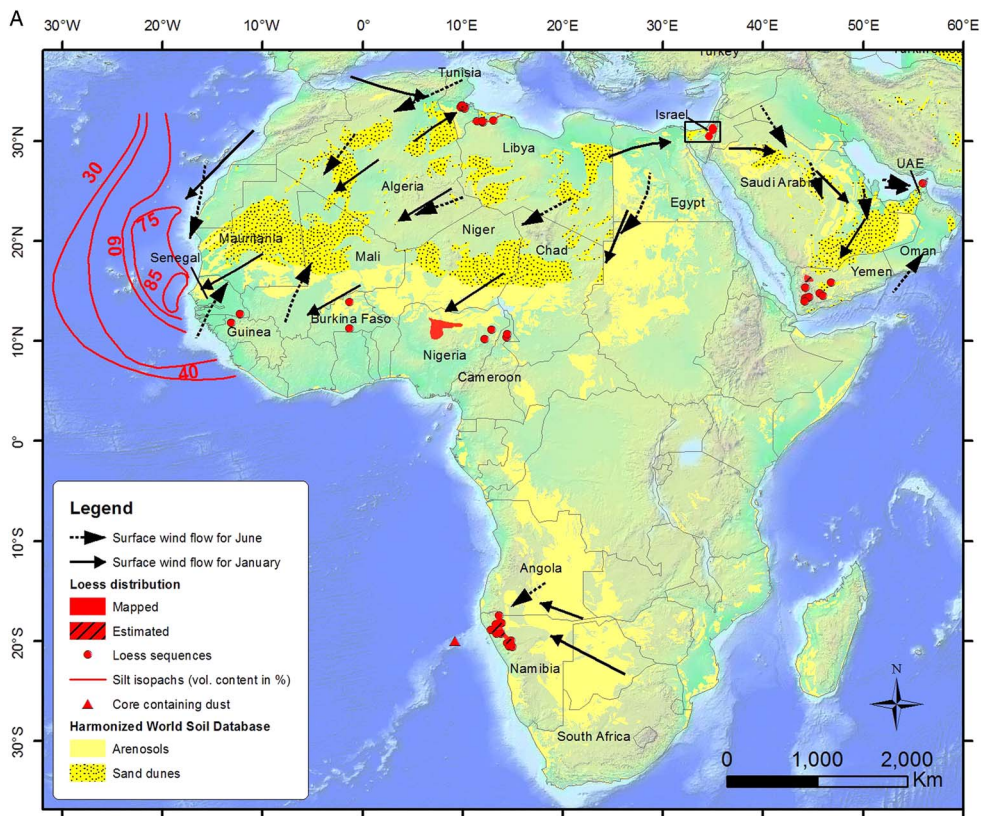
Loess at desert margins (termed here as “desert loess”) refers to eolian silt deposits generated in, and derived from, non-glaciated, low-latitude warm-arid or semiarid regions. The documentation of loess at desert margins since the mid-twentieth century (e.g., Yaalon, 1969; Coude-Gaussen, 1987; McTainsh, 1987) has confounded the traditional view of silt generation solely by glacial grinding (e.g., Smalley and Krinsley, 1978) that is widely attributed to most of the world’s well-known loess deposits. Thus, a number of non-glacial processes that produce silt grains in deserts have long been proposed and debated (e.g., Smalley, 1995; Assallay et al., 1998; Wright, 2001; Smith et al., 2002; Muhs and

Bettis, 2003), including salt weathering, frost weathering, deep weathering, fluvial comminution, and eolian abrasion.

Desert loess is known to exist at the margins of deserts in Africa (Tunisia, Libya, Algeria, Nigeria, and Namibia), in the Middle East (Israel, Yemen, the United Arab Emirates, and Iran), the western United States, the Great Plains of North America, and Australia (Fig. 11A). With the exception of the thick nonglacial loess in the Great Plains of North America, loess of this kind is patchy and varies in thickness from a few meters on uplands to a few tens of meters in valleys. Importantly, desert loess is the parent material for some of the most fertile soils in these regions. A few characteristics are common to all reported desert loess sites in Africa and the Middle East (Crouvi et al., 2010): (1) loess sediments are dominantly coarse silt to very fine sand, with median grain sizes ranging from 50 to 80 μm , and at some sites, the particle-size distribution is reported to be tri- or bimodal; (2) loess mineralogy is mostly quartz and feldspars, with various amounts of carbonate, depending on the degree of soil development in the loess; (3) at most sites, the underlying lithologies are inconsistent with the presence of quartz in the loess, suggesting an external silt source; (4) the shapes of loess particles are reported as subangular to angular for most regions; and (5) most loess bodies were deposited during the last glacial period ($\sim 110\text{--}10\text{ ka}$). Crouvi et al. (2010) noted that all these loess regions are located only a few tens of kilometers downwind from sand dunes (Fig. 11), and based on the mineralogical, spatial, and temporal associations between these two eolian bodies, suggested that the proximal source of the coarse silt in loess is the upwind dunes, via eolian abrasion of sand grains.

The Negev loess (Israel) is one of the world’s best-studied desert loess deposits, with scientific exploration that goes back to the early twentieth century (Fig. 11B; see Crouvi et al., 2017a). The carbonate bedrock lithology of the Negev and its physiography provide a unique opportunity to understand the sources of this silicate-rich loess and to explore silt formative processes in deserts. Grain-size data from the Negev loess have three main characteristics: (1) clear textural bimodality, with one mode in the coarse silt fraction (36–65 μm) and another in the fine silt to clay fraction (2.5–10 μm); (2) grain-size decreases to the north, east, and south, away from the sand dunes that border the loess deposit on the west; and (3) increasing grain-size upward in each individual primary sequence. Recognizing the bimodality of the loess, Dan Yaalon was the first to

Figure 11. (color online) (A) Spatial distribution of loess in Africa and Arabia, active sand seas, and Arenosols (sandy soils) (Food and Agriculture Organization of the United Nations, International Institute for Applied Systems Analysis, ISRIC–World Soil Information, Institute of Soil Science–Chinese Academy of Sciences, and Joint Research Centre of the European Commission, 2009). Near surface dominant wind directions for January and June are based on Breed et al. (1979). Silt (content in %, 24 μm mode) in oceanic sediments off the coast of West Africa deposited during the last glacial maximum (Sarnthein et al., 1981). See text for further details on the Negev loess, Israel. After Crouvi et al. (2010). (B) Map of Israel and its surroundings, showing the distribution of sand dunes (white polygons with black dots) and loessial (dark gray) and sandy (light gray) soils in the Negev and Sinai deserts (the soils were mapped only in Israel). Mean annual rainfall (mm) in Israel for the period 1961–1990 is shown by dashed isohyets. Black arrows are the inferred westerly winds prevalent during sand incursion. Insert shows the location of Israel in the eastern Mediterranean region and the mean annual rainfall isohyets (mm). After Crouvi et al. (2008).



suggest that the Negev loess had two different sources that supplied sediments through two different transport pathways (Yaalon, 1969; Yaalon and Ganor, 1973, 1979; Yaalon and Dan, 1974): distal sources in the Sahara and Arabia deserts supplying fine silt and clays transported by cyclonic winds over thousands of kilometers, and proximal sources in Sinai, such as Wadi El-Arish in northern Sinai, supplying the coarser silts. However, recent studies have shown that the major source of the coarse silt grains is the adjacent, upwind sand dunes that advanced into Sinai and Negev during the late Pleistocene, concurrent with accumulation of the loess (Crouvi, 2009; Crouvi et al., 2008). This conclusion was based on the following observations: (1) increases of the quartzofeldspathic coarse mode upward in the loess deposits, (2) the spatiotemporal association of sand dune activities and dust mass accumulation rates (MARs) of the loess, (3) similarity in mineralogical composition and in isotopic composition of Sr and Nd between the sand dunes and the coarse fraction of the loess (Muhs et al., 2013c; Ben Israel et al., 2015), and (4) location—the loess was located downwind of sand dunes during the late Pleistocene, as evident by the linear orientation of the dunes. In addition, recent studies have shown that the quartz-rich silt fraction in soils in the Judean Mountains and their lowlands, north of the loess, can be regarded as the direct continuation of the dune – loess association (Crouvi et al., 2014; Amit et al., 2016). Because of the fact that these silt grains are farther away from their source than the Negev loess deposits, they are finer-grained and exhibit lower MARs. Finally, because much of the Negev loess formed during the late Pleistocene, it has been undergoing erosion through most of the Holocene, and even more severely during the last 100 yr because of agriculture practices. The erosion is both by water (e.g., Avni, 2005; Avni et al., 2006) and by wind (e.g., Tanner et al., 2016; Crouvi et al., 2017b), transferring the loess into a relatively young and new proximal dust source. Overall, the Negev loess can be regarded today as nonreplenishable natural resource that is slowly disappearing.

One of the main challenges in studies of loess at desert margins is the lack of comprehensive quantitative information about loess properties and their period(s) of formation (e.g., in Yemen, Namibia, and the United Arab Emirates). In other areas, there is no published map of loess distribution, and our knowledge originates mainly from sporadic documentation of the soils and sediments (e.g., the loess belt in the Sahel) and, except for the Nigerian loess, is poorly documented (see Crouvi et al., 2010 for more details).

Questions, challenges, and opportunities unique to loess at desert margins can be grouped into four categories: (1) Sources—despite great advances in grain-size end member modeling, and other approaches, separating between proximal and distal sources of the loess and identifying them is still an ongoing challenge. This dilemma is related to the century-old debate on the formation mechanisms of silts in deserts. (2) Paleoclimatological reconstruction—loess is an excellent climate archive that can shed light on (a) regional environmental changes, such as the appearance and

disappearance of dust sources, (b) regional changes in wind direction and strength, and (c) local climate properties (i.e., precipitation), through analyzing buried soils. These reconstructions are still poorly constrained from most desert loess regions in the world. (3) The continuation of loess downwind, beyond the major deposits, is unclear. What is the effect of loess and its derivatives on the areas and soils located farther downwind? How have additions of fine silt and clay affected the soils here? (4) Loess probably presents a new and intensive dust source that might affect future climate changes. The magnitude and frequency of dust emissions from desert loess regions is still poorly documented.

METHODOLOGICAL APPROACHES TO THE STUDY OF LOESS

Loess and paleosol stratigraphy

By Slobodan B. Marković

Loess covers huge parts of the continents, from currently subtropical areas to subpolar regions. The formation of loess is often not a recent or contemporary process. Instead, loess is usually deposited under extreme conditions ranging from desert to tundralike environments associated with previous glacial phases during the Quaternary period. During these periods, complex natural processes related to the formation, production, and deposition of dust facilitated the formation of loess deposits.

Loess, which is a mixture of different minerals, represents an almost ideal substrate for soil formation. Even slight climate changes are able to initiate rapid soil formation in loess deposits. Thus, even slight shifts from periods of dust accumulation to pedogenesis can be recorded in loess; paleosols within these sequences are some of the most sensitive continental archives of environmental responses to Quaternary climate change. From this point of view, each typical loess deposit or strongly developed pedocomplex can be regarded as a basic climatostratigraphic unit, representing full glacial or interglacial conditions. Other varieties of loess derivatives and weakly developed paleosols in loess are equivalent to stadial and interstadial environments, respectively.

Consequently, it is no surprise that climatostratigraphic research in many loess regions has a long and distinguished history. Many such early loess stratigraphic models represented climatostratigraphic approaches (e.g., Marković et al., 2016). Nonetheless, they had shortcomings. Developed at the beginning of the twentieth century, many of these studies were highly speculative, and the nomenclatures used were usually derived from local place names. With the purpose of creating a common European loess stratigraphy, the Loess Subcommittee (currently Loess Focus Group) of the International Union for Quaternary Research promoted pedostratigraphic criteria as the primary basis for stratigraphic correlations (Fink, 1962; Smalley et al., 2010). This concept culminated in the studies of Bronger and coworkers, who presented their attempts at Eurasian continental loess

correlation in a series of papers (Bronger, 1976, 2003; Bronger and Heinkele 1989; Bronger et al., 1998). Later, investigation of Czechian and Austrian loess exposures provided the background for correlation of terrestrial loess deposits with the oscillations recorded in deep-sea sediments, given that both likely reflect global paleoclimate drivers (Kukla, 1975, 1977; Fink and Kukla, 1977). The glacial cycle concept that Kukla applied to loess-paleosol sequences promoted loess as the most important terrestrial archive of Pleistocene climatic and environmental changes.

Further development of magnetostratigraphic techniques, as applied to loess in China, highlighted scientific interest in the multiple loess-paleosol couplets of the Chinese Loess Plateau (Heller and Liu, 1982, 1984; Liu, 1985). This new approach, based on paleomagnetic polarity zonation, allowed for direct correlations between profiles using loess-paleosol magnetic susceptibility variations and its correspondence with Marine Oxygen Isotope Stage (MIS) stratigraphy. Eventually, this method became the basis for the famous so-called “L&S” (loess and soil) Chinese loess stratigraphic model (Liu, 1985; Kukla, 1987; Kukla and An, 1989; Hao et al., 2012). Enhancement of the magnetic signal attributable to pedogenic processes appears to be valid for loess strata across the vast Eurasian semiarid loess zone as well (Maher and Thompson, 1992), further extending its application (Fig. 12). Data on loess magnetic susceptibility have since proved to be a rapid and consistent tool for interprofile correlations, even over very long distances (Marković et al., 2015). Figure 13 shows the remarkable accordance between Serbian and Chinese loess stratigraphies. The loess magnetic record from Siberian and Alaskan loess provinces has the opposite trends—that is, higher magnetic susceptibility values characterize loess deposits, with lower values in paleosols (e.g., Begét, 1990, 1996; Begét et al., 1990; Heller and Evans, 1995; Chlachula et al., 1998). Additional quantitative chronological approaches, such as current improvements in amino acid racemization, relative geochronology, tephrochronology, and ^{14}C and luminescence dating, have helped to significantly improve the accuracy of loess stratigraphic models, but still only at the level of correlation with the main MISs. In the United States, most of the loess is

younger than Middle Pleistocene in age, and therefore, “classic” regional loess stratigraphic models supported by luminescence and radiocarbon dating are generally more useful for long-range correlations than are data on magnetic susceptibility or amino acid racemization (Bettis et al., 2003).

Loess stratigraphy in the Southern Hemisphere has been investigated less intensively in South America where there is a high diversity of loess and loesslike deposits as a consequence of quite diverse environmental responses to climate forcing (Zárate, 2003; Iriondo and Kröhling, 2007). An additional problem in some regions is similar to the examples mentioned previously for Siberian and Alaskan loess; in this case, the variation in magnetic susceptibility is because of contributions of volcanic material in the loess deposits (e.g., Ruocco, 1989; Heller and Evans, 1995). Similar conditions occur in New Zealand, although here the presence of many (dated) tephra layers became an important advantage for the establishment of loess stratigraphy (Palmer and Pillans, 1996; Roering et al., 2002).

Using the L&S stratigraphic nomenclature, already well accepted for Chinese and Danubian stratigraphic units, can be a useful global approach. The L&S stratigraphic scheme has led to standardized, regionally specific stratigraphies of European loess deposits. The L&S scheme also offers a potential for correlating the confusing diversity of European loess stratigraphic records across the Eurasian loess belt and into central Asia and China (Marković et al., 2015). In order for the L&S system to provide accurate correlations, three conditions need to be met: (1) numerical ages or tie lines to numerical ages (e.g., volcanic ash dated elsewhere) need to be available; (2) absence of unconformities in undated portions of the sections must be demonstrated; and (3) there must be an assumption that global (or at least continental) geoenvironmental conditions fostering loess accumulation and subsequent soil development were more or less isochronous. The last assumption is the most problematic and can only be demonstrated with a much larger set of well-dated key localities than are currently available. Using this very simple labeling system is especially useful for geoscientists who may not be conversant in the region or in loess research. Hence, a unified chronostratigraphic scheme like the L&S scheme makes synchronization between the loess stratigraphic units in different parts of world almost intuitive (Fig. 14).

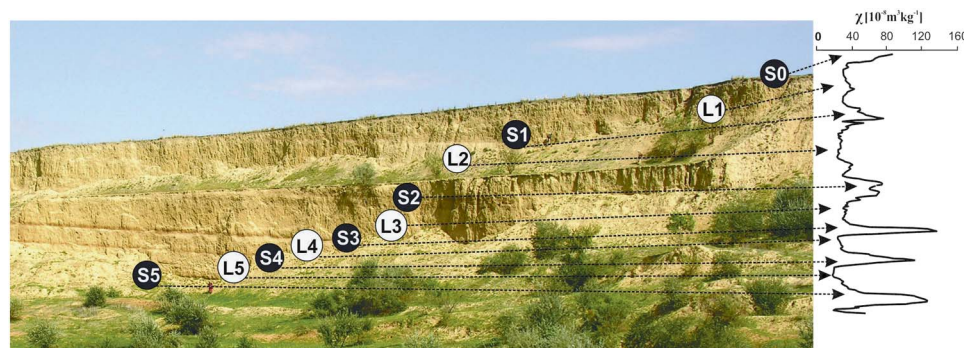


Figure 12. (color online) The Mircea Voda loess section in Dobrogea, Romania, is a good example of alternations of loess layers (from L1 to L5) and pedological horizons, or paleosols (from S0 to S5). These data are additionally illustrated by variations in magnetic susceptibility ranging from low values in loess units to high values in paleosols (Bugge et al., 2009; Timar-Gabor et al., 2011).

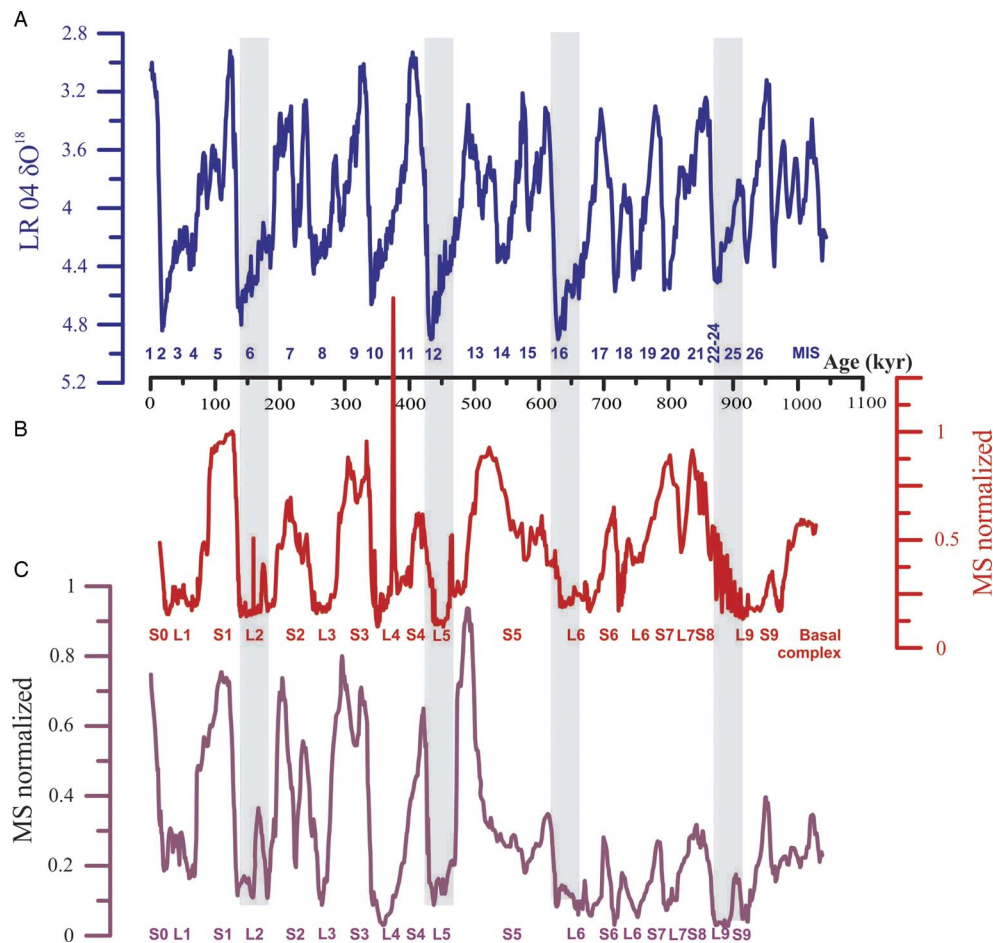


Figure 13. (color online) Direct comparisons between the marine LR04 stack (Lisiecki and Raymo, 2005) (A) and Serbian loess (Marković et al., 2015) (B) and Chinese loess (Sun et al., 2006) (C) magnetic susceptibility (MS) records plotted on time scale. MIS, Marine Oxygen Isotope Stage.

Contrary to successful attempts at correlations between the main loess stratigraphic models and their equivalent MISs (e.g., Lisiecki and Raymo, 2005; Fig. 13A), application of event stratigraphy in loess research is still problematic (*sensu* Björck et al., 1998). For example, direct correlations of the loess record with Greenland stadial-interstadial cycles (Rousseau et al., 2002, 2007; Antoine et al., 2009, 2013) or with Heinrich events (Porter and An, 1995; Stevens et al., 2008) are still under debate. The main problem lies in inadequate age control. Luminescence chronologies from loess sections are not sufficiently precise to make the proposed temporal correlations with the higher-resolution Greenland ice-core records. For example, one-standard-deviation uncertainties on a luminescence age are at best 5%, far too large to allow such fine correlations over this time interval (Roberts, 2008).

Because of the widespread distribution of loess and loesslike deposits, especially in the Northern Hemisphere, accurate loess climatostratigraphic records supported with accurate age control can be regarded as an important first step toward appropriate correlation of sections from distant loess provinces. Nonetheless, they also provide a missing link for a better understanding of temporal and spatial environmental reconstructions during the Quaternary period.

Environmental magnetism in Quaternary loess deposits

By Ulrich Hambach, Christian Zeeden, Qingzhen Hao, Igor Obreht, and Daniel Veres

Introduction and background

Iron is the fourth most common element in the earth's crust and responsible for color in many geologic deposits. Because of its low energetic thresholds in redox processes, iron is involved in numerous bio-/geochemical process chains. It also belongs to the transition elements which exhibit para- and ferromagnetism (*sensu lato*). The combination of these properties makes iron a key tracer and witness of environmental processes and forms the base of rock, environmental, and paleomagnetism.

Since the seminal work of Friedrich Heller and Tungsheng Liu (1982, 1984), environmental magnetic parameters have been recognized as fundamental paleoclimate proxies for Eurasian loess-paleosol sequences (LPSs; see "Loess and paleosol stratigraphy"). Later, George Kukla and Zhisheng An (Kukla et al., 1988; Kukla and An, 1989) further employed low-field magnetic susceptibility (MS) as a

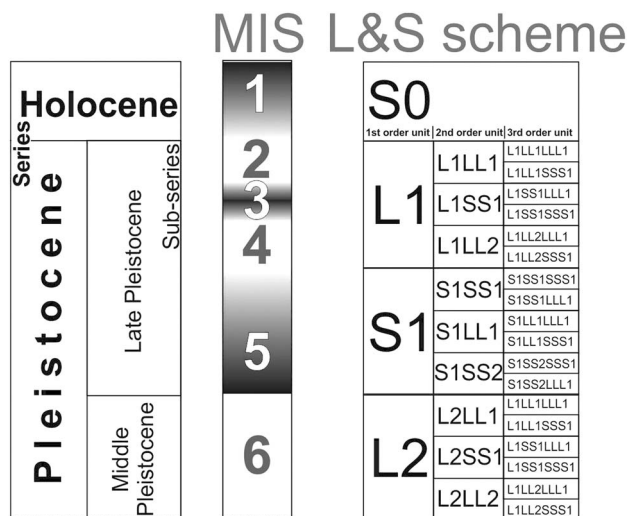


Figure 14. Comparisons between classic Pleistocene stratigraphic subdivisions (Gibbard and Cohen, 2008), Marine Oxygen Isotope Stages (MIS; e.g., Liescke and Raymo, 2005), and L&S (loess and soil) nomenclature initially presented by Kukla and An (1989).

stratigraphic tool, facilitating correlations between terrestrial deposits and the marine record; the latter is based on oxygen-isotope data for oceanic foraminifera, which in turn is a proxy for global ice volume (Lisiecki and Raymo, 2005). This early work demonstrated that MS, combined with magnetic polarity stratigraphy, provides a critical temporal framework for LPSs. Later work confirmed that the MS record closely parallels the oxygen-isotope fluctuations in deep-sea sediments, suggesting a close interconnection between dust deposition on the Chinese Loess Plateau (CLP), global ice volume, and global climate (compare Fig. 15A and B). Since then, MS, a nondestructive and inexpensive measurement, has become a widely applied paleoclimatic proxy and correlation tool in the study of LPSs worldwide (e.g., Heslop et al., 2000; Guo et al., 2002, 2009; Sun et al., 2006; Marković et al., 2011, 2015; Hao et al., 2012; Necula et al., 2015; Zeeden et al., 2016b).

MS records from geochemically and mineralogically quite homogenous loess deposits provide a first order chronostratigraphic link between these terrestrial dust archives and the marine and lacustrine record, potentially resolving orbitally paced climatic variability since the Neogene (Heller and Liu, 1984; Guo et al., 2002; Hao and Guo, 2004). Precipitation controls soil moisture variations, which in turn are a first-order control for diagenesis and pedogenesis in terrestrial dust deposits. Moisture governs the geochemical process chains from silicate weathering of detrital eolian grains up to the neoformation of magnetically highly effective Fe-oxide minerals, whose concentration and particle size in loess and paleosols eventually reflect past climate variations (Heller et al., 1991; Buggle et al., 2014). Unweathered (primary) loess consists predominantly of silt-sized, silicate minerals, with variable amounts of detrital carbonate (e.g., Muhs, 2013b; Maher, 2016). Upon deposition, the loess undergoes “loessification,” a process involving initial silicate weathering, partial carbonate

dissolution and reprecipitation, and neoformation of clay minerals (Sprafke and Obrecht, 2016). Loessification also controls the geochemical dynamics of iron (Fe) and, in so doing, influences the color and magnetic properties of the loess (Maher, 2011). Changes in moisture, accompanied by biological activity, both directly linked to global/regional climate conditions, lead to carbonate dissolution and silicate weathering; these pedogenic processes largely reflect global and regional variations in the hydroclimate regime (Maher, 2016).

In environmental magnetic studies, low-field or initial MS signal is usually determined at ambient temperatures, in low AC-fields of a few hundred A/m, and at different frequencies ranging from a few hundred to thousands of Hz (Evans and Heller, 2003). MS and its dependence on the frequency of the applied magnetic field (MS_{fd}) provide highly sensitive proxies of climate conditions during loess accumulation (Buggle et al., 2014). This signal is, first, based on the mineralogical homogeneity of the original dust/loess and, second, on the subsequent neoformation of ferrimagnetic minerals during the course of silicate weathering and pedogenesis. Thus, intense pedogenesis leads to enhancement of the mineral magnetic signal (Fig. 16). Ultimately though, the MS value of a given magnetic assemblage in an LPS depends on the concentration and composition of the mineral grains, as well as their particle size. Magnetic mineral particles reveal magnetic domain structures, with each domain being spontaneously magnetized to saturation. Particles may consist of a single domain (SD) or multiple domains (MDs) depending on particle size, composition, and internal mineralogical structure. SD particles are either superparamagnetic (SP) with high MS or stable SD (SSD) with low MS. The MS of MD particles, however, is again higher without reaching the level of the SP state (Evans and Heller, 2003; Zeeden et al., 2016a). Hence, it is not sedimentary particle size but the magnetically effective domain state of a particle that controls its magnetic properties (Liu et al., 2012; Buggle et al., 2014). The highest MS values occur in horizons containing higher concentrations of ultrafine particles covering even the SP-SSD threshold. SP particles mainly precipitate in situ, from soil moisture-controlled weathering solutions; their abundance provides therefore a sensitive proxy for sediment and soil humidity (Heller et al., 1991; Maher, 2011; Song et al., 2014; Zeeden et al., 2016a; Gao et al., 2018).

Besides MS, the user can also utilize a range of mineral magnetic parameters and interparametric ratios. In addition to specific hysteresis parameters, laboratory-induced remanences and their dependence on temperature can be employed. Although yielding valuable information, they are less frequently applied, as they are generally time consuming to determine (Maher, 2011; Liu et al., 2012).

MS as the stratigraphic backbone in Eurasian loess deposits

In Eurasian loess deposits, MS is usually enhanced in paleosols, as compared with primary loess (Evans and Heller, 2003). This characteristic is explained by the neoformation of

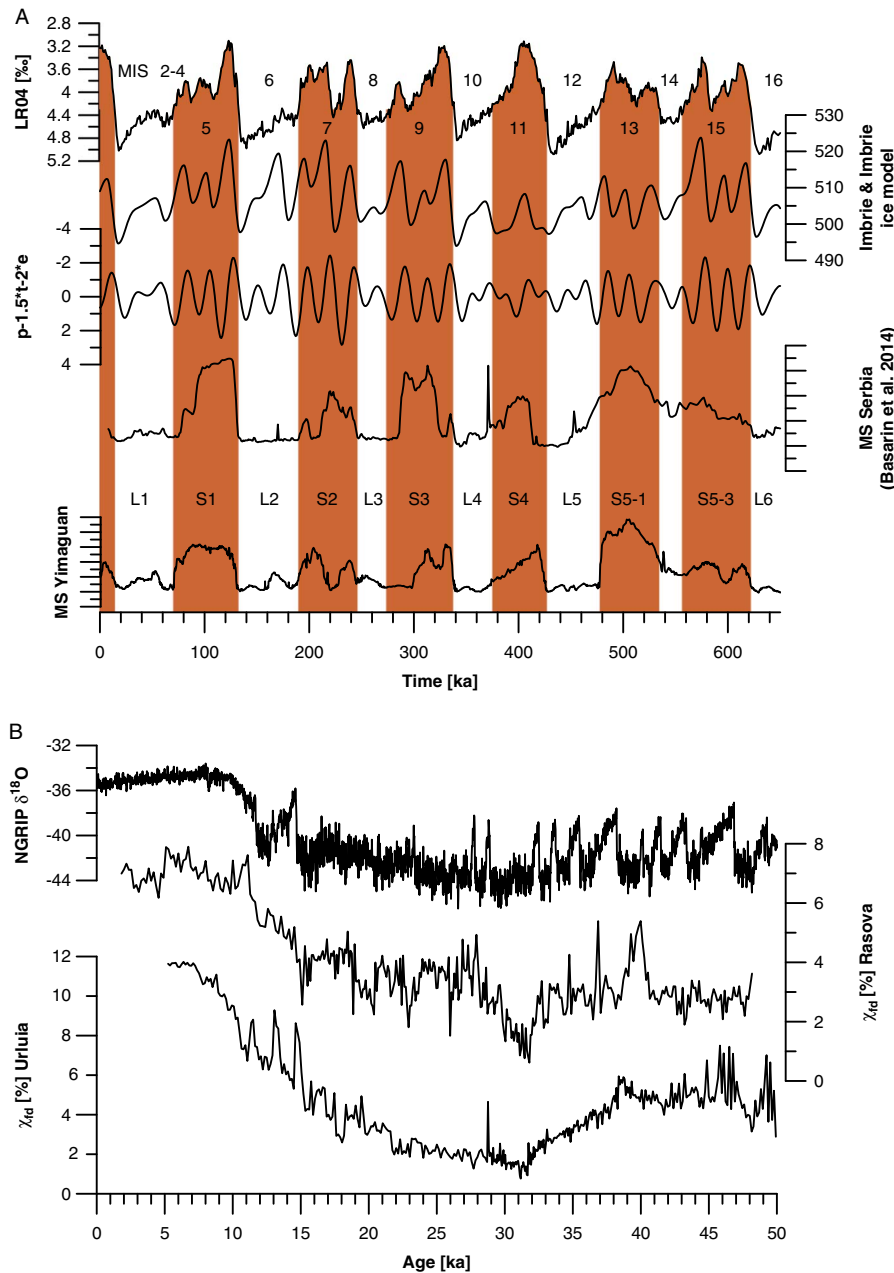


Figure 15. (color online) Comparisons of established Quaternary reference data sets. (A) A comparison of the LR04 benthic isotope stack (Lisiecki and Raymo, 2005), the Imbrie and Imbrie (1980) ice model (parameterized as by LR04), and a mixture of orbital parameters eccentricity (E), tilt/obliquity (T), and precession (P; Laskar et al., 2004), along with loess magnetic susceptibility (MS) data from Europe (Basarin et al., 2014) and the Chinese Loess Plateau (Hao et al., 2012). In both cases, loess MS (and other information) was used for correlative time scale construction. Marine Oxygen Stages (MISs) and loess (L) and paleosol (S) units are indicated, using a $\delta^{18}O$ cutoff of 4.3. (B) A comparison of North Greenland Ice Core Project (NGRIP) $\delta^{18}O$ data (North Greenland Ice Core Project Members et al., 2004) with two data sets of the MS_{fd} from Uurluia (Obrecht et al., 2017) and Rasova (Zeeden et al., 2016a). Note that the Campanian Ignimbrite volcanic tephra causes additional signal at ca. 40 ka. NGRIP.

ultrafine magnetic particles during pedogenesis (Chinese enhancement model; Heller et al., 1991). Figure 16 illustrates the magnetic enhancement trend for the Semlac LPS (recent to ≈ 400 ka; southeastern Pannonian basin, Romania). MS increases here are attributed solely to pedogenesis, via the increase of ultrafine particles extending into the SP-SSD threshold interval (20–40 nm). As this threshold decreases with increasing frequency of the magnetic field, the relative

amount of newly formed ultrafine particles can be determined by the dependence of MS on the applied frequency (here: χ_{Δ} ; Fig. 16; Liu et al., 2012). Therefore, the MS_{fd} is also a valuable and sensitive parameter for incipient soil formation. The interception of the trend line with the ordinate defines the background susceptibility of raw unweathered loess, which fits well to the average value determined for Eurasian loess by Forster et al. (1994). In contrast to this generally accepted

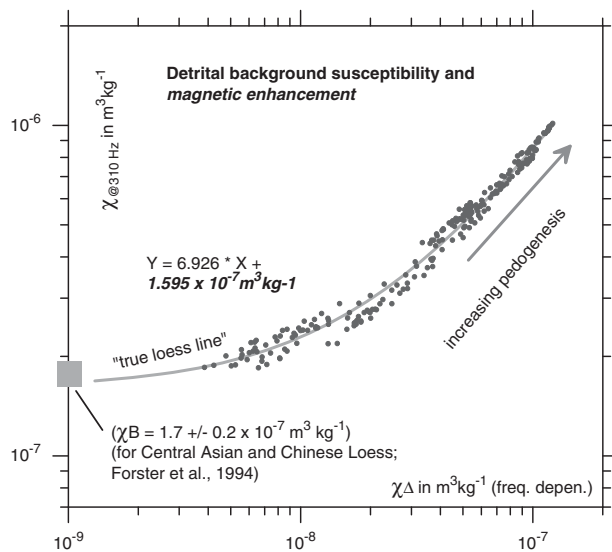


Figure 16. A scatter plot of the χ_{if} (ordinate) versus χ_{Δ} (abscissa) and the trend of the “true loess line” as suggested by Zeeden et al. (2016b) and based on Forster et al. (1994). The gray data points show the magnetic enhancement trend for the Semilac loess-paleosol sequence (recent to ≈ 400 ka; southeastern Pannonian basin, Romania; modified after Zeeden et al., 2016b) as a function of increasing pedogenesis for dry steppe loess. The interception of the “true loess line” with the ordinate defines the background susceptibility of raw, unweathered loess, which fits well to the average value determined for Eurasian loess by Forster et al. (1994).

explanation for magnetic enhancement in LPSs, lowered values of MS in paleosols in high latitude Alaskan and Siberian loess deposits have been explained by increased wind strength during glacial periods, which more efficiently transports dense iron oxide particles (wind-vigor model; e.g., Begét et al., 1990; Evans, 2001). This process, however, is generally inconsequential in controlling climate-induced variations in MS on the midlatitude Eurasian loess steppes (Bugge et al., 2014). Likewise, pervasive hydromorphy as the result of waterlogged conditions, leading to a reduction of MS by the dissolution of magnetic particles, is also not a factor in the dry Eurasian steppes, as it might be elsewhere, especially in the potentially waterlogged Arctic tundra. In summary, loss of magnetic signal in soils/paleosols, because of waterlogging, is mainly observed in loess from areas affected by periglacial conditions (Matasova et al., 2001; Baumgart et al., 2013; Taylor et al., 2014).

Mineral magnetic patterns in LPS records are fairly concordant throughout Eurasia, at least on glacial-interglacial time scales. These records show high similarities to oxygen-isotope fluctuations in deep-sea sediments, and even to the Greenland and Antarctic ice records (Lambert et al., 2008; Guo et al., 2009; Marković et al., 2015). Such well-expressed linkages are not found to the same extent for loess or loesslike deposits from other continents, and we therefore focus here on Eurasia. Moreover, on the CLP, strongly altered and dominantly eolian silt deposits date back to the Early Miocene; no equivalent has yet been found in western Eurasia and on other continents. Nevertheless, the eolian

Red-Earth sequence (also referred to as Red-Clay) in China provides an outstanding paleoclimatic archive for eastern Eurasia. It has been dated by magnetic polarity and MS stratigraphy and defines the onset of desertification in Asia as early as 22 Ma (Guo et al., 2002).

The robust correlations between the LPSs of Europe and the CLP are of major relevance for understanding the temporal and spatial variability in paleoclimate within Eurasia (Bronger, 2003; Marković et al., 2015). Several recent publications have correlated southeastern European LPSs with the CLP, although leaving some inconsistencies (Bugge et al., 2009; Basarin et al., 2014; Marković et al., 2015; Song et al., 2018). Nonetheless, the studies provide valuable reference records with correlative age control. In Figure 15A, we provide a comparison of established Quaternary paleoclimatic reference data sets, the LR04 benthic isotope stack (Lisiecki and Raymo, 2005), the Imbrie and Imbrie (1980) ice model, and a mixture of orbital parameters (Laskar et al., 2004) with the loess MS records from Europe (Basarin et al., 2014) and China (Hao et al., 2012). In both cases, MS was the primary proxy utilized for correlation. Over this long glacial-interglacial time scale, where loess units (L) and soil complexes (S) alternate in the sedimentary profiles, the MS records of LPSs from the CLP and southeastern Europe exhibit similar patterns and amplitudes (Fig. 15). However, prior to ~ 500 ka the MS record of paleosols in the CLP shows less amplitude, whereas for European LPSs, the amplitude remains similar (e.g., Heslop et al., 2000; Sun et al., 2006; Marković et al., 2015; Necula et al., 2015). Moreover, it has been suggested that the Danube basin in southeastern Europe experienced progressive continentalization throughout the Middle Pleistocene (Bugge et al., 2013). On the one hand, such subcontinental-scale climatic differentiations additionally complicate the inferred cross-continental correlation among LPSs. On the other hand, if these areas of difference can be better understood, they would allow for deeper insights into the regionally differentiated past climatic evolution of Eurasia, an issue that has only marginally been explored to date (Obrecht et al., 2016).

MS records resolving millennial-scale climatic fluctuations

Using Eurasian loess deposits to resolve millennial-scale climate variability is a compelling research topic, as such deposits had previously been considered too dry to reflect short-term variability in hydroclimate such as that associated with Greenland stadial-interstadial climate variability. Nonetheless, Yang and Ding’s (2014) data on millennial-scale climatic fluctuations, based on grain-size records across the CLP, revealed a close match to isotopic records of temperature contained in ice cores and speleothems and sea surface temperature records. For the western end of the Eurasian loess belt, Zeeden et al. (2016a) and Obrecht et al. (2017) recently provided the first multisite high-resolution MS and MS_{fd} records for the last 50 ka. Figure 15B shows the comparison of Greenland $\delta^{18}O$ data (North Greenland Ice

Core Project Members et al., 2004) and the MS_{fd} data from southeastern Romania. This work highlighted the quality and resolution of paleoenvironmental data that can be extracted from European loess via mineral magnetic methods. It is evident from these studies that grain size and MS_{fd} can sometimes provide powerful and fine-structured proxy information.

Magnetic fabric in loess

MS in loess deposits has one additional application. Directional measurements of MS on oriented samples are used for fabric analyses in LPSs. The anisotropy of magnetic susceptibility (AMS) method is an established structural indicator even in unconsolidated geologic materials (Parés, 2015). Magnetic fabric can be correctly approximated by a second-order symmetric tensor and fabric magnitude (i.e., degree of anisotropy) and fabric shape (i.e., prolate or oblate). Additionally, the orientation of principal axes of AMS ellipsoids (k_{max} , k_{int} , k_{min}) can be used for fabric characterization and quantification (Tarling and Hrouda, 1993).

AMS data have their largest applicability in estimating near-surface paleowind directions and even wind intensity (Lagroix and Banerjee, 2004; Zhu et al., 2004; Ge et al., 2014). Additionally, their temporal evolution can also be reconstructed from loess by such data (Taylor and Lagroix, 2015; Zeeden et al., 2015). The AMS technique has successfully been applied to western Eurasian (Nawrocki et al., 2006; Bradák, et al., 2018) as well as to Chinese and Siberian loess deposits (Matasova et al., 2001; Liu and Sun, 2012), further illustrating the wide application of loess magnetic properties to paleoenvironmental research.

Geochemical approaches to the study of loess

By E. Arthur Bettis III

Geochemistry of loess sediment can be a powerful tool for understanding its origins, transport pathways, and postdepositional alteration. Loess provides a broad, continental-scale sample of the earth's upper continental crust (Liu et al., 1993; Taylor et al., 1983; Gallet et al., 1998; McLennan, 2001). Importantly for loess studies, loess geochemistry varies at subcontinental scales, reflecting variations in source rock types, alteration along transport pathways, and trends in postdepositional weathering; these data may provide important insights into paleoclimate, periods of pedogenesis, and other aspects of Quaternary history. Three primary approaches, sometimes in combination, are used to investigate loess geochemistry—namely, concentrations of (1) major elements, (2) immobile trace elements (Sc-Th-La-Zr), and (3) rare earth elements (REEs). These data are determined most commonly using X-ray fluorescence (XRF) spectrometry, although inductively coupled plasma-atomic emission spectrometry has also been used. The use of portable XRF devices, both in the field and benchtop, is on the rise, but more studies of their performance

relative to traditional laboratory XRF are needed to ensure the production of comparable data sets.

Major element concentrations in loess reflect the mineral suite present in the sediment. Bivariate plots of co-occurring elements or elemental oxides' concentrations are often used to display compositional differences between loess bodies derived from different source rocks or mixtures of source rocks (Grimley, 2000; Muhs et al., 2003a, 2008b; Újvári et al., 2008). Concentrations of Al_2O_3 and Fe_2O_3 are often positively correlated because minerals common in loess, such as some smectites and chlorite, are relatively rich in Al and in Fe. Loess from different regions or source areas is often distinguishable by plots of such data, because of variations in source rock mineralogy, as illustrated by a midcontinent U.S. example (Bettis et al., 2003). In this example, loess from Indiana plots low on an Fe_2O_3/Al_2O_3 diagram (Fig. 17A) primarily because of dilution by high amounts of CaO and MgO (Fig. 17B), reflecting significant contributions of calcite and dolomite from carbonate rocks. As carbonate contributions to the loess decrease from Indiana westward into the Central Plains of Nebraska, loess data plot higher and farther to the right on the iron/aluminum diagram and display a reverse trend on the Mg/Ca diagram.

Although loess is dominated by silt-size particles, it does have a range of particle sizes, and these various size fractions can have potential mineralogical variability that a geochemical study of the “whole rock” misses. Studies by Eden et al. (1994) and Yang et al. (2006) demonstrated that mineralogy, and thus geochemistry, varies between different particle-size classes in loess, and that it is therefore important to understand both the particle-size distribution and the mineralogy of a loess body before confidently interpreting its geochemistry. Given the likely relationship between loess particle size and mineralogy, one would expect that geochemical variations within a loess body would also occur along a transport pathway from a source area. For example, Peoria Loess in western Iowa, USA, exhibits increasing Al_2O_3 and Fe_2O_3 concentrations with increasing distance from its Missouri River valley source, because sand content (a major contributor to SiO_2 concentrations) decreases as clay contents (dominantly smectite) increase downwind from this approximately linear source area (Muhs and Bettis, 2000).

Paleosols are important components of many loess sequences, and they can provide paleoenvironmental information about periods when loess accumulation was slow or stopped. Comparing abundances of soluble oxides of major elements (e.g., CaO, MgO, Na_2O , K_2O) with abundances of relatively immobile element oxides (typically TiO_2 or ZrO_2) is one way to evaluate the relative degree of weathering in sediment. Muhs et al. (2001) used this approach to demonstrate that the geochemistry of modern soils formed in loess along the Mississippi River valley varies systematically with climate. In a study of the long loess-paleosol record from the Chinese Loess Plateau at Lingtai, Yang et al. (2006) developed a chemical weathering index, $(CaO + MgO + Na_2O)/TiO_2$, to evaluate long-term trends in loess alteration and found greater mineral weathering during the previous

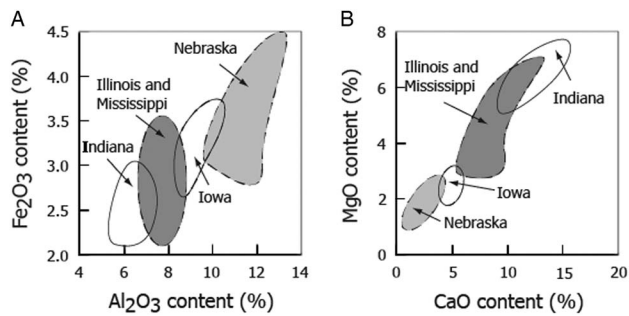


Figure 17. Contents of various major elements in last-glacial loess of midcontinent United States. Fe and Al contents generally increase east to west from Indiana to Nebraska (A), as calcite and dolomite (reflected by CaO and MgO percentages, respectively) generally decrease (B). These changes reflect decreasing contributions of carbonate rock sources to the loess from east to west. After Pye and Johnson (1988), Muhs and Bettis (2000), and Muhs et al. (2001).

five interglacial periods than during the present interglacial period. They found evidence for greater weathering of both loess and intervening paleosols prior to the mid-Pleistocene. They attributed this trend to greater prevalence of colder and drier conditions that fostered less weathering in the loess source areas since the mid-Pleistocene.

Trace element geochemistry is also an important tool for loess provenance studies (Jahn et al., 2001; Sun, 2002a, 2002b; Muhs et al. 2007, 2016; Buggle et al., 2008; Hu and Yang, 2016). Elements commonly used are those with low mobility in near-surface, low-temperature environments: Cr, Sc, Ta, Th, Zr, Hf, As, Sb, and Y; the REEs La to Lu; as well as Ti, a minor element. The Sc-Th-La suite of elements is one of the most useful, and these data are usually plotted as a ternary diagram (Taylor and McLennan, 1985). Muhs et al. (2007, 2008c) used this approach to demonstrate that silts in loess mantles on the California Channel Islands have trace element concentrations more like granitic terrain sources of the Mojave Desert (mainland California) than the trace element concentrations characteristic of the islands' andesite and basalt bedrock. Clays in these soils, on the other hand, fall between the fields of Mojave dust and those of the local bedrock, suggesting that the loess clay minerals represent a mixture of clays formed in situ, as well as clays from distant sources.

REEs also have low mobility under near-surface conditions but have an advantage over other trace elements for loess provenance studies because they occur in both heavy and light minerals. Thus, they can provide information about both proximal and distal eolian sources. REE plots typically use abundances normalized to chondritic meteorites. "Flat" REE curves normalized in this manner can distinguish little differentiated oceanic crust sources from upper continental crust sources, which exhibit enrichment of light REEs and depletion of heavy REEs. The sign and degree of the Eu "anomaly" provides additional insights into differentiating these sources (Taylor and McLennan, 1985). Sun (2002a, 2002b) used REEs and other geochemical and mineralogical data to isolate potential distal sources of

Chinese Loess Plateau sediments and concluded that likely sources for the Chinese Loess Plateau are silts deflated from alluvial fans flanking the Qilian Mountains in China and the Gobi Altay and Hangayan Mountains in Mongolia.

As these few examples indicate, geochemical approaches can provide insight into a wide range of loess topics, including source area identification and differentiation, paleoclimatic patterns, and weathering profile evolution. Multiparameter approaches and the spread of new technologies such as portable XRF will continue to advance loess geochemical studies that help us better understand loess systems and sediments.

The "spatial signatures" approach to loess research

By Randall J. Schaetzl

Loess deposits represent some of the world's best terrestrial archives of paleoenvironmental information. The loess itself is a storehouse of information for the period of deposition, and any intercalated paleosols or weathering profiles can provide data on intervening periods of nondeposition (or slowed deposition) and soil formation. Knowing this, much has been learned about past terrestrial environments by studying thick loess deposits, many of which have several intercalated paleosols and span more than one glacial-interglacial or dry-moist cycle of the Quaternary period (Heller et al., 1993; Rousseau and Kukla, 1994; Akram et al., 1998; Buggle et al., 2009, 2011; Marković et al., 2009). Put another way, thick loess sequences often provide important temporal environmental proxy data at a given location or within a given region (Muhs and Bettis, 2000). In some areas, most of the loess deposit dates mainly to the last glaciation, or at least to only one instance of recent deposition (e.g., Gild et al., 2017). Here, this type of "deep" temporal exploration is not possible, or at least less fruitful than in areas of thick loess that spans more geologic time.

All loess, regardless of thickness, can provide investigators with an opportunity to peer into the spatial variation across past landscapes. In other words, thinner loess deposits may not provide insight into multiple past environments, but by examining the same deposit spatially, information on various environmental aspects of that landscape while the loess was being deposited can be gained. Although not commonly performed, similar exploration of spatial trends is possible in thicker loess deposits that span multiple climate cycles.

Indeed, loess is one of the best deposits to examine for spatial patterns and information. Loess has long been known to become thinner and finer-textured away from the source area (Smith, 1942; Ruhe, 1954, 1973; Fehrenbacher et al., 1965; Frazee et al., 1970; Kleiss, 1973). Mineralogical changes within the same loess deposit, but across space, are also often predictable and insightful as to provenance (Muhs and Bettis, 2000; Bettis et al., 2003; Chen et al., 2007; Buggle et al., 2008). Such information is often developed by studying loess deposits across space, knowing a priori the loess source(s). By knowing which spatial trends in loess deposits

are most informative, subsequent work can then examine the spatial properties of such data, for loess with “less certain” paleoenvironmental histories. This research has done much to elucidate new loess source areas, refine our understanding of loess transport systems, and even determine the strength and directional properties of paleowinds (Stanley and Schaetzl, 2011; Luehmann et al., 2013, 2016; Schaetzl and Attig, 2013; Martignier et al., 2015; Nyland et al., 2017; Schaetzl et al., 2017; Muhs et al., 2018). In summary, much can be learned about loess deposits by studying their spatial properties.

Historically, researchers have typically examined the spatial properties of loess deposits along transects (e.g., Frazee et al., 1970; Rutledge et al., 1975; Handy, 1976; Muhs and Bettis, 2000; Martignier et al., 2015; Fig. 18). This early work helped the loess community to understand the distribution of dust from a source and the processes involved in its generation, transport, and accumulation. Recent work by Schaetzl and colleagues (Scull and Schaetzl, 2011; Stanley and Schaetzl, 2011; Luehmann et al., 2013, 2016; Schaetzl and Attig, 2013) has expanded on this approach by obtaining loess samples across spatial grids, some of which may include several hundred samples. Typically, these samples are analyzed for grain size and thickness data; future work is likely to include mineralogy and elemental geochemistry data as well. A GPS or a GPS-ready laptop computer can be used to provide geospatial data for each sample site. Samples are routinely taken with a bucket auger, being careful to obtain some sediment from the entire length of the auger (i.e., the full vertical thickness of the loess deposit must be incorporated into the sample). Finally, it is suggested that sampling loess within 10–20 cm of any underlying lithologic discontinuity be avoided, as there exists the potential for mixing and contamination (Schaetzl and Luehmann, 2013). Data obtained from the loess, which are presumed to represent loess that was deposited during a discrete time interval, allow the investigator to tease out patterns that can then be used to infer dust source areas or paleowind directions (Schaetzl et al., 2017). Simple characterization techniques such as isoline interpolation or graduate circle symbols are useful for data exploration and interpretation, although more advanced applications such as kriging and inverse distance weighting methods are also commonly applied to such data (Fig. 19).

In summary, much can be gleaned from loess data, when examined spatially. Loess is a highly “spatially organized” deposit, innately lending itself to sampling and analysis across space (landscapes). Although still in its infancy, the spatial signatures, or spatial analysis, approach to loess research discussed here has great potential for future studies of loess depositional and paleoenvironmental systems.

Biomarkers and stable isotopes in loess as paleoenvironmental indicators

By Michael Zech and Roland Zech

The last few decades have seen considerable advances in biogeochemical analytical techniques (e.g., gas chromatography,

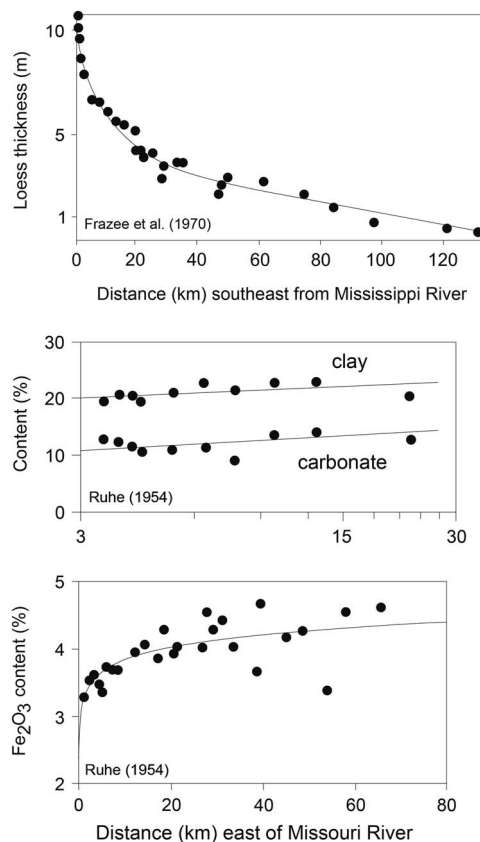


Figure 18. Examples of loess data derived from two-dimensional transects away from a known loess source. Both rivers are in the central United States. The use of scatter plots and regression equations in the analysis of such data is commonplace.

high-performance liquid chromatography, and isotope ratio mass spectrometry [IRMS]). These techniques have enabled investigators to study organic molecules, and their stable isotopic composition preserved in various sedimentary archives, as new and valuable proxies for paleoenvironmental and climate change. When those organic molecules have more or less specific sources (e.g., they are leaf wax or bacterially derived), they are called biomarkers or molecular fossils (Eganhouse, 1997; Eglinton and Eglinton, 2008). Although biomarker and stable isotope tools have been often employed by organic geochemists in the study of marine and lacustrine sediments, applications of these methods to loess research have only recently begun (Zech et al., 2011). Concerning the origin of bulk organic matter as well as of individual biomarkers in loess, neither a partial contribution by far and middle distance eolian transport nor a partial contribution by postsedimentary illuviation processes nor postsedimentary “contamination” by roots/(rhizo-) microbial input can be fully excluded. Hence, such processes need to be carefully considered and evaluated as exemplarily highlighted for leaf wax–derived *n*-alkanes at the end of the third paragraph in this section.

Amino acids of land snails embedded in loess deposits were among the first loess-associated organic molecules investigated (Oches and McCoy, 2001). The time-dependent

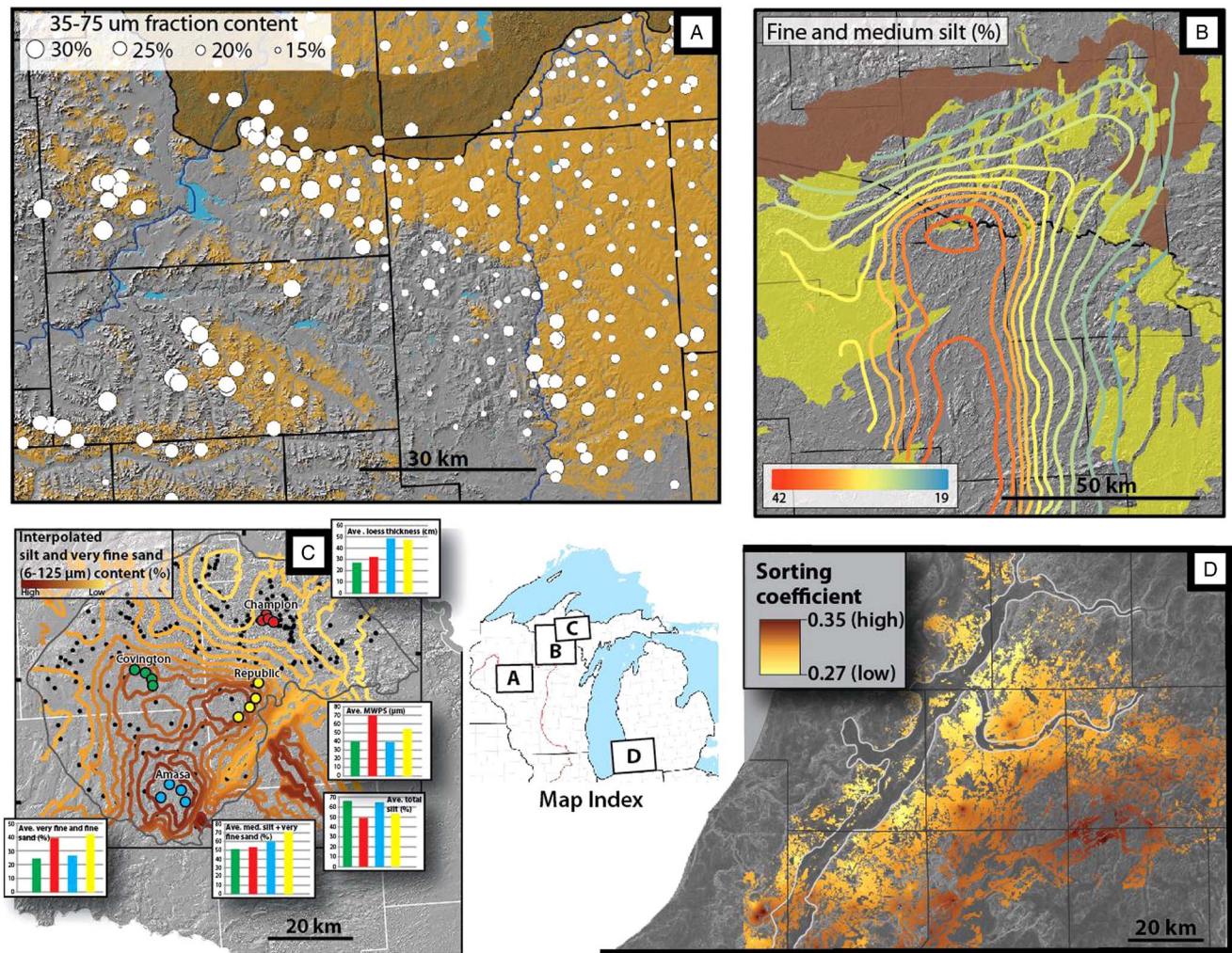


Figure 19. Examples of spatial display/analytical approaches that have been applied to loess data in the United States. (A) Graduated circle map of a loess textural attribute across the loess-covered plains of central Wisconsin. Loess is mapped here on areas shown as light brown; the dark-brown area is the Late Wisconsin (Marine Oxygen Isotope Stage 2) end moraine. Major rivers, which flow north-to-south in this area, are also shown. The size of the circles, in this case, is proportional to content of the 35–75 μm fraction in the loess (coarse silt and the finest of the very fine sand). Loess samples were obtained in areas that are not currently mapped as having loess, but the loess here contains little of this size fraction. Areas with larger amounts of the mapped size fraction are downwind (to the southeast) of topographic obstructions to loess transport: (1) bedrock uplands, (2) the end moraine, and (3) major river valleys. (B) Kriged, interpolated isoline map of the contents of fine and medium silt (6–35 μm) in the thin loess of Michigan's western Upper Peninsula and northeastern Wisconsin. Potential loess source areas are shown in yellow (outwash plains) and brown (end moraines). Isolines are only shown in areas where mapped thicknesses of loess occur. After Schaetzl and Attig (2013). (C) Kriged, interpolated isoline map of the contents of silt and very fine sand (6–125 μm) across the thin loess of Michigan's western Upper Peninsula. This map also shows sample site locations (some are covered by the isolines). The loess here varies considerably across the landscape. Luehmann et al. (2013) identified four "core" areas of loess in this region. The figure also provides compiled data, as histograms, for other kinds of loess data within the heart of each loess "core": average loess thickness, mean weighted particle size (μm), total silt (6–50 μm), medium silt through very fine sand (25–125 μm), and total very fine and fine sand (50–250 μm). (D) Interpolated, kriged map of sorting coefficients (Trask, 1932) for a thin (<1 m) loess deposit in southwestern Michigan. Across this study area, loess deposits are discontinuous, and therefore, in this display method, interpolated data are shown only in areas where soils are mapped that presumably formed in loess. That is, the figure is also a loess distribution map. The presumed loess source for this area is the glacial meltwater valley, outlined in white. After Luehmann et al. (2016). (For interpretation of the references to color in this figure legend, the reader is referred to the web version of this article.)

racemization of amino acids is used as geochronometer by quantifying the D-enantiomers that have formed from L-enantiomers. One of the recent biomarker approaches used in loess research focusses on glycerol dialkyl glycerol tetraethers (GDGTs), which are membrane lipids of soil bacteria. These markers can be used to reconstruct mean annual temperature and soil pH from loess-paleosol sequences (Jia et al.,

2013; Schreuder et al., 2016). However, one should keep in mind potential pitfalls of GDGT-based reconstructions. For three case studies of well-studied loess-paleosol sequences, Zech et al. (2012b) found major disagreements between GDGT-based temperature reconstructions, as compared with expectations based on available stratigraphic, pedological, and geochemical data. This finding is in agreement with a

climate transect study of Dirghangi et al. (2013) reporting that the GDGT method only produces reliable results in humid study areas with mean annual precipitation values >700–800 mm/yr.

During the last decade, the quantification of the leaf wax-derived long-chain *n*-alkanes nC_{27} , nC_{29} , nC_{31} , and nC_{33} from loess sediments has emerged as a potential tool for reconstructing vegetation changes. Well-preserved *n*-alkanes in the organic matter of loess deposits are mostly interpreted in terms of expanding grassland versus forest, respectively (Zhang et al., 2006; Bai et al., 2009; Zech et al., 2009). It has to be emphasized that such a differentiation based on *n*-alkane patterns does not necessarily work on a global scale (Bush and McInerney, 2013), and therefore, regional calibration studies on modern plants may be necessary, as shown by the work of Schäfer et al. (2016b) in Europe. Further issues needing consideration are variable *n*-alkane concentrations of different vegetation types, potential degradation effects, and the effects of postsedimentary root or rhizomicrobial sources. Gymnosperms yield mostly significantly lower *n*-alkane abundances compared with angiosperms (Diefendorf et al., 2011). Although this issue makes the *n*-alkane method insensitive for reconstructing conifers (Zech et al., 2012a), it might be overcome in future studies by investigating additional terpenoid and terpenoid-derived biomarkers such as retene and cadalene (Bugge and Zech, 2015), as well as *n*-alkanoic acid (Schäfer et al., 2016a, 2016b). Concerning degradation effects on *n*-alkane patterns, two possible correction procedures were suggested by Bugge et al. (2010) and Zech et al. (2009, 2013a). There is also a discussion as to whether *n*-alkane biomarkers in loess sequences are significantly affected by postdepositional root and rhizomicrobial sources (e.g., Wiesenberg and Gocke, 2013 vs. Zech et al., 2013b). This controversy stimulated compound-specific as well as bulk *n*-alkane ^{14}C dating in loess research. Accordingly, comparisons of *n*-alkane ^{14}C results with independent luminescence dating corroborate the stratigraphic integrity of the leaf wax-derived *n*-alkane biomarkers in loess deposits (Häggi et al., 2014; Haas et al., 2017; Zech et al., 2017). Moreover, ^{14}C dating of bulk leaf waxes, which is a relatively straightforward procedure, might become a valuable chronological tool in loess research.

By about 1990, the online coupling of elemental analysis with IRMS had facilitated the stable carbon ($\delta^{13}C$) and nitrogen ($\delta^{15}N$) isotope analysis of soil and sediment samples. This is achieved by converting the sample carbon and nitrogen into CO_2 and N_2 in a reactor and subsequent transfer of those gases into the IRMS using helium (He) as a carrier gas. Given that the $\delta^{13}C$ values of plants vary according to photosynthetic pathway, this tool can be applied in loess research to reconstruct C3 and C4 vegetation changes (Liu et al., 2005; Hatté et al., 2013; Zech et al., 2013d). Potentially challenging issues to be kept in mind are methodological constraints caused by biases during acid pretreatment, when removing carbonates from loess samples (Brodie et al., 2011), as well as degradation effects (Zech et al., 2007),

sedimentation of reworked and/or transported organic matter, and illuviation and root contamination. Like the $\delta^{13}C$ composition of bulk organic material, $\delta^{15}N$ in soils and sediments is also affected by degradation (Zech et al., 2011). The few studies that have applied $\delta^{15}N$ to loess deposits therefore have tentatively interpreted the results in terms of a more open versus more closed nitrogen (N) cycle (Schatz et al., 2011; Zech et al., 2013d; Obrecht et al., 2014).

The large potential for the application of stable hydrogen (δ^2H) and oxygen ($\delta^{18}O$) isotopes in paleoclimatology is based on the finding that the isotopic composition of precipitation is mainly climatically controlled (Dansgaard, 1964; Rozanski et al., 1993). Although applications of this method to ice cores, speleothems, and lacustrine archives have boosted our understanding of paleoclimate during the last decades, applications to loess were hindered because loess and the buried soils within are complex from a chemical point of view, comprising a variety of H and O pools. Even worse, some of those pools are prone to exchange reactions with percolating water. In a pioneering study, Liu and Huang (2005) applied compound-specific δ^2H analyses of leaf wax-derived *n*-alkanes to loess deposits. Follow-up studies corroborated that a robust reconstruction of the isotopic composition of paleoprecipitation (δ^2H_{prec}) is hindered by unknown isotopic enrichment of leaf water because of variable evaporative enrichment (Zech et al., 2013d). Meanwhile, it has become increasingly clear that δ^2H of *n*-alkanes in soils and sediments reflects leaf water rather than precipitation (Zech et al., 2015). The same holds true for $\delta^{18}O$ of plant-derived sugar biomarkers (Tuthorn et al., 2014). This latter new method, developed by Zech and Glaser (2009), has been successfully applied to organic-rich permafrost loess-paleosol sequences and lake sediments (Zech et al., 2013c, 2014) and awaits adaptation to organic-poor loess.

The coupling of the $\delta^2H_{n-alkane}$ with the $\delta^{18}O_{sugar}$ biomarker methods has exciting potential for paleoclimate research and, particularly, for loess research. First, this coupling has the potential to reconstruct $\delta^2H/\delta^{18}O_{prec}$ much more robustly than a method based on $\delta^2H_{n-alkane}$ or $\delta^{18}O_{sugar}$ alone (Fig. 20). This is realized by tracing back the leaf water evaporation line until it intersects with the global meteoric water line. Additionally, the coupling allows for the calculation of paleo-relative humidity, based on a leaf water enrichment model (Gat and Bowser, 1991) and the reconstructed so-called deuterium excess of leaf water. This innovative “paleohygrometer” approach was validated recently by Tuthorn et al. (2015) by applying it to modern topsoils along an Argentinean climate transect, and it was further successfully applied to a Late Quaternary paleosol sequence from Mt. Kilimanjaro (Hepp et al., 2017).

Terrestrial gastropods in loess (paleoecology, paleoclimate, geochronology)

By David A. Grimley and Jessica L. Conroy

Gastropod assemblages have been a major component of loess studies for well over a century, ever since they were

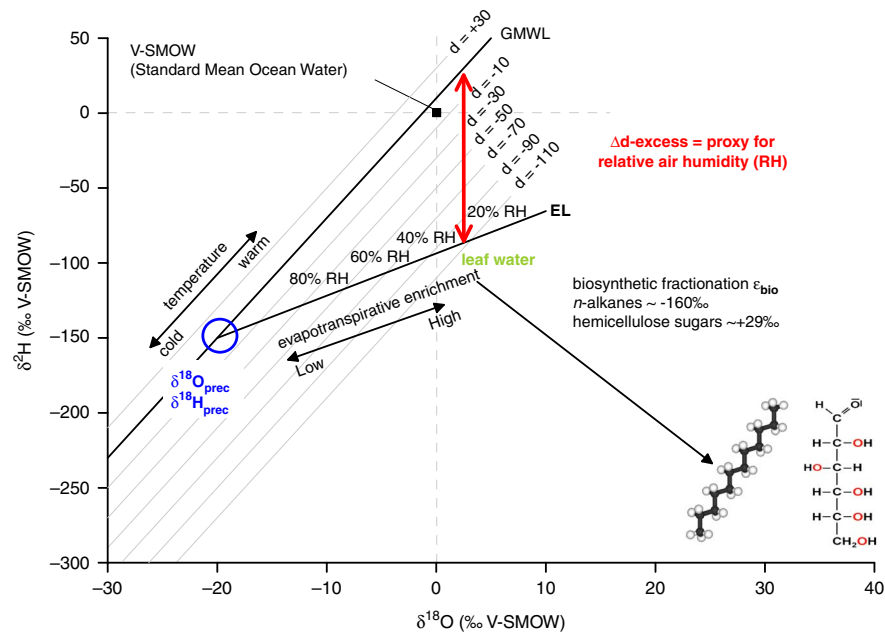


Figure 20. (color online) Conceptual diagram of the proposed “paleohygrometer” based on a coupled ^2H - ^{18}O biomarker approach (modified after Zech et al., 2013c; Tuthorn et al., 2015). Apart from enabling the reconstruction of relative atmospheric humidity (RH) by using $\delta^2\text{H}_{\text{n-alkane}}$ and $\delta^{18}\text{O}_{\text{sugar}}$ and resultant deuterium (d-) excess of leaf water, the approach additionally allows for the reconstruction of $\delta^2\text{H}/\delta^{18}\text{O}_{\text{prec}}$ much more robustly than one based on $\delta^2\text{H}_{\text{n-alkane}}$ or $\delta^{18}\text{O}_{\text{sugar}}$ alone. V-SMOW, Vienna standard mean ocean water.

used as key evidence that North American loess deposits have an eolian, rather than fluvial, origin (Shimek, 1899). More recently, the presence of land snails has aided in the eolian interpretation of Miocene-Pliocene silt deposits in China (Li et al., 2006). Biostratigraphically, mollusks have been used to differentiate and characterize loess units (Leonard and Frye, 1960; Rousseau, 2001), although only rarely have molluscan species disappeared from the Pleistocene geologic record. Rather, species have tended to shift geographically in response to climatic and habitat changes, becoming exotic rather than extinct (although many are now threatened by human impacts).

Important habitat and ecological inferences are routinely provided by fossil terrestrial gastropod assemblages worldwide. For example, their assemblages can reveal whether past landscapes were a dense or open woodland, boreal or deciduous forest, steppelike grassland, or tundra (Miller et al., 1994; Marković et al., 2007; Rech et al., 2012). Climatically, many terrestrial gastropods are sensitive to temperature and humidity, more so than aquatic gastropod species buffered by lakes or rivers, and can thus serve as important proxies for paleoclimate. Land snails are mainly dormant during periods of cold temperature, so they are best used as indicators of summer or warm-season climate in mid- to high latitudes. It was recognized decades ago that many fossil gastropod species in Pleistocene loess (Fig. 21) are distinct from local modern faunas and mostly represent cooler glacial or interstadial environments (e.g., Baker, 1931). Today, more accurate range maps of terrestrial gastropods (e.g., Nekola and Coles, 2010, for North America) can provide modern analog distributions and thus better estimates of paleoclimate (Moine et al., 2002; Nash et al., 2017). Many examples of

climatic (and ecological) interpretations from gastropod assemblages in loess-paleosol sequences are reported in Asia (Rousseau et al., 2000; Li et al., 2006), Europe (Rousseau, 1991; Marković et al., 2007), and North America (Rousseau and Kukla, 1994; Rossignol et al., 2004). Such data can fill gaps in the geologic record or can complement other terrestrial-aquatic climate records, including pollen, plant macrofossils, insects, mammals, and ostracodes (Miller et al., 1994; Karrow et al., 2001).

From a geochronological standpoint, many terrestrial gastropod genera have now been shown to be reliable for radiocarbon dating applications, based on dating of modern snails in carbonate-rich environments and comparisons with wood and plant macrofossil ages (Pigati et al., 2010, 2013). Various tests, including comparisons with independent ages and stratigraphic boundaries in loess (Pigati et al., 2013), have confirmed that many small terrestrial genera (when well cleaned of detrital grains and secondary carbonate) are statistically accurate or have <500 yr offset from small amounts of old carbon; only a few genera should be avoided (Pigati et al., 2010, 2015). For example, *Succinea*, *Catinella*, and *Discus*, three genera common to North American loess records (Fig. 21), typically provide accurate radiocarbon ages with <300 yr offset (Pigati et al., 2010, 2015). Such success is in large part because of the fact that most terrestrial gastropod genera do not readily incorporate old carbon from mineral grains into their shells, but rather obtain carbon from plants and the atmosphere.

Beyond the limit of radiocarbon dating (>50 ka), amino acid racemization studies of gastropod shells have been used successfully to provide chronologies for loess units (Clark et al., 1989; Oches and McCoy, 2001; Marković et al., 2006;

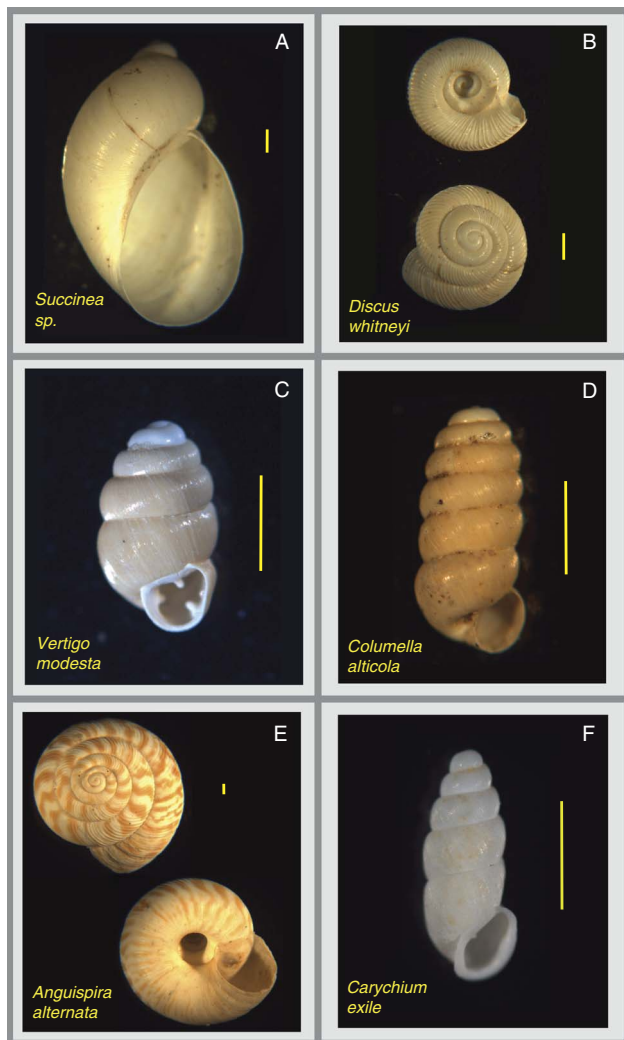


Figure 21. Examples of six species of fossil terrestrial gastropods of the more than 25 genera and 50 species found in last-glacial loess (Peoria Silt) of the central United States. (A) *Succinea* sp. from Scott County, Illinois (Leonard and Frye, 1960; ABL#7). (B) *Discus whitneyi* from Rocks Section, Union County, Kentucky. (C) *Vertigo modesta* from Demazenod Section, St. Clair County, Illinois. (D) *Columella alticola* from Rocks Section, Union County, Kentucky. (E) *Anguispira alternata* from Burdick Branch Section, Madison County, Illinois (Leonard and Frye, 1960; ABL#2). (F) *Carychium exile* from New Cottonwood School Section, Cass County, Illinois (Nash et al., 2017). The yellow scale bar is 1 mm in all images. Shells of the genera *Succinea* (panel A) and *Discus* (panel B) are among the best for radiocarbon dating. The shells pictured in panels C and D, where found, are representative of much cooler boreal environments to perhaps borderline tundra conditions (Nekola and Coles, 2010). Species in panel E and F have relatively broad distributions today in forested landscapes of the eastern United States and southern Canada. (For interpretation of the references to color in this figure legend, the reader is referred to the web version of this article.)

Grimley and Oches, 2015). Early, middle, and late Pleistocene loess units, where fossiliferous, can thus be reliably separated, which can be particularly important in regions lacking datable volcanic ashes or beds. Although amino acid

age estimates have only ~20% to 30% precision and include temperature history assumptions, the current use of multiple amino acids (e.g., glutamic acid, aspartic acid) that racemize at different rates is providing more reliable age and uncertainty estimates (Kaufman and Manley, 1998; Kosnik et al., 2008). More studies will help to further expand molluscan amino chronologies for use in correlating Pleistocene units.

In addition to their utility as chronometers and indicators of past environments, expressed via community composition, gastropod shell aragonite holds additional paleoenvironmental information in stable isotope ratios of carbon and oxygen (henceforth expressed in standard delta notation, $\delta^{13}\text{C}$ and $\delta^{18}\text{O}$). Since the pioneering work of Yapp (1979), gastropod $\delta^{13}\text{C}$ and $\delta^{18}\text{O}$ data have been investigated in loess deposits across diverse paleoenvironments (e.g., Kehrwald et al., 2010; Yanes et al., 2012; Colonese et al., 2013; Yanes, 2015; Banak et al., 2016; Nash et al., 2017). Ideally, shell $\delta^{13}\text{C}$ values can be interpreted in the context of changes in gastropod diet between C3 and C4 plants, which may reflect changes in local vegetation (Stott, 2002). However, gastropod shell $\delta^{13}\text{C}$ values are also influenced by plant water stress, ingested inorganic carbonate (e.g., limestone), exchange with atmospheric CO_2 , and varying metabolic rates, all of which can complicate interpretations (Zhang et al., 2014; Yanes, 2015). Shell $\delta^{18}\text{O}$ values are controlled by temperature and body water $\delta^{18}\text{O}$, which in turn is a function of the $\delta^{18}\text{O}$ value of precipitation and atmospheric water vapor, as well as the degree of evaporation, which is strongly influenced by relative humidity (Balakrishnan and Yapp, 2004). Despite the seeming complexity of shell $\delta^{18}\text{O}$, at large spatial scales shell $\delta^{18}\text{O}$ values largely reflect the $\delta^{18}\text{O}$ value of warm season precipitation (Yanes, 2015). For example, Kehrwald et al. (2010) showed the power of gastropod $\delta^{18}\text{O}$ values across large spatial gradients to indicate past atmospheric circulation patterns. Additionally, the availability of a straightforward proxy system model for gastropod $\delta^{18}\text{O}$ (Balakrishnan and Yapp, 2004), developed long before the growing popularity and use of such models in other paleoclimate archives (Evans et al., 2013), can aid in the interpretation of the climate signal stored in gastropod $\delta^{18}\text{O}$. Future applications of gastropod stable isotope values for paleoclimate reconstruction will be aided by incorporation of this model, as well as comparison with general circulation model simulations of past climate (e.g., Eagle et al., 2013; Nash et al., 2017). Finally, studies using clumped stable isotopes (C, O) in gastropod shell carbonate as paleothermometers are also ongoing (Eagle et al., 2013) and provide a promising avenue of future research.

In sum, terrestrial gastropods are a multipurpose tool of tremendous value to stratigraphic, ecological, chronological, and climatic studies of Pleistocene loess sequences (and even where resedimented into adjacent lacustrine-wetland records). In the future, high-resolution gastropod studies and chronologies of glacial and nonglacial loess should help to reveal additional detailed records of millennial to centennial variations in sedimentation rates, ecology, and climate. Such research may help decipher the relationships among finer-scale glacial

fluctuations, global and regional climate variability, loess sedimentation systems, and incipient paleosol development.

Identifying abrupt climate changes in loess-paleosol sequences

By Denis-Didier Rousseau

Understanding the impacts of atmospheric mineral aerosols (dust) on climate dynamics during past glacial periods is a major challenge in modeling the glacial climate (Mahowald et al., 2006). Dust content in Greenland ice cores consistently suggests that atmospheric dynamics were highly variable during the last climate cycle (LCC; last 130 ka), with extremely dusty intervals alternating with nondusty intervals on millennial and shorter time scales. The dust transported to Greenland may have originated from northern Chinese deserts, suggesting that climate variations in these sources reinforced or reduced dust emissions. Do other Northern Hemisphere paleodust deposits, exposed to the strengthened general atmospheric circulation, also record these abrupt climate changes?

Extensive investigations of European loess along a longitudinal transect at 50°N reveal that the millennial-scale climate variations observed in the North Atlantic marine and Greenland ice-core records are well preserved in loess sequences (Rousseau et al., 2007, 2011, 2017a, 2017b). Among them, the Nussloch site, on the right bank of the Rhine valley, yields an important record of the LCC (Antoine et al., 2001, 2009). At this site, the sequence for the interval 45 to 18 ka is exceptionally detailed and supported by an intensive dating effort combining accelerator mass spectrometry ^{14}C and luminescence methods (Hatté et al., 1999; Lang et al., 2003; Rousseau et al., 2007; Tissoux et al., 2010; Moine et al., 2017). Alternating paleosols and paleodust units (loess) preserved in the LCC record at Nussloch correspond one to one with Greenland interstadial (GI, paleosol) and stadial (GS, paleodust) events identified in the Greenland ice cores (Fig. 22) (Dansgaard et al., 1993; Johnsen et al., 2001; Moine et al., 2008, 2017; Rousseau et al., 2002, 2007, 2017a, 2017b; Antoine et al., 2009). The morphology of each paleosol observed at Nussloch can be related to the duration of the corresponding GIs (Rousseau et al., 2007, 2017a, 2017b). GI 8, for example, the longest interstadial event during the 40–15 ka period, corresponds in the Nussloch stratigraphy to a well-developed Arctic brown soil, whereas the much shorter GI 3 and 2, among others, correspond to tundra gley soils of variable thickness, or to weakly oxidized horizons marked, in part, by slightly increased organic contents (Rousseau et al., 2002, 2007, 2017a, 2017b; Antoine et al., 2009). Rock magnetic investigations (Taylor et al., 2014) of the sediment above the Arctic brown soil at Nussloch revealed bands of iron oxide dissolution associated with the formation of tundra gley soils. Iron oxide dissolution and the possible iron reprecipitation leading to oxidized horizons represent a diagenetic alteration occurring at the base of the active layer (i.e., at the interface with permafrost)

during seasonal warm and moist intervals. This observation supported the correlation between the paleosols and the GIs of variable duration, correlations that have been confirmed by recent ^{14}C dates obtained on earthworm calcite granules collected in the paleosols (Moine et al., 2017).

Uncertainties concerning the duration of soil forming intervals pose important chronological challenges, especially for interglacial soils in which the upper profile is often eroded. Nevertheless, the Arctic brown and tundra gley paleosols do not show evidence of erosion at the outcrops. Furthermore, biological remains such as mollusk shells (Moine et al., 2008) and earthworm calcite granules (Prud'homme, 2016, 2017), encountered in the upper 10 cm of these paleosols, support the interpretation of lack of erosion. This issue is essential to address so that an accurate time scale (Moine et al., 2017) can be used for model-data comparisons. Rousseau et al. (2017a) further showed the importance of an accurate chronology for correctly estimating the mass accumulation rate of the sequences for comparison with model estimates, because without a detailed chronology and taking into account periods of soil formation, the temporal structure of dust accumulation intervals cannot be determined.

The succession of paleosol-loess unit couplets at Nussloch is not unique but has been observed with local and regional variations in sequences ranging from western Europe eastward to Ukraine (Antoine et al., 2009, 2013; Rousseau et al., 2011, 2017a, 2017b). These paleosol-loess alternations are characteristic of the Eurasian loess sequences deposited at about 50°N and higher (north of the Alps and the Carpathians); such sequences seem to also exist in Siberia as described by Chlachula (2003) and Haesaerts et al. (2005) and at lower latitudes in North America (Rousseau et al., 2007) south of the last-glacial border. Tundra gleys and other indications of permafrost do not occur in southern European loess sections but GI–GS forcings may be evident in grain-size or $\delta^{13}\text{C}$ records in Serbia (Antoine et al., 2009a; Hatté et al., 2013; Marković et al., 2015) and in the Carpathian region (Ujvari et al., 2010; Varga, 2011). A pattern similar to the southern European sequences, but without any paleosol identified in the LCC, has been identified in grain-size variations in the Chinese Loess Plateau (Vandenberghe et al., 1997; Vandenberghe, 2003, 2013; Stevens et al., 2006; Sun et al., 2012). In these sequences, GS corresponds to coarser loess intervals, whereas finer-grained intervals correspond to GI. Similar patterns were also observed in cores from the Japan Sea and related to variations in the position of the polar jet stream as it affected eastward transport of dust particles from East Asian deserts (Nagashima et al., 2007, 2011). It is interesting to note that, based on loess data, not only the last glacial period, but also most of Marine Oxygen Isotope Stage 5 (120–71 ka) experienced several dust episodes at the European scale (Rousseau et al., 2013), which are also correlated with abrupt events recorded in the Greenland ice cores.

Modeling results point to vegetation changes in response to millennial-scale climate variability as a key factor in modulating dust emission (and, consequently, also

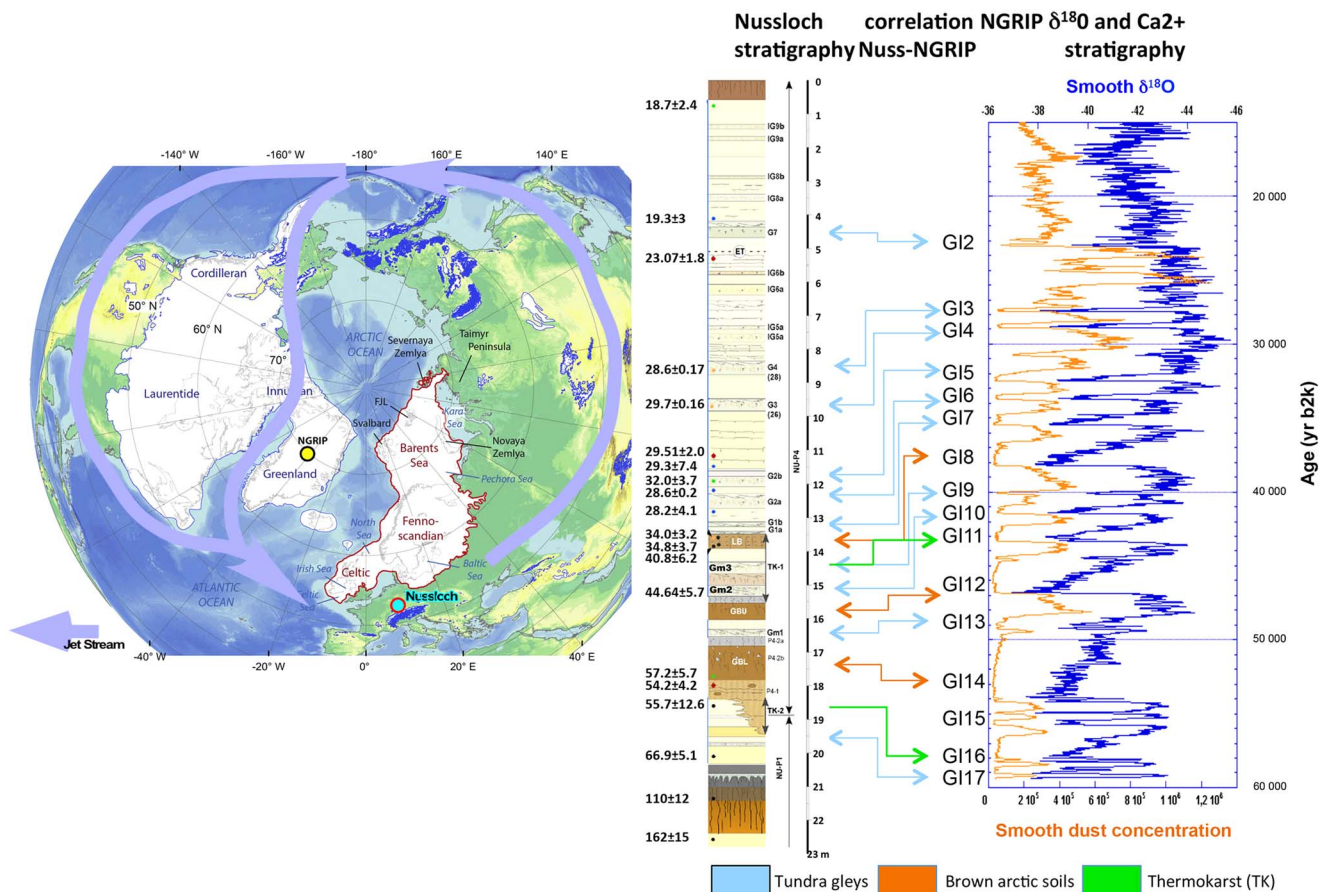


Figure 22. Stratigraphic correlations between Nussloch paleosols and NGRIP interstadial events (GIs) (modified from Rousseau et al., 2017a, 2017b). Map of Northern Hemisphere during the last glacial maximum (Patton et al., 2016) showing the location of the main ice sheets, the reconstructed jet stream tracks (Kutzbach, 1987), and the reference sequence of Nussloch. $\delta^{18}\text{O}$ (‰, in blue) and the dust concentration (part/ μL , in brown) records in the NGRIP ice core over the interval between 60 ka and 15 ka. Nussloch stratigraphic column modified from Antoine et al. (2016). (For interpretation of the references to color in this figure legend, the reader is referred to the web version of this article.)

deposition). Model results also point to strong seasonality in the annual dust cycle, mainly active in springtime, when the snow cover melts, soils begin to thaw, surface winds are still strong (although weaker than in winter), and the surface is exposed to wind erosion because of patchy vegetation cover. The colder the climate, the later the emission season starts, and the later it ends (about one month delay for a given region between the warmest and the coldest simulated climate state, GI vs. Heinrich stadial events) (Sima et al., 2009, 2013; Rousseau et al., 2014)

Understanding how the climate system has operated at both regional and global scales during abrupt climatic changes, and at millennial time scales, is a key issue in the last Intergovernmental Panel on Climate Change report (Masson-Delmotte et al., 2013). Much emphasis has been given to numerous other classical factors such as greenhouse gases and orbital parameters. Paleodust data, however, have been almost neglected because of the strong uncertainties associated with the loess paleorecord, uncertainties about its origin and transport, and the lack of reliable intercomparisons between models and paleodata. Future investigations should attempt to fill this gap.

“Thin” loess deposits

By Randall J. Schaetzl

Most of the world’s best-known loess deposits occur in exposures commonly exceeding meters in thickness, thereby providing ready access to the sediment and any intercalated paleosols (Roberts et al., 2003; Basarin et al., 2009; Marković et al., 2009; Obrecht et al., 2015). Such deposits are today readily recognized as loess and have proved to be valuable, land-based paleoenvironmental archives (Ding et al., 1993, 1999; Lu and An, 1998; Miao et al., 2007; Buggle et al., 2009; Yang and Ding, 2014; Marković et al., 2015). Less studied but perhaps more widespread are thinner and/or discontinuous loess deposits. For the purposes of this section, thin loess deposits are defined as those <2 m in total thickness (Fig. 23A).

Thin loess deposits are part of a continuum from thicker loess deposits to deposits so thin and intermixed with the underlying sediment as to be initially unrecognizable (Yaalon and Ganor, 1973; Muhs, 2013a; Luehmann et al., 2016). Therefore, in the past, many such thin loess deposits went unrecognized or misinterpreted. Although much research

on thin loess deposits has been focused in the east-central United States (Rutledge et al., 1975; Carey et al., 1976; Foss et al., 1978; Schaetzl and Loope, 2008; Stanley and Schaetzl, 2011; Jacobs et al., 2012; Luehmann et al., 2013, 2016; Schaetzl and Attig, 2013), thin loess deposits occur worldwide (e.g., Litaor, 1987; Hesse and McTainsh, 2003; Muhs and Benedict, 2006; Greene et al., 2009; Lehmkuhl et al., 2014; Gild et al., 2017; Waroszewski et al., 2017).

Most commonly, thin loess deposits represent the end member of a loess sheet/deposit that is much thicker nearer to its primary source area. The thinning patterns of many loess sheets are well known and can be predicted using statistical models (Fehrenbacher et al., 1965; Frazee et al., 1970; Kleiss, 1973; Ruhe, 1973). By recognizing thin loess deposits as the distal “end members” of thicker loess deposits, the thinning and fining trends of loess may be more accurately described and analyzed. Some thin loess deposits, on the other hand, represent locally sourced sediment that has no association with a “thick end member” (Schaetzl, 2008; Luehmann et al., 2013). Source regions for such loess deposits may have been short lived, small in areal extent, or simply low overall dust producers.

For many, the identification of thin loess deposits has proved to be problematic. Normally, the silty textures and pale colors help to identify loess, where present in thick deposits. However, thinner loess is often intermixed with the underlying sediment, sometimes making a clear assessment based on texture ambiguous (Schaetzl and Weisenborn, 2004; Schaetzl, 2008; Nyland et al., 2017). Methods used to identify loess in thin deposits include (1) changes in texture, often from fine-grained, usually silty, textures in the loess to different textures below (these changes are easiest to interpret where the lithologic contact and texture changes are sharp, and especially where the underlying sediment contains coarse fragments); (2) the presence of quartz or illite (mica) in soils/sediments that have otherwise formed on quartz- and

mica-free rocks such as basalt (e.g., Rex et al., 1969); (3) different values of quartz oxygen isotope ratios or Ti/Zr ratios between the loess and the underlying substrate; and (4) distinct and regular changes in loess particle size across the landscape (Hesse and McTainsh, 2003; Muhs, 2013a). Usually, for methods 1–3, data are plotted as depth functions in order to note changes in one or more of these properties with depth (Allan and Hole, 1968; Carey et al., 1976).

Although most loess deposits are originally silt dominated, various postdepositional processes have, in some locations, modified their textural character. For this reason, they have often been misinterpreted, or simply not recognized as loess, thereby requiring inventive methods for their discernment (e.g., Scheib et al., 2013). Examples from soils in Michigan, USA, illustrate this phenomenon. Here, thin loess commonly overlies sandy sediment. Postdepositional pedoturbation (mixing) has modified the original loess textures—that is, sand from below has been mixed into the loess, resulting in coarse-loamy textures (Schaetzl and Hook, 2008; Schaetzl and Luehmann, 2013). Alternatively, sandy sediments in the lower part of the loess deposit may have been locally sourced (i.e., deposited via saltation); this process may have occurred synchronously with early stages of loess deposition, when much of the landscape was not yet loess covered or fully vegetated. Either scenario can result in loess deposits that are sandier than is typical, especially at depth (Schaetzl and Luehmann, 2013; Luehmann et al., 2016; Fig. 23A), hindering their recognition in the field. Such “compromised” loess often has distinctly bimodal particle-size curves (Fig. 23B). Ongoing research has shown that, in many areas, soils not known for having loess parent materials actually do have silty surface horizons, or if they have coarse-textured lower profiles, then the upper profile is loamy. Many of these soils have been impacted by thin loess contributions, but until recently, this type of depositional history was not recognized (Munroe et al., 2015).

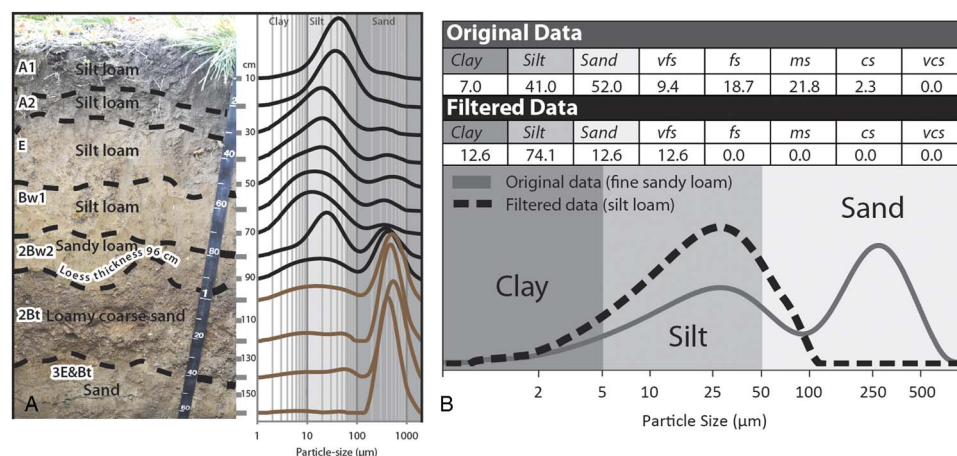


Figure 23. (color online) Textural data for two different thin loess deposits in Michigan, USA. (A) A profile image, with corresponding texture data, for a soil formed in ≈ 96 cm of loess over glacial outwash. Texture curves indicate the varying amounts of mixing of the two sediments, both above and below the lithologic contact. Tape increments in centimeters. After Luehmann et al. (2016). (B) Example of texture data for a thin loess deposit in northern Michigan. Note the distinct bimodality in the raw data, but not in the filtered data. After Luehmann et al. (2013).

Because many thin loess deposits have been texturally altered by postdepositional mixing or by additions of other (coarser) eolian sediment during the loess deposition period (Schaetzl and Luehmann, 2013), using texture data from thin loess deposits to examine possible source areas or paleowind-flow patterns can be problematic. For this reason, Luehmann et al. (2013) developed a textural “filtering” operation that works in most spreadsheet software packages. The filtering method removes the sand data from bimodal particle-size texture curve and recalculates the remaining particle-size data to better reflect the character of the original loess (Fig. 23B). The filtering method has been successfully used in studies of thin loess in midcontinent United States (Schaetzl and Attig, 2013; Luehmann et al., 2016; Nyland et al., 2017) and awaits further application and refinement elsewhere.

Most thick loess deposits are the focus of scientists who study paleoenvironments, eolian systems, or stratigraphy. Alternatively, thin loess deposits commonly fall within the realm of soil specialists, many of whom also have an interest in eolian systems. The intellectual draw of thin loess deposits to the soil science community is to be expected: soil development is dramatically affected by even small additions of loess (Simonson, 1995). Small additions of loess to a preexisting soil often have notable impacts on the soil’s texture, hydrology, erodibility, and fertility. Soils formed in thin loess deposits are affected not only by the combination of the two sediment types, but also by the hydrologic impacts of the lithologic contact itself, across which soil permeability values change markedly. Loess is commonly finer than the underlying sediment, which causes wetting fronts to “hang” at the contact zone for some time, leading potentially to increased duration times for saturated conditions, and heightened weathering. This effect can also preferentially cause deposition of illuvial substances at the lithologic contact (Schaetzl, 1998) and can reduce the rate at which weathering by-products in the overlying loess are removed from the soil. Thus, some soils formed in thin loess develop heightened concentrations of soluble substances in the overlying loess (Wilding et al., 1963; Indorante, 1998). If the loess overlies a paleosol, these impacts may be even more dramatic.

In sum, thin loess deposits, much more widespread and important than previously thought, are gaining attention worldwide by pedologists, geologists, and eolian scientists. They have great potential to inform the scientific community about paleowind patterns, and knowledge of thin loess additions in soils can help explain many pedogenic characteristics.

From cover sand to loess systems: a continuous spectrum

By Jef Vandenberghe

Periglacial eolian sands

Sedimentary facies, origin, and transport processes: Eolian sands form in periglacial environments with different facies and morphology, from in situ to reworked deposits and

composing sheet or dune forms. They extend over a vast belt in North Europe from northern France to northern Russia (Koster, 1988; Kasse, 1997, 2002; Vandenberghe and Kasse, 2008), but patchy deposits are also reported in England (Catt, 1977; Bateman, 1998), North America (Lea, 1990; Lea and Waythomas, 1990), and southwestern France (Sitzia et al., 2015; Bertran et al., 2016). Their periglacial origin has been evidenced since the pioneering work of Edelman and Crommelin (1939) and Van der Hammen et al. (1967). Because of their variegated nature, this section discusses the different kinds of cover sand deposits, focusing on their facies, depositional systems, environmental conditions, and chronological evolution, and especially their relations with loess deposits. Because of this diversity, periglacial eolian sands have to be categorized. The discussion that follows examines the different categories.

Typical “(primary) cover sands” (Fig. 24A) are characterized by a specific, very finely horizontal-parallel laminated structure. These sands were deposited as a “cover” bed, preserving the preexisting topography, hence their name. As demonstrated by mineralogical analyses, they have been homogenized by saltation over distances on the order of tens of kilometers (Vandenberghe and Krook, 1981, 1985). As a result, their grain size is surprisingly constant (around 150 μm modal size) over wide surfaces, independent of the underlying substrate.

“Reworked (secondary) cover sands” (Fig. 24B) originate from primary cover sand by postdepositional runoff or/and fluvial processes. This reworking has resulted in sedimentary structures typical of flowing water (e.g., channel and ripple cross lamination, thin concave-upward lenses of coarse-grained sand), sheetwash (e.g., parallel strata), and even shallow pools of standing water (e.g., clay or silt drapes, humic beds) (Ruegg, 1983; Koster, 1988). However, because this transport is limited to relatively short distances (tens or hundreds of meters), the deposits have largely maintained the mineralogical and granulometric composition of the source cover sand. This mixed genesis, also described for present-day periglacial environments (Good and Bryant, 1985), is at the origin of their respective designation as “fluvio-eolian” or even “lacustro-eolian” sediments (Vandenberghe and Van Huissteden, 1988; Van Huissteden et al., 2000), analogous to similar loess deposits (Vandenberghe, 2013; Vandenberghe et al., 2018).

“Periglacial dune sands” (Fig. 24C) are characterized by their well-expressed dune morphology, some up to a few tens of meters in relief. Their sedimentary structure consists of (low- to high-angle) cross bedding, (sub)horizontal lamination, and occasionally homogeneous beds. Transport was by saltation or in low-suspension clouds (De Ploey, 1977) over short distances (tens or hundreds of meters). In contrast to the cover sands, these sands have a variable granulometric and mineralogical composition because of their local provenance.

Evolution, age, and environmental conditions of European periglacial eolian sands: In contrast to loess, periglacial

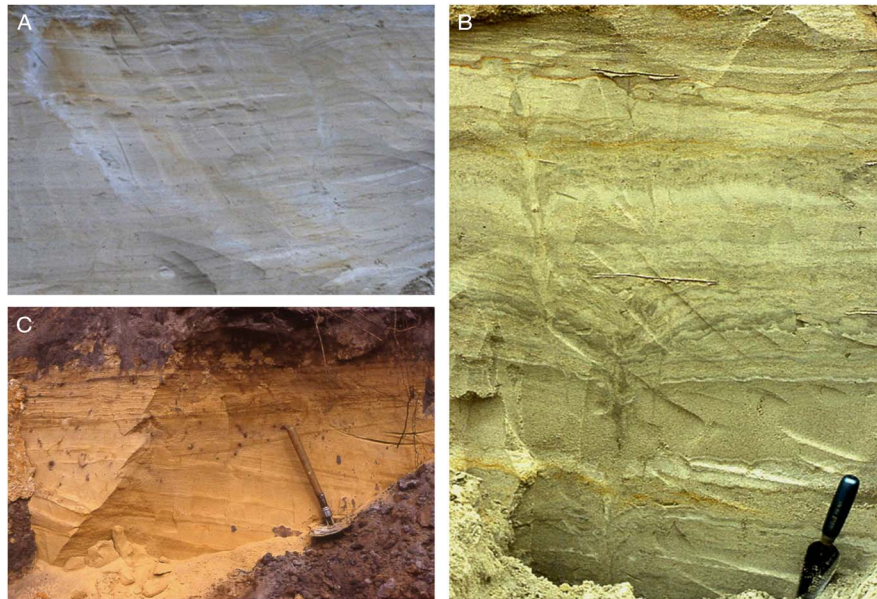


Figure 24. (color online) (A) Characteristic horizontal parallel laminated cover sand in the type region of Lutterzand (eastern Netherlands); vertical extent of image is 100 cm. (B) Fluvio-eolian sands consisting of alternating beds of medium-coarse sands, fine sands, and silty fine sands interrupted by phases of nondeposition during which frost cracks could form (e.g., indicated by arrows; eastern Netherlands). Length of trowel is 15 cm. (C) Typical cross-laminated and high-angle bedded sand in a dune of Younger Dryas age (Bosscherheide, Netherlands); activation surfaces are indicated by arrows. Length of spade is 50 cm.

eolian sands mostly date to the last full glacial period in Europe (Weichselian pleniglacial period, ca. 62–14.7 ka, ~Marine Oxygen Isotope Stages [MISs] 4–2). Nonetheless, there do exist some rare, Early Pleistocene cover sand deposits (Kasse, 1993).

During the Weichselian Early and Middle Pleniglacial (ca. 62–30 ka, ~MISs 3–4), reworked eolian sands were dominant (Van Huissteden, 1990). This system is consistent with the generally humid conditions during that period, which favored reworking by water on top of a mostly frozen substrate (Böse, 1991; Kasse, 1999). The reworking also involved mixing with loess. This system of deposition persisted until ca. 17 ka, although the silt component gradually decreased over time. Sometimes the primary eolian sands were interbedded with water-laid sediments during dry climatic phases or/and in dry topographic positions (Vandenberghe, 1985; Gozdzik, 1991). Similar processes of dominant reworking, occasionally interrupted by pure eolian activity, before 17 ka have also been documented in adjacent loess regions (Mücher and Vreeken, 1981; Huijzer, 1993; Meszner et al., 2014; Lehmkuhl et al., 2016).

At the end of the last glacial period (after 17 ka), postdating the last permafrost maximum, the “typical” (primary) cover sands were deposited across the entire North European cover sand belt (Ruegg, 1983; Vandenberghe, 1985, 1991; Schwan, 1988; Kasse, 2002; Kasse et al. 2007). This period of pure eolian activity was fostered by increased aridity with reduced vegetation cover, attributed to (apart from drier climatic conditions) the disappearance of permafrost that allowed for increased infiltration (Kasse, 1997). This important eolian phase started with widespread deflation, resulting in the formation of a characteristic desert pavement (“Beuningen Gravel Bed”; Van der Hammen et al., 1967). This prominent

(litho-)stratigraphic marker horizon occurs from northern France to northeastern Europe (e.g., Zagwijn and Paepe, 1968; Lautridou and Sommé, 1981). It was dated by luminescence techniques from the type sections in the eastern Netherlands at 17–15 ka (Bateman and Van Huissteden, 1999; Vandenberghe et al., 2013), confirmed both in the Netherlands (Kasse et al., 2007) and Belgium (Buylaert et al., 2009).

Finally, during the late glacial period (14.7–11.9 ka) dune formation was most prominent, although cover sand deposition may have locally continued (Kasse, 1999). Especially during the Older and Younger Dryas, dunes expanded considerably in north-central Europe (e.g., Nowaczyk, 1986; Bohncke et al., 1995; Zeeberg, 1998), and during the very dry end of the Younger Dryas (10.5–10.1 ka) in North Europe (e.g., Vandenberghe, 1983; Bohncke et al., 1993). Dunes formed especially along valley margins where sand supplied from (braided) floodplains was captured by the vegetation on the adjacent higher dry areas (Vandenberghe, 1983, 1991). In poorly vegetated areas, dune formation continued into the early Holocene (Kozarski, 1990; Schwan, 1991; Manikowska, 1994).

The transitional zone between loess and cover sand

Macroscopically, there is often a sharp spatial boundary between areas of late pleniglacial cover sands and loess areas. However, loess adjacent to the cover sand belt shows distinct transitional properties (e.g., in average grain-size distribution). One example occurs in central Flanders (called the “sandloess belt” by Paepe and Sommé, 1970), at the northern fringe of the Central Loess Plateau (e.g., Liu, 1985; Nugteren and Vandenberghe, 2004), and in southwestern France (Bertran

et al., 2011). Texturally, the transitional sandloess here is distinctly bimodal, with a fine cover sand grain size ($\sim 150 \mu\text{m}$) and a typical silt-loess mode ($\sim 40 \mu\text{m}$). This double composition reflects transport both by saltation and in suspension. Possible source regions of both cover sand and loess (possibly the vast Nordic proglacial areas, floodplains, or large river deltas) and wind directions (varying from north to southwest) are still under discussion (e.g., Lautridou et al., 1984; Schwan, 1988; Renssen et al., 2007; Schatz et al., 2015). The spatial distribution of the sandloess facies illustrates the downwind transition from cover sand to sandloess to loess, roughly north-northwest to south-southeast both in western Europe (Renssen et al., 2007) and in northern China (Nugteren and Vandenberghe, 2004). Further, it appears that in the southern Netherlands and Flanders this sandloess occurred more to the north (in proximal position) before the Beuningen desert pavement formed than after (i.e., the cover sand belt advanced distally after that episode; Vandenberghe and Krook, 1985).

The periglacial loess depositional system

Generally, three modes of primary loess deposition, each with specific grain-size distributions, may be distinguished (Bagnold, 1941; Pye, 1995; Vandenberghe, 2013). Fine sandy deposits are principally transported by saltation (type 1a in Vandenberghe, 2013), whereas two finer-grained populations are transported in suspension (types 1b–c).

Loess type 1b (mainly medium-to-coarse silt [25 to $65 \mu\text{m}$]) is transported in short-term, near-surface to low-suspension clouds (Tsoar and Pye, 1987) probably during cyclonal dust storm outbreaks and especially under cold conditions (Prins et al., 2007). Grain sizes of 35 – $40 \mu\text{m}$ are common worldwide in primary loess (e.g., in central and eastern Europe: Bokhorst et al., 2011; Novothny et al., 2011; Vandenberghe et al., 2014b; in China: Prins et al., 2007; Vriend et al., 2011; Ijmker et al., 2012; Dietze et al., 2013; Nottebaum et al., 2015; in North America: Muhs and Bettis, 2003). However, this grain size may vary slightly according to differing wind energy, and thus transport capacity, which can be influenced by the local topography and surface conditions, including vegetation cover (Schaetzl and Attig, 2013; Vandenberghe, 2013). The sandloess type from the transitional zone (see previous discussion) may be considered as a mixture of loess types 1a and 1b.

Loess type 1c is a fine (clayey) silt with modal diameters between 4 and $22 \mu\text{m}$. It has been interpreted as background dust transported in high-suspension clouds over long distances (Zhang et al., 1999; Prins et al., 2007; Vriend et al., 2011) and incorporated in the high-level westerlies (Pye and Zhou, 1989; Pye, 1995; Sun et al., 2002); compare the “small dust” (Stuut et al., 2009) and the very fine dust transported from central Asia. This dust type is deposited mostly in combination with the coarser-grained silt fraction 1b. It is deposited continuously over time, but it is best expressed in relatively warm conditions when cyclonic dust storms are relatively weak (Vandenberghe et al., 2006; Prins et al., 2007; Vriend et al., 2011).

Loess and past cultures

By Piotr Owczarek and Ian Smalley

Changes to farming and stock keeping, along with other measures of development of past cultures, were crucial to the growth and rapid expansion of human groups (Dani and Masson, 1992; Simmons, 2011). The agrarian Neolithic societies in Europe and the rich ancient proto-urban and urban civilization in Asia developed under favorable environmental conditions created by access to water and fertile loess soils. The appearance of early man in China and the development of the Chinese culture have long been associated with loess (Andersson, 1934; Clark and Pigott, 1965; Watson, 1966). The traditional view, as expressed by these scholars, indicates that the distribution of loess corresponds approximately to the areas assigned to the Neolithic tradition of the north, in particular the painted pottery of the Yang-shao people. Ho (1976) demarcated loess regions as the “Cradle of the East” and has clearly demonstrated the links between loess and the Chinese Neolithic. This loess-based Chinese society is the only one of the great ancient civilizations to have survived to the present day. Roxby (1938) was perhaps the first to link the societal development specifically to loess, and his ideas were developed by Smalley (1968). Smalley postulated unreasonable amounts of glaciation as a precursor to loess deposit formation, but recent studies have shown that loess material originated in High Asia and its deposition was much influenced by the Yellow River (Stevens et al., 2013a). The formation mechanisms for the Chinese loess and the links to early societies now seem to be firmly established.

Central Asia, regarded by many authors as one of the classic loess provinces (Dodonov, 2007), includes different loess deposits extending from the marginal zones of Taklamakan desert, valleys and piedmont of the Pamir-Alay and Tian Shan mountains, to the southeastern coast of the Caspian Sea (Dodonov, 1991; Dodonov and Zhou, 2008) (Fig. 25). These areas played a key role in the development of the first agricultural civilizations in this part of Asia. The earliest known remains of production-based economy in central Asia date to the sixth millennium BC (Sarianidi, 1992). Early agricultural sites here are known from the area between the Pamir forelands, the upper Amu Darya (Oxus) River, and southern margin of the Karakum desert. These settlements developed on loess patches, as did the First Persian Empire (Achaemenid Empire), and in the next millennia Parthia, Khwarezm, Sogdiana, and Bactria (Dani and Masson, 1992). In the past, more humid climatic conditions occurred in these modern semidesert or desert landscapes (Yang et al., 2009; Chen et al., 2010). The rise and fall of societies inhabiting central Asia coincided with these climatic fluctuations (Yin et al., 2016).

The first Neolithic cultures also appeared in areas of loess in Europe. Clark (1952) produced an interesting map suggesting the relationship of the settlement of central Europe by Neolithic Danubian peasants to locations of loess deposits. He placed Neolithic sites on a base map of the Grahmann (1932) loess map of Europe and showed impressive correlations. Neolithic and earlier Bronze Age

settlement systems on the central European uplands and Carpathian forelands also correspond strongly with areas of loess (Kruk et al., 1996; Kruk and Milisauskas, 1999). The spread of the Neolithic to central Europe, between the sixth and fourth millennium BC (Gronenborn, 2010), took place along fertile loess uplands occurring on the northern Sudetes and Carpathians forelands.

Loess deposits are interconnected along the course of the Silk Route (Fig. 25), whose peak of influence occurred during the Tang dynasty, in the second part of the first millennium AD (Liu, 2010). From Chang'an (Xi'an) in the Chinese Empire, through the rich ancient kingdoms of Loulan, Khotan, Sogdiana, and Khwarezm to the coast of the Caspian Sea, the route clearly coincided with loess areas, where many agricultural settlements occurred. The development of a network of towns and settlements along the Silk Road during this period was possible thanks to fertile loess soils and abundant water (oases, rivers) (Dani and Masson, 1992; Abazow, 2008; Owczarek et al., 2017). Climate change during the last two millennia, along with human impacts such as deforestation and intensive agriculture, influenced the rise and fall and, in some cases, even the emergence of new settlements in this area, especially in the western piedmont of Pamir and Tian Shan mountains in the Sogdiana (Marshak, 2003). An example of the close relationship between favorable environmental conditions and climate change may be the ancient cities of Niya, Loulan, and Panjikent. Niya and Loulan, centers of the rich Khotan and Loulan kingdoms, were located on the southern and eastern edge of the Taklamakan desert (Yong and Sun, 1994). Both of the cities were developed on the basis of irrigation of loess

soils on the terraces of the Niya and Tarim Rivers. Increases in precipitation at ca. 2.1–1.9 ka, noted in the Tarim basin (Wünnemann et al., 2006; Chen et al., 2010), led to the rapid political and economic development of this area. These rich cities lost their importance after the second century AD, because of long-term drought and shifting and drying of river channels and lakes, and were completely abandoned by the early fifth century (Yong and Sun, 1994). As these kingdoms located on the edge of the Taklamakan desert in the Tarim basin declined, the Sogdiana in western central Asia grew. The Sogdian settlement network, like those of Samarqand and Bukhara, developed on loess patches in the piedmont of Pamir-Alay along the Zarafshan River. One of the towns erected along the Silk Road in the fifth century was Panjikent, which by the end of the seventh century was the most important urban settlement in this part of central Asia (Grenet and de la Vaissière, 2002; Marshak, 2003). The city was founded on the upper, loess-mantled terrace of the Zarafshan River (Owczarek et al., 2017). The ancient town was abandoned in the ninth and tenth centuries. The fall of Panjikent was associated with a political crisis connected to Arab conquest in AD 722 (Grenet and de la Vaissière, 2002), during a shift to a drier climate in the eighth to ninth centuries, and an accompanying decline in natural and agricultural resources because of human impacts and erosion of its loess soils (Owczarek et al., 2017).

The cultural and economic development of human societies is strongly affected by environmental resources. Areas with fertile soil and access to water, characteristics common to most areas of loess, have been shown throughout history to be predisposed for a “Neolithic revolution,”

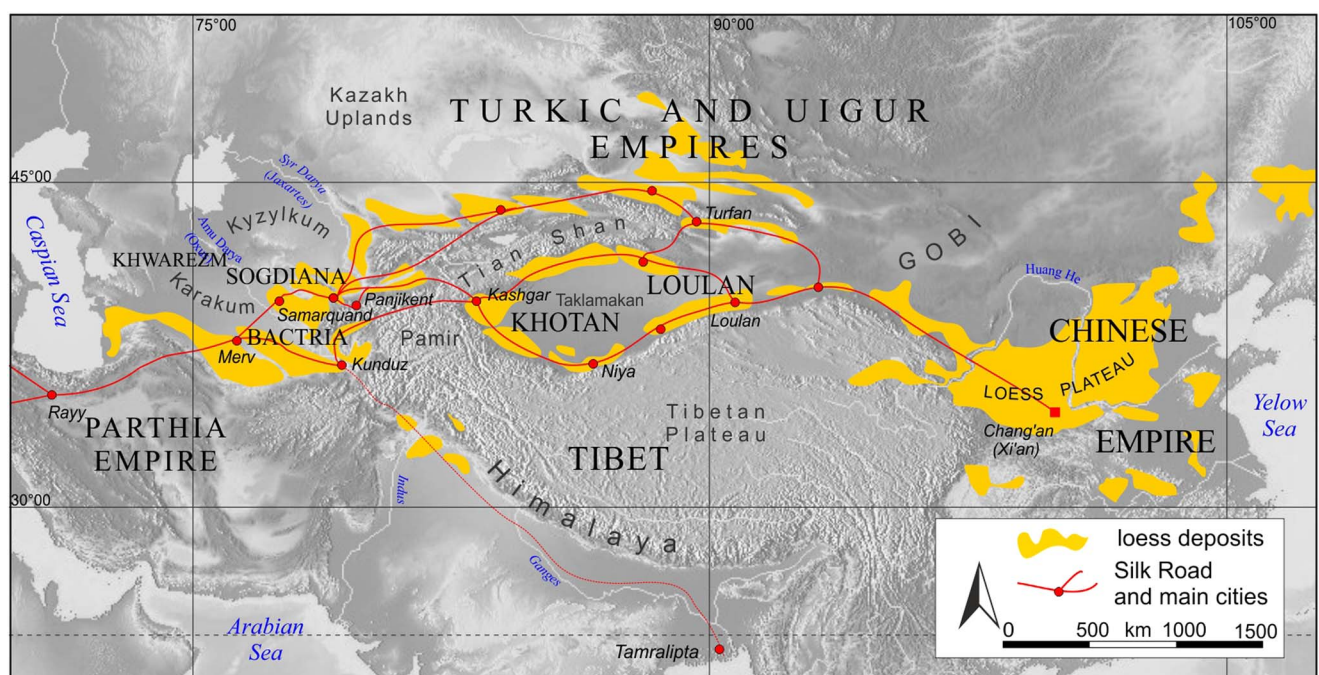


Figure 25. (color online) Map of loess and loesslike deposits in Asia, with the locations of the most important towns and Silk Road branches on the background of the main kingdoms and empires of the second to third centuries AD. After Dodonov (2007), Dodonov and Zhou (2008), and Owczarek et al. (2017).

which became a later impulse for the development of modern societies.

Loess geochronology

By Helen M. Roberts

Loess deposits often provide impressive paleoclimatic and paleoenvironmental records. Accurate geochronological data play a critical role in understanding these important terrestrial archives. A number of approaches have been used to establish the timing of events preserved within the loess record, including relative dating techniques and methods to establish age equivalence, as well as radiometric dating techniques to establish numerical ages. The purpose of this section is to consider these different geochronological approaches and their contribution to the study of loess and comment on the likely future research directions for loess geochronology.

The striking visible changes between alternating intercalated loess and paleosol units that can be seen in many loess exposures attests directly to the rhythm of changing climatic conditions through time. This stratigraphy offers a simple relative chronology back through time, across glacial-interglacial cycles, solely based on appearance. If assumptions are made about continuous accumulation rates and preservation of the loess deposits over time, then simple top-down layer counting of the loess-paleosol units can be used to establish the likely ages of the individual units, which in turn allows correlation to other loess sequences on the basis of likely age equivalence, and correlation to other dust-bearing deposits such as terrestrial lake deposits, marine sediments, and ice cores. Correlations of all kinds are dramatically strengthened where isochronous stratigraphic markers preserved in the deposits (e.g., a geochemically distinct tephra) can be identified and used to establish age equivalence; this is especially key for loess deposits. Where the age of these distinctive markers is already known from records elsewhere, this is particularly valuable—for example, the widespread Campanian Ignimbrite/Y5 tephra, dated to ~40 ka, is a key chronostratigraphic marker across the Mediterranean and southeastern Europe (Veres et al., 2013).

Records of paleomagnetic reversals and geomagnetic excursions because of changes in the earth's geomagnetic field have also played an important role in linking long terrestrial loess sequences to each other and enabling correlation to other long records such as the marine record of Lisiecki and Raymo (2005). However, the delay between the deposition of sediment and the immobilization of the magnetic signal results in the apparent downward displacement of the paleomagnetic signature preserved in different records (Zhou and Shackleton, 1999; Sun et al., 2013; Zhao et al., 2014). This “lock-in effect” requires careful consideration or potentially much higher-resolution sampling (Maher, 2016), if high-precision magnetostratigraphy is to be used to link sites with greater temporal precision and accuracy.

Beyond this broad framework of tie points offered through stratigraphy, opportunistic tephra correlation, and magneto-

stratigraphy, further detail and opportunities for correlation between these indirectly dated records can be provided by fluctuations in records of magnetic susceptibility, grain size, dust flux, and the degree of amino-acid racemization in land snails, which are used to establish age equivalence on the basis of the pattern of their signatures within loess and paleosol units. Magnetic susceptibility and grain-size fluctuations in particular have been widely used for correlation between loess records on the basis of “wobble matching” (e.g., Yang and Ding, 2014; Marković, this issue); they are often interpreted as climate-related signatures, inasmuch as climate cycles largely drive silt generation and loess depositional systems. In some cases, a chronology is established by linking these records to other nonloess records for which more detailed chronological information may have already been established, such as records from lacustrine, marine and ice cores, and speleothems (e.g., Bloemendal et al., 1995; Porter and An, 1995; Vandenberghe et al., 1997; Yang and Ding, 2014); in other cases, these records are directly tuned to orbital cycles (Ding et al., 2002b; Sun et al., 2006).

Where only a broad chronostratigraphic framework or methods to establish age equivalence are used, or where proxy records of climate are tuned to orbital frequencies, it is necessary to assume that (1) loess accumulation rates were essentially continuous over time, with no major hiatuses or erosional events, and (2) the rates were constant between chronological tie points. However, these assumptions are being increasingly recognized as an oversimplification of the nature of many loess records, as large (i.e., order of magnitude) fluctuations in accumulation rates have been reported within (Roberts et al., 2003; Muhs et al., 2013a; Stevens et al., 2016), as well as between, loess units (Sun and An, 2005). Additionally, significant hiatuses have been identified (Lu et al., 2006; Terhorst et al., 2011). Additionally, indirect dating methods and/or tuning of proxy records to a climate driver, such as orbital cycles, has other potential problems: (1) it involves assumptions about the nature and timing of the records or proxies being investigated, (2) it brings the potential for circular reasoning, and (3) it precludes the opportunity to investigate leads and lags between proxy records of climate change. In contrast, independent numerical dating using radiometric techniques allows loess-paleosol sequences to be linked unambiguously to each other, and to other records with accurate, independent numerical chronologies. This approach allows proxy records and their correlations to be explored within and between sites, rather than being assumed to have the same meaning, timing, and significance at each site. For example, a comparison of several Chinese loess sections with independent radiometric age control (Dong et al., 2015) revealed the time-transgressive nature across the sites of rapid changes in the magnetic susceptibility signal inferred to represent the Pleistocene/Holocene transition. The sites spanned a climatic gradient across the Chinese Loess Plateau, and the age for the inferred Pleistocene/Holocene transition was asynchronous across the sites, varying by ~3–4 ka along the northwest (drier, less weathered) to southeast (wetter, more weathered) transect.

Furthermore, none of these independently derived numerical ages were synchronous with the age of the Marine Oxygen Isotope Stage 2/1 boundary that would otherwise have been assumed for the Pleistocene/Holocene transition at each site, had there been no independent radiometric chronology to support the magnetic susceptibility data (Dong et al., 2015). This example emphasizes the importance of independent numerical dating, where possible.

The key radiometric dating techniques that have helped establish numerical chronologies for loess-paleosol sequences are (1) radiocarbon dating and (2) luminescence dating. Since the earliest application to loess-paleosol sequences, radiocarbon dating has benefited from advances in methods of analysis, improvements in instrumentation, and extensions and refinements to the radiocarbon calibration curve (e.g., Hajdas, 2008). The radiocarbon method relies on finding suitable, sufficient, in situ organic material for dating and has therefore been particularly applied to paleosols and snail shells in loess deposits (Pigati et al., 2013; Wang et al., 2014), although other organic materials such as calcareous earthworm granules have also been used (Moine et al., 2017). One key issue regarding the use of radiocarbon techniques for dating loess deposits is the relatively low maximum age that can be achieved, compared with the temporally extensive nature of many loess records. Luminescence dating techniques extend beyond the upper age limit of radiocarbon dating and have played an increasingly significant role in deciphering the chronology of loess-paleosol sequences, as both the accuracy and precision of techniques have improved over time.

Luminescence dating exploits the steady buildup of a time-dependent signal acquired during burial of mineral grains of quartz and feldspar. The event being dated is the last exposure to sunlight during transport, prior to deposition and burial. Luminescence techniques are therefore highly appropriate for application to loess sequences, as the fine-grained nature of this eolian sediment implies long-transport distances, and hence ample time for bleaching of any preexisting luminescence signal prior to deposition; additionally, the method dates the deposition event directly. The method does not typically suffer from lack of suitable materials for dating, being applied to mineral grains of quartz and feldspar, which are abundant in loess and available throughout the sedimentary sequence. One important parameter that does need to be considered though is water content over the depositional period, as water in the pore spaces between grains absorbs radiation that would otherwise reach the sediment grains. Careful assessment must be made as the final luminescence age calculated can change by a little over 1% per 1% change in water content. A combination of local knowledge of water history at the site and measurements of the lower and upper limits of water content are therefore used to define a suitable average value for the water content over the depositional history of the sediments (see also Nelson and Rittenour, 2015).

Today, a family of luminescence techniques exists, and the range of signals available for dating continues to expand. The optically stimulated luminescence (OSL) signal from quartz

grains, measured using a single-aliquot regenerative dose protocol, remains the luminescence signal of choice for dating where conditions are appropriate (see review by Roberts, 2008). Unfortunately, the annual dose rate in loess is relatively high, and hence the maximum age limit for quartz OSL is typically significantly less than 100 ka (Chapot et al., 2012). In contrast, infrared-stimulated luminescence (IRSL) signals from feldspar have a greater saturation dose and hence a greater potential upper age limit. In the past, however, the widespread use of feldspars for dating was impeded by the phenomenon of anomalous fading, leading to age underestimations. A resurgence of interest in the use of feldspars for dating has recently occurred, driven by the discovery of more stable “post-IR IRSL” signals with minimal rates of anomalous fading (see reviews by Buylaert et al., 2012; Li and Li, 2012). Feldspars offer a higher upper age limit of several hundreds of thousand years in loess. Ongoing and future luminescence work relevant to loess studies will likely focus on the development of techniques to reliably extend the upper limit of dating even further. Examples include the infrared photon-luminescence signal from feldspars, which appears not to suffer from anomalous fading (Prasad et al., 2017); the use of the thermally transferred OSL signal from quartz (Wang et al., 2006); and the violet-stimulated luminescence signal, which has been used by Ankjærgaard et al. (2016) to significantly extend the age range from quartz by an order of magnitude to ~600 ka in loess.

Aided by the expansion of the range of radiometric techniques available, and an increasingly large number of ages generated, future work within the area of loess geochronology will likely focus on investigating the validity of previous assumptions regarding the steady accumulation rates and quasi-continuous nature of loess accumulation. Future research can address questions relating to the degree of continuity of thick loess records and explore the existence and durations of major hiatuses in the loess sedimentary record. The increased use of independent radiometric dating will also permit further investigation of the degree of (a)synchrony of the proxy records preserved across networks of loess-paleosol sequences, and cross correlations to other long sedimentary records such as marine and ice-core records. This work will, however, necessitate an increasingly dense sampling strategy for radiometric dating, in order to capture the detail required to address these questions. An increased density of independent numerical age determinations will also enable the application of Bayesian statistics to such data sets, giving rise to age-depth models that will further increase the accuracy and precision of loess-paleosol chronologies.

Zircon U-Pb and single-grain provenance techniques in loess research

By Thomas Stevens

Knowledge of loess sources provides information on past dust sources and production, allows proper interpretation of climate proxies, and can yield insights into landscape

evolution (Smalley et al., 2009; Nie et al., 2015). However, substantial debates still exist over the dust sources of many of the world's loess deposits (Aleinikoff et al., 2008; Crouvi et al., 2008; Újvári et al., 2012; Stevens et al., 2013b). Because of the dominance of silt-size particles and the well-known distance-sorting properties of eolian systems, bulk sediment techniques have traditionally been used to address these debates (Chen et al., 2007; Buggle et al., 2008). Although they provide valuable information on the fine silt/clay sources and overall compositional characteristics of loess, bulk sediment analyses average out provenance signatures, which may mask specific provenance data if the loess was derived from multiple sources (Stevens et al., 2010).

In order to circumvent such problems, there has been a surge in use of single-grain techniques to identify loess sources (Aleinikoff et al., 1999, 2008; Stevens et al., 2010; Újvári et al., 2012). To date, most such studies have focused on U-Pb ages of multiple individual zircon grains ($ZrSiO_4$). Zircons are heavy minerals (4.65 g/cm³) that are resistant to weathering and act as geochemically closed systems through most surface and crustal processes. They crystallize at high temperatures from silica-rich melts and at high grades of metamorphism, with Pb and U retained up to ~900°C. They are nearly ubiquitous in upper crustal rocks and as an accessory mineral in detrital sediments (Hawkesworth and Kemp, 2006). Zircons reject radiogenic Pb during their formation, which means that the ages of individual grains, isolated from bulk samples via density and magnetic separation, can be constrained using U-Pb isotopic analysis, often measured using laser ablation inductively coupled mass spectrometry or secondary ion mass spectrometry (Fedo et al., 2003). Zircon U-Pb ages can be highly diagnostic of sediment source, because of the variety of distinct formation ages of their protosource terranes, and the often characteristic zircon U-Pb age distributions in different detrital sediments and rocks. As such, the technique is one of the most widely used provenance methods (Fedo et al., 2003), and zircon U-Pb age data are abundant for many loess potential source areas.

Provenance assignment is undertaken via comparisons of zircon U-Pb age assemblages in target loess sediments to zircon U-Pb data in potential source areas. This comparison is usually based on some graphical form of probability density estimation—for example, a probability density function or kernel density estimator diagram (Fig. 26)—but also potentially via mixture modeling or other statistical approaches. The identification of discrete peaks of specific zircon U-Pb ages or age ranges in a sample facilitates the identification or exclusion of possible sources based on the presence of zircons of these ages in potential source rock samples. A specific example from China is shown in Figure 26, and described subsequently. Because preparation and analysis of samples is relatively time consuming, sampling is often undertaken at rather coarse intervals (meters to tens of meters scale) within a loess section. To ensure sufficient yield of zircons, it is advisable to take ~1 kg of loess material per sample at the cleaned section. After extraction, grains are usually imaged (often using cathodoluminescence) to check

for damage, zonation, and so forth, and to set up targets for analyses. Analyses numbers vary greatly between studies (discussed subsequently), but at a minimum, it is generally accepted that >110 zircon ages are needed to utilize age peak presence as a provenance indicator (Vermeesch, 2004), whereas to analyze the absence of ages or the relative heights of peaks generally requires substantially more data (Pullen et al., 2014).

Significant zircon U-Pb data sets exist from both North American (Aleinikoff et al., 1999, 2008) and European (Újvári et al., 2012) loess, although the majority of data are from Chinese Loess Plateau deposits (Stevens et al., 2010, 2013b; Pullen et al., 2011; Xiao et al., 2012; Che and Li, 2013; Licht et al., 2016; Fenn et al., 2017). Debate about the origin/provenance of Chinese loess has been rather polarized, with multiple potential source areas, some being thousands of kilometers apart. Chinese Loess Plateau zircon U-Pb age distributions exhibit a distinctive “double peak” of ages of around 260–290 Ma and 440–460 Ma; these ages comprise 80–90% of the zircon grains (Fig. 26). Small numbers of grains have ages of 700–1100 Ma and 1700–2000 Ma. The protosources of these zircon grains must be crystalline/high-grade metamorphic rocks formed at those times, with prime candidates being northern Tibetan Plateau and Gobi Altay

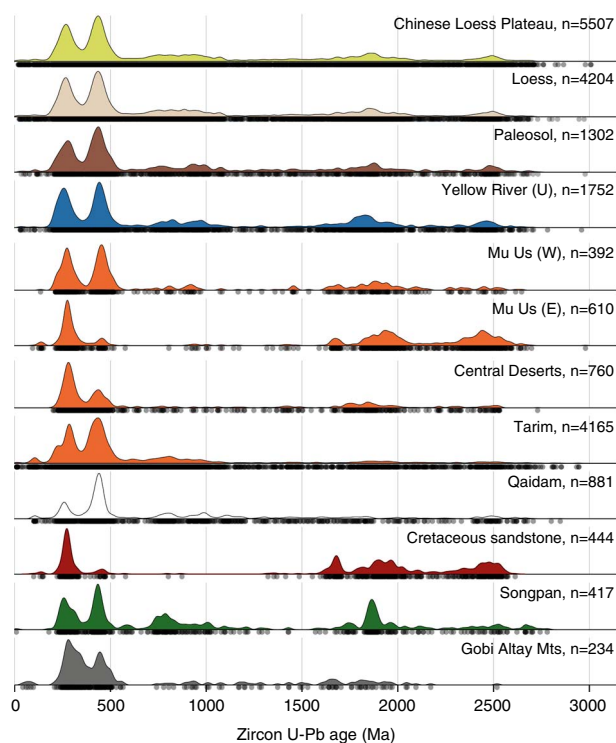


Figure 26. (color online) Kernel density estimator diagrams (Vermeesch, 2012) of compiled zircon U-Pb age data from studies of the Chinese Loess Plateau. Compiled from Fenn et al. (2017; see paper for sources). “Chinese Loess Plateau” includes all data from the plateau combined, whereas “loess” and “paleosol” are combined data for Chinese Loess Plateau loess and soil units, respectively. Yellow River (U) refers to the upper river reaches (Nie et al., 2015); Mu Us (E) and (W) refer to data from eastern and western parts of the desert, respectively (Stevens et al., 2013b).

mountain terranes (Stevens et al., 2010). These age peaks can be compared to data obtained from potential source sediments, as they may be indicative of the most recent sediment transport step. Nie et al. (2015) proposed that the Yellow River system was the source for Chinese Loess Plateau deposits, as it transported eroded northeastern Tibetan Plateau sediment (Fig. 26) that is readily available for deflation and eolian transport to the Chinese Loess Plateau. This major revision of prevailing ideas implies that the summer monsoon controls incision of the Tibetan Plateau and may be responsible for the accelerated rates of loess deposition on the plateau, post-3.6 Ma. A number of further U-Pb studies have tested these conclusions (Bird et al., 2015; Licht et al., 2016; Zhang et al., 2016; Fenn et al., 2017). Licht et al. (2016) argued that although many potential Chinese loess source areas yield similar zircon age peaks, deriving large data sets ($n=400\text{--}1000$ grains per sample) permits differences in peak proportions to be used to differentiate these source areas. As such, they grouped age data together into loess, paleosol, and potential source area groups and applied mixture-modeling techniques; their work supports the idea that the Yellow River system is indeed the dominant sediment source to the Chinese Loess Plateau (Fig. 26). Licht et al. (2016) further argued that sediments from the northern Tibetan Plateau Qaidam basin also contributed an equal proportion of sediment to both loess and paleosol units (Fig. 26). As different dust storm tracks likely existed between glacial and interglacial phases, this similar source assemblage implies that predeposited glacial loess material was eroded during interglacial periods and contributed to accretion of soil units, in a process of internal reworking or “eolian cannibalism” (Licht et al., 2016).

A key challenge is to extend these comprehensive analyses to Pliocene red clay deposits that underlie the loess. Although some red clay zircon U-Pb studies have been published (Nie et al., 2014; Shang et al., 2016; Gong et al., 2017), the necessary preparation and analysis of smaller zircon grains in the red clays make this work difficult. A further challenge is that the large sample numbers in recent studies require improved analysis and visualization of the resultant data sets. One method to address this is multidimensional scaling (MDS; Vermeesch, 2013). MDS constructs a two-dimensional map of individual points that represents samples with multiple analyses numbers; distances on the map indicate the degree of similarity among points (cf. Stevens et al., 2013a). Such dimensional reduction techniques are likely to become more important with the increasing importance of “big data” (an Internet-era term used by Vermeesch and Garzanti [2015] to describe the large and complex multisample, multimethod data sets now being generated in many provenance studies). Big data sets also open up the potential for quantification of source contributions from zircon U-Pb data; this is a major topic of interest, with a number of recent approaches proposed (Stevens et al., 2010; Licht et al., 2016; Zhang et al., 2016). However, a note of caution has also recently been sounded by Fenn et al. (2017), who demonstrated that grouping of sample

data together can result in spurious trends. Clearly, high analysis numbers and statistical representativity are important, although the number of analyses required depends on the complexity of source assemblages and the specific property of U-Pb age distributions being examined (Vermeesch, 2004; Pullen et al., 2014). Nonetheless, the goal should be larger numbers of analyses from individual samples, with caution exercised in grouping sample data sets (Fenn et al., 2017).

Zircon U-Pb data are not without limitations—for example, (1) the effect of sedimentary recycling through multiple phases is hard to diagnose; (2) zircon sources may not always be representative of those of the main sediment body; (3) as zircon is a heavy mineral, zircon U-Pb ages will likely reflect more proximal sources; and (4) zircon fertility in source rocks exerts a key control over detrital zircon assemblages (Sláma and Košla, 2012). As such, a major goal of future research should be to introduce other single-grain analyses that complement zircon U-Pb age analyses. Some initial attempts at this have been made in Chinese loess, combining zircon U-Pb dating with zircon fission-track and heavy mineral analysis (Stevens et al., 2013a; Nie et al., 2014, 2015) and with garnet chemistry (Fenn et al., 2017). In central-eastern European loess deposits, attempts have been made to combine zircon U-Pb dating with both geochemistry of rutile (Újvári et al., 2013) and zircon Hf isotopes (Újvári and Klötzli, 2015), as well as bulk geochemical indicators (Újvári et al., 2012). Zircon U-Pb analyses have also been combined with Pb isotope analysis of isolated aliquots of K-feldspars in loess in the United States (Aleinikoff et al., 1999, 2008). Garnet type and rutile trace element composition in particular have great potential to complement zircon U-Pb dating, especially where source terranes show overlapping zircon U-Pb ages but are composed of rocks of varying metamorphic grade and formation temperatures (Újvári et al., 2013; Fenn et al., 2017).

In sum, single-grain provenance analysis is a rapidly emerging tool in loess research. Although in many loess regions major breakthroughs in constraining loess-dust sources can be made through the straightforward application of detrital zircon U-Pb dating, multitechnique single-grain approaches promise even more accurate and precise dust sourcing for loess deposits globally.

ACKNOWLEDGMENTS

We wish to thank the many people who helped to make the Eau Claire LoessFest a success, especially Doug Faulkner, Garry Running, and Kent Syverson of the University of Wisconsin–Eau Claire; John Attig of the Wisconsin Geological and Natural History Survey; and Kristine Gruley and Joseph Mason of the University of Wisconsin–Madison. Chase Kasmerchak of Michigan State University was a key support person for field trip and conference planning. We thank Michigan State University and the University of Wisconsin–Eau Claire for financial and logistical support and acknowledge receipt of grants in support of the LoessFest from INQUA and the National Science Foundation. This special issue

was the idea of Nick Lancaster, editor of Quaternary Research. Nick brought in Art Bettis and Randall Schaetzl as guest editors. The authorship order for this introduction is, after the two editors, alphabetical order by last name of the primary authors, and then again in alphabetical order by last name of the secondary authors. The editors also wish to thank the many reviewers of the papers that follow for their constructive input and expertise. We would especially like to thank Dan Muhs and Peter Jacobs for their thorough reviews of the final “assembled” manuscript. Dan Muhs deserves a special commendation for his thorough and insightful comments and suggestions on the sections entitled “Loess in Alaska” and “Geochemical Approaches to the Study of Loess.” We believe that the 19 contributions in this introduction, and the 19 papers in this LoessFest issue proper, nicely represent the diversity of loess research being done today worldwide and exemplify some of the best that this discipline has to offer. Enjoy.

REFERENCES

- Abazow, R., 2008. *Palgrave Concise Historical Atlas of Central Asia*. Palgrave Macmillan, New York.
- Akram, H., Yoshida, M., Ahmad, M.N., 1998. Rock magnetic properties of the late Pleistocene loess-paleosol deposits in Haro River area, Attock Basin, Pakistan: is magnetic susceptibility a proxy measure of paleoclimate? *Earth, Planets and Space* 50, 129–139.
- Aleinikoff, J.N., Muhs, D.R., Bettis, E.A. III, Johnson, W.C., Fanning, C.M., Benton, R., 2008. Isotopic evidence for the diversity of late Quaternary loess in Nebraska: glaciogenic and nonglaciogenic sources. *Geological Society of America Bulletin* 120, 1362–1377.
- Aleinikoff, J.N., Muhs, D.R., Saner, R.R., Fanning, C.M., 1999. Late Quaternary loess in northeastern Colorado: Part II—Pb isotopic evidence for the variability of loess sources. *Geological Society of America Bulletin* 111, 1876–1883.
- Allan, R.J., Hole, F.D., 1968. Clay accumulation in some Hapludalfs as related to calcareous till and incorporated loess on drumlins in Wisconsin. *Soil Science Society of America Proceedings* 32, 403–408.
- Amit, R., Enzel, Y., Crouvi, O., 2016. Distance-impacted grain size of loess and dust result in the formation of diverse soil types around the Mediterranean. *Geological Society of America, Abstracts with Programs* 48. <http://dx.doi.org/10.1130/abs/2016AM-282202>.
- An, Z., Kukla, G.J., Porter, S.C., Xiao, J., 1991a. Magnetic susceptibility evidence of monsoon variation on the Loess Plateau of central China during the last 130,000 years. *Quaternary Research* 36, 29–36.
- An, Z.S., Kukla, G., Porter, S.C., Xiao, J.L., 1991b. Late Quaternary dust flow on the Chinese Loess Plateau. *Catena* 18, 125–132.
- Andersson, J.G., 1934. *Children of the Yellow Earth*. Kegan Paul, Trench, Trubner, London.
- Ankjærgaard, C., Guralinik, B., Buylaert, J.-P., Reimann, T., Yi, S.W., Wallinga, J., 2016. Violet stimulated luminescence dating of quartz from Luochuan (Chinese Loess Plateau): agreement with independent chronology up to ~600 ka. *Quaternary Geochronology* 34, 33–46.
- Antoine, P., Catt, J., Lantidou, J.-P., Sommé, J., 2003. The loess and coversands of northern France and southern England. *Journal of Quaternary Sciences* 18, 309–318.
- Antoine, P., Coutard, S., Guerin, G., Deschodt, L., Goval, E., Loch, J.-L., Paris, C., 2016. Upper Pleistocene loess-paleosol records from Northern France in the European context: Environmental background and dating of the Middle Palaeolithic. *Quaternary International* 411, 4–24.
- Antoine, P., Rousseau, D.-D., Zoller, L., Lang, A., Munaut, A.-V., Hatte, C., Fontugne, M., 2001. High-resolution record of the last glacial-interglacial cycle in the Nussloch loess-paleosol sequences, Upper Rhine Area, Germany. *Quaternary International* 76–77, 211–229.
- Antoine, P., Rousseau, D.-D., Degeai, J.-P., Moine, O., Lagroix, F., Kreuzer, S., Fuchs, M., Hatté, C., Gauthier, C., Svoboda, J., Lisá, L., 2013. High-resolution record of the environmental response to climatic variations during the Last Interglacial–Glacial cycle in Central Europe: the loess-paleosol sequence of Dolní Věstonice (Czech Republic). *Quaternary Science Reviews* 67, 17–38.
- Antoine, P., Rousseau, D.-D., Moine, O., Kunesch, S., Hatté, C., Lang, A., Tissoux, H., Zöller, L., 2009. Rapid and cyclic aeolian deposition during the Last Glacial in European loess: a high-resolution record from Nussloch, Germany. *Quaternary Science Reviews* 28, 2955–2973.
- Assallay, A.M., Rogers, C.D.F., Smalley, I.J., Jefferson, I.F., 1998. Silt: 2–62 micron, 9–4 phi. *Earth-Science Reviews* 45, 61–88.
- Aubekerov, B.J., 1993. Stratigraphy and Paleogeography of the Plain Zones of Kazakhstan during the Late Pleistocene and Holocene. In: Velichko, A.A. (Ed.) *Development of Landscape and Climate of Northern Asia, Late Pleistocene and Holocene*. [In Russian.] Nauka, Moscow, pp. 101–110.
- Auclair, M., Lamothe, M., Lagroix, F., Banerjee, S.K., 2007. Luminescence investigation of loess and tephra from Halfway House section, central Alaska. *Quaternary Geochronology* 2, 34–38.
- Avni, Y., 2005. Gully incision as a key factor in desertification in an arid environment, the Negev highlands, Israel. *Catena* 63, 185–220.
- Avni, Y., Porat, N., Plakht, J., Avni, G., 2006. Geomorphic changes leading to natural desertification versus anthropogenic land conservation in an arid environment, the Negev Highlands, Israel. *Geomorphology* 82, 177–200.
- Bagnold, R., 1941. *The Physics of Blown Sand and Desert Dunes*. Chapman and Hall, London.
- Bai, Y., Fang, X., Nie, J., Wang, Y., Wu, F., 2009. A preliminary reconstruction of the paleoecological and paleoclimatic history of the Chinese Loess Plateau from the application of biomarkers. *Palaeogeography, Palaeoclimatology, Palaeoecology* 271, 161–169.
- Baker, F.C., 1931. Pulmonate mollusca peculiar to the Pleistocene period, particularly the loess deposits. *Journal of Paleontology* 5, 270–292.
- Balakrishnan, M., Yapp, C.J., 2004. Flux balance models for the oxygen and carbon isotope compositions of land snail shells. *Geochimica Cosmochimica Acta* 68, 2007–2024.
- Balco, G., Stone, J.O.H., Mason, J.A., 2005. Numerical ages for Plio-Pleistocene glacial sediment sequences by Al-26/Be-10 dating of quartz in buried paleosols. *Earth and Planetary Science Letters* 232, 179–191.
- Banak, A., Mandić, O., Sprovieri, M., Lirer, F., Pavelić, D., 2016. Stable isotope data from loess malacofauna: evidence for climate changes in the Pannonian Basin during the Late Pleistocene. *Quaternary International* 415, 15–24.
- Basarin, B., Buggle, B., Hambach, U., Marković, S.B., Dhand, K.O., Kovačević, A., Stevens, T., Guo, Z., Lukić, T., 2014. Time-scale and astronomical forcing of Serbian loess-paleosol sequences. *Global and Planetary Change* 122, 89–106.
- Basarin, B., Vandenberghe, D.A.G., Marković, S.B., Catto, N., Hambach, U., Vasiliniuc, S., Derese, C., Rončević, S., Vasiljević, D.A., Rajić, L., 2009. The Belotinac section (southern Serbia) at

- the southern limit of the European loess belt: initial results. *Quaternary International* 240, 128–138.
- Bateman, M.D., 1998. The origin and age of coversand in north Lincolnshire, UK. *Permafrost and Periglacial Processes* 9, 313–325.
- Bateman, M.D., Van Huissteden, J., 1999. The timing of last-glacial periglacial and aeolian events, Twente, eastern Netherlands. *Journal of Quaternary Science* 14, 277–283.
- Baumgart, P., Hambach, U., Meszner, S., Faust, D., 2013. An environmental magnetic fingerprint of periglacial loess: records of Late Pleistocene loess–palaeosol sequences from eastern Germany. *Quaternary International* 296, 82–93.
- Begét, J., 1990. Middle Wisconsinan climate fluctuations recorded in central Alaskan loess. *Géographie Physique et Quaternaire* 44, 3–13.
- Begét, J., Edwards, M., Hopkins, D., Keskinen, M., Kukla, G., 1991. Old Crow tephra found at the Palisades of the Yukon, Alaska. *Quaternary Research* 35, 291–297.
- Begét, J.E., 1996. Tephrochronology and paleoclimatology of the last interglacial-glacial cycle recorded in Alaskan loess deposits. *Quaternary International* 34–36, 121–126.
- Begét, J.E., Hawkins, D.B., 1989. Influence of orbital parameters on Pleistocene loess deposition in central Alaska. *Nature* 337, 151–153.
- Begét, J.E., Stone, D.B., Hawkins, D.B., 1990. Paleoclimatic forcing of magnetic susceptibility variations in Alaskan loess during the Quaternary. *Geology* 18, 40–43.
- Ben Israel, M., Enzel, Y., Amit, R., Erel, Y., 2015. Provenance of the various grain-size fractions in the Negev loess and potential changes in major dust sources to the eastern Mediterranean. *Quaternary Research* 83, 105–115.
- Berger, G.W., 2003. Luminescence chronology of late Pleistocene loess-paleosol and tephra sequences near Fairbanks, Alaska. *Quaternary Research* 60, 70–83.
- Bertran, P., Bateman, M.D., Hernandez, M., Mercier, N., Millet, D., Sitzia, L., Tastet, J.-P., 2011. Inland aeolian deposits of southwest France: facies, stratigraphy and chronology. *Journal of Quaternary Science* 26, 374–388.
- Bertran, P., Liard, M., Sitzia, L., Tissoux, H., 2016. A map of Pleistocene aeolian deposits in western Europe, with special emphasis on France. *Journal of Quaternary Sciences* 31, 844–856.
- Bettis, E.A. III, Muhs, D.R., Roberts, H.M., Wintle, A.G., 2003. Last Glacial loess in the conterminous USA. *Quaternary Science Reviews* 22, 1907–1946.
- Bird, A., Stevens, T., Rittner, M., Vermeesch, P., Carter, A., Andò, S., Garzanti, E., et al., 2015. Quaternary dust source variation across the Chinese Loess Plateau. *Palaeogeography, Palaeoclimatology, Palaeoecology* 435, 254–264.
- Björck, S., Walker, M.J.C., Cwynar, L.C., Johnsen, J., Knudsen, K.L., Lowe, J.J., Wohlfarth, B., 1998. An event stratigraphy for the Last Termination in the North Atlantic region based on the Greenland ice-core record: a proposal by the INTIMATE group. *Journal of Quaternary Science* 13/4, 283–292.
- Bloemendal, J., Liu, X.M., Rolph, T.C., 1995. Correlation of the magnetic-susceptibility stratigraphy of Chinese loess and the marine oxygen-isotope record: chronological and paleoclimatic implications. *Earth and Planetary Science Letters* 131, 371–380.
- Bohncke, S., Kasse, C., Vandenberghe, J., 1995. Climate induced environmental changes during the Vistulian Lateglacial at Zabinko, Poland. *Quaestiones Geographicae*, special issue 4, 43–64.
- Bohncke, S., Vandenberghe, J., Huijzer, A.S., 1993. Periglacial environments during the Weichselian Late Glacial in the Maas valley, the Netherlands. *Geologie en Mijnbouw* 72, 193–210.
- Boixadera, J., Poch, R.M., Lowick, S.E., Balasch, J.C., 2015. Loess and soils in the eastern Ebro Basin. *Quaternary International* 376, 114–133.
- Bokhorst, M., Vandenberghe, J., Sümege, P., Lanczont, M., Gerasimenko, N.P., Matviishina, Z.N., Markovic, S.B., Frechen, M., 2011. Atmospheric circulation patterns in central and eastern Europe during the Weichselian Pleniglacial inferred from loess grain-size records. *Quaternary International* 234, 62–74.
- Böse, M., 1991. A palaeoclimatic interpretation of frost-wedge casts and aeolian sand deposits in the lowlands between Rhine and Vistula in the Upper Pleniglacial and Late Glacial. *Zeitschrift für Geomorphologie* 90, 15–28.
- Bradák, B., Újvári, G., Seto, Y., Hyodo, M., Végh, T., 2018. A conceptual magnetic fabric development model for the Paks loess in Hungary. *Aeolian Research* 30, 20–31.
- Breed, C.S., Fryberger, S.G., Andrews, S., McCauley, C., Lennartz, F., Gebel, D., Horstman, K., 1979. Regional studies of sand seas, using Landsat (ERTS) imagery. In: McKee, E.D. (Ed.), *A Study of Global Sand Seas*. U.S. Geological Survey, Reston, VA, pp. 305–397.
- Brodie, C., Leng, M., Casford, J., Kendrick, C., Lloyd, J., Yongqiang, Z., Bird, M., 2011. Evidence for bias in C and N concentrations and $\delta^{13}\text{C}$ composition of terrestrial and aquatic organic materials due to pre-analysis acid preparation methods. *Chemical Geology* 282, 67–83.
- Bronger, A., 1976. Zur quartären Klima- und Landschaftsentwicklung des Karpatenbeckens auf (paläo) pedologischer und bodengeographischer Grundlage. Kieler geographische Schriften 45. Selbstverlag des Geographischen Instituts der Universität Kiel, Kiel, Germany.
- Bronger, A., 2003. Correlation of loess-paleosol sequences in East and central Asia with SE central Europe: towards a continental Quaternary pedostratigraphy and paleoclimatic history. *Quaternary International* 106/107, 11–31.
- Bronger, A., Heinkele, T., 1989. Micromorphology and genesis of paleosols in the Luochuan loess section, China: pedostratigraphical and environmental implications. *Geoderma* 45, 123–143.
- Bronger, A., Winter, R., Sedov, S., 1998. Weathering and clay mineral formation in two Holocene soils and in buried paleosols in Tadjikistan towards a Quaternary paleoclimatic record in central Asia. *Catena* 34, 19–34.
- Buggle, B., Glaser, B., Hambach, U., Gerasimenko, N., Marković, S., 2011. An evaluation of geochemical weathering indices in loess-paleosol studies. *Quaternary International* 240, 12–21.
- Buggle, B., Glaser, B., Zöller, L., Hambach, U., Marković, S., Glaser, I., Gerasimenko, N., 2008. Geochemical characterization and origin of southeastern and eastern European loesses (Serbia, Romania, Ukraine). *Quaternary Science Reviews* 27, 1058–1075.
- Buggle, B., Hambach, U., Glaser, B., Gerasimenko, N., Marković, S.B., Glaser, I., Zöller, L., 2009. Stratigraphy and spatial and temporal paleoclimatic trends in east European loess paleosol sequences. *Quaternary International* 196, 86–106.
- Buggle, B., Hambach, U., Kehl, M., Marković, S.B., Zöller, L., Glaser, B., 2013. The progressive evolution of a continental climate in SE-central European lowlands during the Middle Pleistocene recorded in loess paleosol sequences. *Geology* 41, 771–774.
- Buggle, B., Hambach, U., Müller, K., Zöller, L., Marković, S.B., Glaser, B., 2014. Iron mineralogical proxies and Quaternary

- climate change in SE-European loess–paleosol sequences. *Catena* 117, 4–22.
- Buggle, B., Wiesenberg, G., Glaser, B., 2010. Is there a possibility to correct fossil n-alkane data for postsedimentary alteration effects? *Applied Geochemistry* 25, 947–957.
- Buggle, B., Zech, M., 2015. New frontiers in the molecular based reconstruction of Quaternary paleovegetation from loess and paleosols. *Quaternary International* 372, 180–187.
- Bush, R., McInerney, F., 2013. Leaf wax n-alkane distributions in and across modern plants: implications for paleoecology and chemotaxonomy. *Geochimica et Cosmochimica Acta* 117, 161–179.
- Buylaert, J.-P., Ghysels, G., Murray, A.S., Thomsen, K.J., Vandenberghe, D., De Corte, F., Heyse, I., Van den haute, P., 2009. Optical dating of relict sand wedges and composite-wedge pseudomorphs in Flanders, Belgium. *Boreas* 38, 160–175.
- Buylaert, J.-P., Jain, M., Murray, A. S., Thomsen, K. J., Thiel, C., Sohbaty, R., 2012. A robust feldspar luminescence dating method for Middle and Late Pleistocene sediments. *Boreas* 41, 435–451.
- Campbell, G.E., Walker, R.T., Abdrakhmatov, K., Jackson, J., Elliott, J.R., Mackenzie, D., Middleton, T., Schwenninger, J.L., 2015. Great earthquakes in low strain rate continental interiors: an example from SE Kazakhstan. *Journal of Geophysical Research: Solid Earth* 120, 5507–5534.
- Carey, J.B., Cunningham, R.L., Williams, E.G., 1976. Loess identification in soils of southeastern Pennsylvania. *Soil Science Society of America Journal* 40, 745–750.
- Catt, J.A., 1977. Loess and coversands. In: Shotton, F.W. (Ed.), *British Quaternary Studies: Recent Advances*. Oxford University Press, Oxford, pp. 221–229.
- Chapot, M.S., Roberts, H.M., Duller, G.A.T., Lai, Z.P., 2012. A comparison of natural and laboratory-generated dose response curves for quartz optically stimulated luminescence signals from Chinese Loess. *Radiation Measurements* 47, 1045–1052.
- Che, X., Li, G., 2013. Binary sources of loess on the Chinese Loess Plateau revealed by U-Pb ages of zircon. *Quaternary Research* 80, 545–551.
- Chen, F.H., Chen, J.H., Holmes, J., Boomer, I., Austin, P., Gates, J.B., Wang, N.L., Brooks, S.J., Zhang, J.W., 2010. Moisture changes over the last millennium in arid central Asia: a review, synthesis and comparison with monsoon region. *Quaternary Science Reviews* 29, 1055–1068.
- Chen, J., An, Z.S., Head, J., 1999. Variation of Rb/Sr ratios in the loess-paleosol sequences of central China during the last 130,000 years and their implications for monsoon paleoclimatology. *Quaternary Research* 51, 215–219.
- Chen, J., Li, G.J., Yang, J.D., Rao, W.B., Lu, H.Y., Balsam, W., Sun, Y.B., Ji, J.F., 2007. Nd and Sr isotopic characteristics of Chinese deserts: implications for the provenances of Asian dust. *Geochimica et Cosmochimica Acta* 71, 3904–3914.
- Chlachula, J., Evans, M.E., Rutter, N.W., 1998. A magnetic investigation of a Late Quaternary loess/paleosol record in Siberia. *Geophysical Journal International* 132, 128–132.
- Clark, G., Pigott, S., 1965. *Prehistoric Societies*. Hutchinson, London.
- Clark, J.G.D., 1952. *Prehistoric Europe: The Economic Basis*. Methuen, London.
- Clark, P.U., Nelson, A.R., McCoy, W.D., Miller, B.B., Barnes, D.K., 1989. Quaternary aminostratigraphy of Mississippi valley loess. *Geological Society of America Bulletin* 101, 918–926.
- Clark, P.U., Pollard, D., 1998. Origin of the middle Pleistocene transition by ice sheet erosion of regolith. *Paleoceanography* 13, 1–9.
- Colonese, A.C., Zanchetta, G., Fallick, A.E., Manganello, G., Saña, M., Alcade, G., Nebot, J., 2013. Holocene snail shell isotopic record of millennial-scale hydrological conditions in western Mediterranean: data from Bauma del Serrat del Pont (NE Iberian Peninsula). *Quaternary International* 303, 43–53.
- Coude-Gaussen, G., 1987. The perisaharan loess: sedimentological characterization and paleoclimatical significance. *GeoJournal* 15, 177–183.
- Cremaschi, M., Zerboni, A., Nicosia, C., Negrino, F., Rodnight, H., Spötl, C., 2015. Age, soil-forming processes, and archaeology of the loess deposits at the Apennine margin of the Po plain (northern Italy): new insights from the Ghiardo area. *Quaternary International* 376, 173–188.
- Crouvi, O., 2009. Sources and Formation of Loess in the Negev Desert during the Late Quaternary, with Implications for Other Worldwide Deserts. PhD dissertation, Institute of Earth Sciences, The Hebrew University of Jerusalem, Jerusalem.
- Crouvi, O., Amit, R., Ben Israel, M., Enzel, Y., 2017a. Loess in the Negev desert: sources, loessial soils, paleosols, and palaeoclimatic implications. In: Enzel, Y., Bar-Yosef, O. (Eds.), *Quaternary of the Levant: Environments, Climate Change, and Humans*. Cambridge University Press, Cambridge, pp. 471–482.
- Crouvi, O., Amit, R., Enzel, Y., Gillespie, A.R., 2010. The role of active sand seas in the formation of desert loess. *Quaternary Science Reviews* 29, 2087–2098.
- Crouvi, O., Amit, R., Enzel, Y., Porat, N., Sandler, A., 2008. Sand dunes as a major proximal dust source for late Pleistocene loess in the Negev desert, Israel. *Quaternary Research* 70, 275–282.
- Crouvi, O., Barzilai, O., Goldsmith, Y., Amit, R., Porat, N., Enzel, Y., 2014. Middle to Late Pleistocene drastic change in eolian silt grains additions into Mediterranean soils at the Levant's desert fringe. Israel Geological Society of America Annual Meeting, Vancouver, British Columbia. https://gsa.confex.com/gsa/2014AM/finalprogram/abstract_247871.htm.
- Crouvi, O., Dayan, U., Amit, R., Enzel, Y., 2017b. An Israeli haboob: sea breeze activating local anthropogenic dust sources in the Negev loess. *Aeolian Research* 24, 39–52.
- Dani, A.H., Masson, V.M. (Eds.), 1992. *History of Civilizations of Central Asia. Vol. 1, The Dawn of Civilization: Earliest Times to 700 B.C.* UNESCO, Paris.
- Danin, A., Ganor, E., 1991. Trapping of airborne dust by mosses in the Negev desert, Israel. *Earth Surface Processes and Landforms* 16, 153–162.
- Dansgaard, P., 1964. Stable isotopes in precipitation. *Tellus* 16, 436–468.
- Dansgaard, W., Johnsen, S.J., Clausen, H.B., Dahi-Jensen, D., Gundestrup, N.S., Hammer, C.U., Hvidberg, C.S., Steffensen, J.P., Sveinbjörnsdóttir, A.E., Jouzel, J., Bond, G., 1993. Evidence for general instability of past climate from a 250-kyr ice-core record. *Nature* 364, 218–220.
- De Ploey, J., 1977. Some experimental data on slopewash and wind action with reference to Quaternary morphogenesis in Belgium. *Earth Surface Processes* 2, 101–115.
- Dettman, D.L., Kohn, M.J., Quade, J., Ryerson, F.J., Ojha, T.P., Hamidullah, S., 2001. Seasonal stable isotope evidence for a strong Asian monsoon throughout the past 10.7 m.y. *Geology* 29, 31–34.
- Diefendorf, A., Freeman, K., Wing, S., Graham, H., 2011. Production of n-alkyl lipids in living plants and implications for the geologic past. *Geochimica et Cosmochimica Acta* 75, 7472–7485.
- Dietze, E., Wünnemann, B., Hartmann, K., Diekmann, B., Jin, H., Stauch, G., Yang, S., Lehmkuhl, F., 2013. Early to mid-Holocene

- lake high-stand sediments at Lake Gonggi Cona, northeastern Tibetan Plateau, China. *Quaternary Research* 79, 325–336.
- Ding, Z., Rutter, N., Liu, T.S., 1993. Pedostratigraphy of Chinese loess deposits and climatic cycles in the last 2.5 Myr. *Catena* 20, 73–91.
- Ding, Z., Sun, J., Rutter, N.W., Rokosh, D., Liu, T., 1999. Changes in sand content of loess deposits along a north-south transect of the Chinese Loess Plateau and the implications for desert variations. *Quaternary Research* 52, 56–62.
- Ding, Z.L., Derbyshire, E., Yang, S.L., Sun, J.M., Liu, T.S., 2005. Stepwise expansion of desert environment across northern China in the past 3.5 Ma and implications for monsoon evolution. *Earth and Planetary Science Letters* 237, 45–55.
- Ding, Z.L., Derbyshire, E., Yang, S.L., Yu, Z.W., Xiong, S.F., Liu, T.S., 2002a. Stacked 2.6-Ma grain size record from the Chinese loess based on five sections and correlation with the deep-sea $\delta^{18}\text{O}$ record. *Paleoceanography* 17, 5-1–5-21.
- Ding, Z.L., Ranov, V., Yang, S.L., Finaev, A., Han, J.M., Wang, G.A., 2002. The loess record in southern Tajikistan and correlation with Chinese loess. *Earth and Planetary Science Letters* 200, 387–400.
- Ding, Z.L., Yu, Z.W., Rutter, N.W., Liu, T.S., 1994. Towards an orbital time scale for Chinese loess deposits. *Quaternary Science Reviews* 13, 39–70.
- Dirghangi, S., Pagani, M., Hren, M., Tipple, B., 2013. Distribution of glycerol dialkyl glycerol tetraethers in soils from two environmental transects in the USA. *Organic Geochemistry* 59, 49–60.
- Dodonov, A.E., 1991. Loess of central Asia. *GeoJournal* 24, 185–194.
- Dodonov, A.E., 2002. Quaternary of Middle Asia: Stratigraphy, Correlation, Paleogeography. [In Russian.] Geos, Moscow.
- Dodonov, A.E., 2007. Loess records: central Asia. In: Elias, S. (Ed.), *The Encyclopedia of Quaternary Sciences*. Elsevier, Amsterdam, pp. 1418–1429.
- Dodonov, A.E., Baiguzina, L.L., 1995. Loess stratigraphy of central Asia: palaeoclimatic and palaeoenvironmental aspects. *Quaternary Science Reviews* 14, 707–720.
- Dodonov, A.E., Sadchikova, T.A., Sedov, S.N., Simakova, A.N., Zhou, L.P., 2006. Multidisciplinary approach for paleoenvironmental reconstruction in loess-paleosol studies of the Darai Kalon section, southern Tajikistan. *Quaternary International* 152–153, 48–58.
- Dodonov, A.E., Zhou, L., 2008. Loess deposition in Asia: its initiation and development before and during the Quaternary. *Episodes* 31, 222–225.
- Dong, Y., Wu, N., Li, F., Huang, L., Wen, W., 2015. Time-transgressive nature of the magnetic susceptibility record across the Chinese Loess Plateau at the Pleistocene/Holocene transition. *PLoS ONE* 10, e0133541.
- Eagle, R.A., Risi, C., Mitchell, J.L., Eiler, J.M., Seibt, U., Neelin, J.D., Li, G., Tripathi, A.K., 2013. High regional climate sensitivity over continental China constrained by glacial-recent changes in temperature and the hydrological cycle. *Proceedings of the National Academy of Sciences of the United States of America* 110, 8813–8818.
- Edelman, C.H., Crommelin, R.D., 1939. Ueber die periglaziale Natur des Jungpleistozäns in den Niederlanden. *Abhandlungen Natur Verzeichnis Bremen* 31/2, 307–318.
- Eden, D.N., Qizhong, W., Hunt, J.L., Whitton, J.S., 1994. Mineralogical and geochemical trends along the Loess Plateau, North China. *Catena* 21, 73–90.
- Eganhouse, R.P. (Ed.), 1997. *Molecular Markers in Environmental Geochemistry*. ACS Symposium Series 671. American Chemical Society, Washington, DC.
- Eglinton, T., Eglinton, G., 2008. Molecular proxies for paleoclimatology. *Earth and Planetary Science Letters* 275, 1–16.
- Ehlers, J., Eissmann, L., Lippstreu, L., Stephan, H.-J., Wansa, S., 2004. Pleistocene glaciation of North Germany. In: Ehlers, J., Gibbard, P.L. (Eds.), *Quaternary Glaciations – Extent and Chronology, Part I: Europe. Developments in Quaternary Sciences*, Vol. 2. Elsevier, Amsterdam, pp. 135–146.
- Ehlers, J., Grube, A., Stephan, H.J., Wansa, S., 2011. Pleistocene glaciation of North Germany – new results. In: Ehlers, J., Gibbard, P.L., Hughes, P.D. (Eds.), *Quaternary Glaciations – Extent and Chronology: A Closer Look. Developments in Quaternary Sciences*, Vol. 15. Elsevier, Amsterdam, pp. 149–162.
- Espizúa, L.E., 2004. Pleistocene glaciations in the Mendoza Andes, Argentina. In: Ehlers, J., Gibbard, P.L. (Eds.), *Quaternary Glaciations – Extent and Chronology, Part III: South America, Asia, Africa, Australasia, Antarctica. Developments in Quaternary Sciences*, Vol. 2. Elsevier, Cambridge, pp. 69–73.
- Evans, M.E., 2001. Magnetoclimatology of aeolian sediments. *Geophysical Journal International* 144, 495–497.
- Evans, M.E., Heller, F., 2003. *Environmental Magnetism – Principles and Applications of Enviromagnetics*. Academic Press, Amsterdam.
- Evans, M.N., Tolwinski-Ward, S.E., Thompson, D.M., Anchukaitis, K.J., 2013. Applications of proxy system modeling in high resolution paleoclimatology. *Quaternary Science Reviews* 76, 16–28.
- Fedo, C.M., Sircombe, K.N., Rainbird, R.H., 2003. Detrital zircon analysis of the sedimentary record. *Reviews in Mineralogy and Geochemistry* 53, 277–303.
- Fehrenbacher, J.B., White, J.L., Ulrich, H.P., Odell, R.T., 1965. Loess distribution in southeastern Illinois and southwestern Indiana. *Soil Science Society of America Proceedings* 29, 566–572.
- Feng, Z.D., Ran, M., Yang, Q.L., Zhai, X.W., Wang, W., Zhang, X.S., Huang, C.Q., 2011. Stratigraphies and chronologies of late Quaternary loess-paleosol sequences in the core area of the central Asian arid zone. *Quaternary International* 240, 156–166.
- Fenn, K., Stevens, T., Bird, A., Limonta, M., Rittner, M., Vermeesch, P., Andò, S., et al., 2017. Insights into the provenance of the Chinese Loess Plateau from joint zircon U-Pb and garnet geochemical analysis of last glacial loess. *Quaternary Research* (in press). <https://doi.org/10.1017/qua.2017.86>.
- Fink, J., 1956. Zur Korrelation der Terrassen und Löss in Österreich. *Eiszeitalter und Gegenwart* 7, 49–77.
- Fink, J., 1962. Studien zur absoluten und relativen Chronologie der fossilen Böden in Österreich, II Wetzleinsdorf und Stillfried. *Archaeologia Austriaca* 31, 1–18.
- Fink, J., Haase, G., Ruske, R., 1977. Bemerkungen zur Lößkarte von Europe 1:2,5 Mio. *Petermanns Geographische Mitteilungen* 2, 81–94.
- Fink, J., Kukla, G., 1977. Pleistocene climates in central Europe: at least 17 interglacials after the Olduvai event. *Quaternary Research* 7, 363–371.
- Fisher, R.V., 1961. Proposed classification of volcanoclastic sediments and rocks. *Geological Society of America Bulletin* 72, 1409–1414.
- Fitzsimmons, K., Marković, S.B., Hambach, U., 2012. Pleistocene environmental dynamics recorded in the loess of the middle and lower Danube basin. *Quaternary Science Reviews* 41, 104–118.
- Fitzsimmons, K.E., Sprafke, T., Zielhofer, C., Günter, C., Deom, J.-M., Sala, R., Iovita, R., 2016. Loess accumulation in the Tian Shan piedmont: Implications for palaeoenvironmental change in

- arid central Asia. *Quaternary International* (in press). <https://doi.org/10.1016/j.quaint.2016.07.041>.
- Fitzsimmons, K.E., Iovita, R., Sprafke, T., Glantz, M., Talamo, S., Horton, K., Beeton, T., Alipova, S., Bekseitov, G., Ospanov, Y., Deom, J.-M., Sala, R., Taimagambetov, Z., 2017. A chronological framework connecting the early Upper Palaeolithic across the Central Asian piedmont. *Journal of Human Evolution* 113, 107–126.
- Follmer, L.R., 1996. Loess studies in central United States: evolution of concepts. *Engineering Geology* 45, 287–304.
- Food and Agriculture Organization of the United Nations (FAO), International Institute for Applied Systems Analysis (IIASA), ISRIC–World Soil Information, Institute of Soil Science–Chinese Academy of Sciences, and Joint Research Centre of the European Commission, 2009. *Harmonized World Soil Database (version 1.1)*. FAO, Rome; IIASA, Laxenburg, Austria.
- Forman, S.L., Bettis, E.A. III, Kemmis, T.J., Miller, B.B., 1992. Chronological evidence for multiple periods of loess deposition during the Late Pleistocene in the Missouri and Mississippi River Valleys, U.S.: implications for the activity of the Laurentide Ice Sheet. *Palaeogeography, Palaeoclimatology, Palaeoecology* 93, 71–83.
- Forman, S.L., Pierson, J., 2002. Late Pleistocene luminescence chronology of loess deposition in the Missouri and Mississippi river valleys, United States. *Palaeogeography, Palaeoclimatology, Palaeoecology* 186, 25–46.
- Forster, T., Evans, M.E., Heller, F., 1994. The frequency dependence of low field susceptibility in loess sediments. *Geophysical Journal International* 118, 636–642.
- Foss, J.E., Fanning, D.S., Miller, F.P., Wagner, D.P., 1978. Loess deposits of the eastern shore of Maryland. *Soil Science Society of America Journal* 42, 329–334.
- Frazeo, C.J., Fehrenbacher, J.B., Krumbein, W.C., 1970. Loess distribution from a source. *Soil Science Society of America Proceedings* 34, 296–301.
- Gallet, S., Jahn, B., Torii, M., 1996. Geochemical characterization of the Luochuan loess-paleosol sequence China, and paleoclimatic implications. *Chemical Geology* 133, 67–88.
- Gallet, S., Jahn, B., Van Vliet-Lanoë, B., Dia, A., Rossello, E.A., 1998. Loess geochemistry and its implications for particle origin and composition of the upper continental crust. *Earth and Planetary Science Letters* 156, 157–172.
- Gao, X.B., Hao, Q.Z., Wang, L., Oldfield, F., Bloemendal, J., Deng, C.L., Song, Y., et al., 2018. The different climatic response of pedogenic hematite and ferrimagnetic minerals: Evidence from particle-sized modern soils over the Chinese Loess Plateau. *Quaternary Science Reviews* 179, 69–86.
- Gat, J.R., Bowser, C., 1991. The heavy isotope enrichment of water in coupled evaporative systems. In: Taylor, H.P., O'Neil, J.R., Kaplan, I.R. (Eds.), *Stable Isotope Geochemistry: A Tribute to Samuel Epstein*. The Geochemical Society, San Antonio, TX, pp. 159–168.
- Ge, J.Y., Guo, Z.T., Zhao, D.A., Zhang, Y., Wang, T., Yi, L., Deng, C.L., 2014. Spatial variations in paleowind direction during the last glacial period in North China reconstructed from variations in the anisotropy of magnetic susceptibility of loess deposits. *Tectonophysics* 629, 353–361.
- Ghafari, A., Khormali, F., Balsam, W., Karimi, A., Ayoubi, S., 2016. Climatic interpretation of loess-paleosol sequences at Mobarakabad and Aghband, Northern Iran. *Quaternary Research* 86, 95–109.
- Gibbard, P.L., Cohen, K.M., 2008. Global chronostratigraphical correlation table for the last 2.7 million years. *Episodes* 31, 243–247.
- Gild, C., Geitner, C., Sanders, D., 2017. Discovery of a landscape-wide drape of late-glacial aeolian silt in the western Northern Calcareous Alps (Austria): first results and implications. *Geomorphology* 301, 39–52.
- González Bonorino, F., 1966. Soil clay mineralogy of the Pampas plain, Argentina. *Journal of Sedimentary Petrology* 36, 1026–1035.
- Gong, H., Xie, W., Zhang, R., Zhang, Y., 2017. U-Pb ages of detrital zircon and provenances of Red Clay in the Chinese Loess Plateau. *Journal of Asian Earth Sciences* 138, 495–501.
- Good, T.R., Bryant, I.D., 1985. Fluvio-aeolian sedimentation – an example from Banks Island, N.W.T., Canada. *Geografiska Annaler: Series A. Physical Geography* 67, 33–46.
- Gozdzik, J., 1991. Sedimentological record of aeolian processes from the Upper Plenivistulian and the turn of Pleni- and Late Vistulian in central Poland. *Zeitschrift für Geomorphologie, Supplementband* 90, 51–60.
- Grahmann, R., 1932. Der Löss in Europa. *Mitteilungen der Gesellschaft für Erkunde Leipzig* 51, 5–24.
- Greene, R.S.B., Cattle, S.R., McPherson, A.A., 2009. Role of eolian dust deposits in landscape development and soil degradation in southeastern Australia. *Australian Journal of Earth Sciences* 56, S55–S65.
- Grenet, F., de la Vaissière, E., 2002. The Last Days of Panjikent. *Silk Road Art and Archaeology* 8, 155–196.
- Grichuk, V.P., 1992. Main types of vegetation (ecosystems) for the maximum cooling of the last glaciation. In: Frenzel, B., Pecs, B., Velichko, A.A. (Eds.), *Atlas of Palaeoclimates and Palaeoenvironments of the Northern Hemisphere*. INQUA/Hungarian Academy of Sciences, Budapest, pp. 123–124.
- Grimley, D.A., 1996. Stratigraphy, Magnetic Susceptibility, and Mineralogy of Loess-Paleosol Sequences in Southwestern Illinois and Eastern Missouri. PhD dissertation, University of Illinois, Urbana.
- Grimley, D.A., 2000. Glacial and nonglacial sediment contributions to Wisconsin Episode loess in the central United States. *Geological Society of America Bulletin* 112, 1475–1495.
- Grimley, D.A., Ochse, E.A., 2015. Amino acid geochronology of gastropod-bearing Pleistocene units in Illinois, central USA. *Quaternary Geochronology* 25, 10–25.
- Gronenborn, D., 2010. Climate, crises, and the neolithisation of central Europe between IRD-events 6 and 4. In: Gronenborn, D., Petrasch, J. (Eds.), *The Spread of the Neolithic to Central Europe: International Symposium, Mainz 24 June–26 June 2005*. Verlag des Römisch-Germanischen Zentralmuseums, Mainz, Germany, pp. 61–81.
- Grützner, C., Carson, E., Walker, R.T., Rhodes, E.J., Mukambayev, A., Mackenzie, D., Elliott, J.R., Campbell, G., Abdрахmatov, K., 2017. Assessing the activity of faults in continental interiors: palaeoseismic insights from SE Kazakhstan. *Earth and Planetary Science Letters* 459, 93–104.
- Gullentops, F., 1954. Contributions à la chronologie du pleistocène et des formes du relief en Belgique. *Mémoires Institut Géologique de Louvain* 18, 125–252.
- Guo, Z.T., Ruddiman, W.F., Hao, Q.Z., Wu, H.B., Qiao, Y.S., Zhu, R.X., Peng, S.Z., Wei, J.J., Yuan, B.Y., Liu, T.S., 2002. Onset of Asian desertification by 22 Myr ago inferred from loess deposits in China. *Nature* 416, 159–163.
- Guo, Z.T., Berger, A., Yin, Q.Z., Qin, L., 2009. Strong asymmetry of hemispheric climates during MIS-13 inferred from correlating China loess and Antarctica ice records. *Climate of the Past* 5, 21–31.
- Haase, D., Fink, J., Haase, G., Ruske, R., Pécsi, M., Richter, H., Altermann, M., Jäger, K.D., 2007. Loess in Europe—its spatial

- distribution based on a European Loess Map, scale 1:2,500,000. *Quaternary Science Reviews* 26, 1301–1312.
- Haas, M., Bliedner, M., Borodynkina, I., Salazar, G., Szidat, S., Eglinton, T., Zech, R., 2017. Radiocarbon dating of leaf waxes in the loess-paleosol sequence Kurtak, central Siberia. *Radiocarbon* 59, 165–176.
- Haesaerts, P., Borziak, I., Chirica, V., Damblon, F., Koulakovska, L., van der Plicht, J., 2003. The east Carpathian loess record: a reference for the middle and late pleniglacial stratigraphy in central Europe. *Quaternaire* 14, 163–188.
- Haesaerts, P., Chekha, V.P., Damblon, F., Drozdov, N.I., Orlova, L.A., Van der Plicht, J., 2005. The loess-paleosol succession of Kurtak (Yenisei Basin, Siberia): a reference record for the Karga stage (MIS 3). *Quaternaire* 16, 3–24.
- Haesaerts, P., Damblon, F., Gerasimenko, N., Spagna, P., Pirson, S., 2016. The Late Pleistocene loess-paleosol sequence of middle Belgium. *Quaternary International* 411, 25–43.
- Häggi, C., Zech, R., McIntyre, C., Zech, M., Eglinton, T., 2014. On the stratigraphic integrity of leaf-wax biomarkers in loess paleosol. *Biogeosciences* 11, 2455–2463.
- Hajdas, I., 2008. Radiocarbon dating and its application in Quaternary studies. *E&G – Quaternary Science Journal* 57, 2–24.
- Hamilton, T.D., Craig, J.L., Sellmann, P.V., 1988. The Fox permafrost tunnel: a late Quaternary geologic record in central Alaska. *Geological Society of America Bulletin* 100, 948–969.
- Handy, R., 1976. Loess distribution by variable winds. *Geological Society of America Bulletin* 87, 915–927.
- Hao, Q., Guo, Z., 2004. Magnetostratigraphy of a late Miocene-Pliocene loess-soil sequence in the western Loess Plateau in China. *Geophysical Research Letters* 31, L092099.
- Hao, Q.Z., Wang, L., Oldfield, F., Peng, S.Z., Qin, L., Song, Y., Xu, B., Qiao, Y., Bloemendal, J., Guo, Z.T., 2012. Delayed build-up of Arctic ice sheets during 400,000-year minima in insolation variability. *Nature* 490, 393–396.
- Hatté, C., Fontugne, M., Rousseau, D.D., Antoine, P., Zöller, L., Tisnérat-Laborde, N., Bentaleb, I., 1998. $\delta^{13}\text{C}$ variations of loess organic matter as a record of the vegetation response to climatic changes during the Weichselian. *Geology* 26, 583–586.
- Hatté, C., Gauthier, C., Rousseau, D.D., Antoine, P., Fuchs, M., Lagroix, F., Markovic, S.B., Moine, O., Sima, A., 2013. Excursions to C-4 vegetation recorded in the upper Pleistocene loess of Surduk (northern Serbia): an organic isotope geochemistry study. *Climate of the Past* 9, 1001–1014.
- Hawkesworth, C.J., Kemp, A.I.S., 2006. Using hafnium and oxygen isotopes in zircons to unravel the record of crustal evolution. *Chemical Geology* 226, 144–162.
- Heller, F., Evans, M.A., 1995. Loess magnetism. *Reviews of Geophysics* 33, 211–240.
- Heller, F., Liu, T., 1982. Magnetostratigraphical dating of loess deposits in China. *Nature* 300, 431–433.
- Heller, F., Liu, T., 1984. Magnetism of Chinese loess deposits. *Journal of the Royal Astronomical Society* 77, 125–141.
- Heller, F., Liu, X., Liu, T., Xu, T., 1991. Magnetic susceptibility of loess in China. *Earth and Planetary Science Letters* 103, 301–310.
- Heller, F., Shen, C.D., Beer, J., Liu, X.M., Liu, T.S., Bronger, A., Suter, M., Bonani, G., 1993. Quantitative estimates of pedogenic ferromagnetic mineral formation in Chinese loess and paleoclimatic implications. *Earth and Planetary Science Letters* 114, 385–390.
- Hepp, J., Zech, R., Rozanski, K., Tuthorn, M., Glaser, B., Greule, M., Keppler, F., Huang, Y., Zech, W., Zech, M., 2017. Late Quaternary relative humidity changes from Mt. Kilimanjaro, based on a coupled ^2H - ^{18}O biomarker paleohyrometer approach. *Quaternary International* 438B, 116–130.
- Heslop, D., Langereis, C.G., Dekkers, M.J., 2000. A new astronomical timescale for the loess deposits of northern China. *Earth and Planetary Science Letters* 184, 125–139.
- Hesse, P.P., McTainsh, G.H., 2003. Australian dust deposits: modern processes and the Quaternary record. *Quaternary Science Reviews* 22, 2007–2035.
- Ho, P., 1976. *The Cradle of the East: An Enquiry into the Indigenous Origins of Techniques and Ideas of Neolithic and Early Historic China 5000-1000 BC*. Chinese University of Hong Kong Press, Hong Kong.
- Höfle, C., Edwards, M.E., Hopkins, D.M., Mann, D.H., 2000. The full-glacial environment of the northern Seward Peninsula, Alaska, reconstructed from the 21,500-year-old Kitluk paleosol. *Quaternary Research* 53, 143–153.
- Höfle, C., Ping, C.-L., 1996. Properties and soil development of late-Pleistocene paleosols from Seward Peninsula, northwest Alaska. *Geoderma* 71, 219–243.
- Hopkins, D.M., 1963. *Geology of the Imuruk Lake area, Seward Peninsula, Alaska*. U.S. Geological Survey Bulletin 1141-C. U.S. Government Printing Office, Washington, DC.
- Hu, J., Yang, X., 2016. Geochemical and geomorphological evidence for the provenance of the eolian deposits in the Badain Jaran Desert, northwestern China. *Quaternary Science Reviews* 131, 179–192.
- Huijzer, A.S., 1993. Cryogenic Microfabrics and Macrostructures: Interrelations, Processes and Paleoclimatic Significance. PhD dissertation, Vrije Universiteit, Amsterdam.
- Hunt, R.M., 1990. Taphonomy and sedimentology of Arikaree (lower Miocene) fluvial, eolian, and lacustrine paleoenvironments, Nebraska and Wyoming: a paleobiota entombed in fine-grained volcanoclastic rocks. In: Lockley, M.G., Rice, A. (Eds.), *Volcanism and Fossil Biotas*. Geological Society of America, Special Paper 244. Geological Society of America, Boulder, CO, pp. 69–112.
- Ijmker, J., Stauch, G., Dietze, E., Hartmann, K., Diekmann, B., Lockot, G., Opitz, S., Wünnemann, B., Lehmkuhl, F., 2012. Characterisation of transport process and sedimentary deposits by statistical end-member mixing analysis of terrestrial sediments in the Donggi Cona lake catchment, NE Tibet Plateau. *Sedimentary Geology* 281, 166–179.
- Imbrie, J., Imbrie, J.Z., 1980. Modeling the climatic response to orbital variations. *Science* 207, 943–953.
- Indorante, S.J., 1998. Introspection of natric soil genesis on the loess-covered till plain in south central Illinois. *Quaternary International* 51, 41–42.
- Iriondo, M., 1990. Map of the South American plains – its present state. *Quaternary of South America and Antarctic Peninsula* 6, 297–308.
- Iriondo, M.H., Kröhlhling, D.M., 2007. Non-classical types of loess. *Sedimentary Geology* 202, 352–368.
- Jacobs, P.M., Knox, J.C., 1994. Provenance and petrology of a long-term Pleistocene depositional sequence in Wisconsin's Driftless Area. *Catena* 22, 49–68.
- Jacobs, P.M., Mason, J.A., Hanson, P.R., 2012. Loess mantle spatial variability and soil horizonation, southern Wisconsin, USA. *Quaternary International* 265, 42–53.
- Jensen, B.J.L., Evans, M.E., Froese, D.G., Kravchinsky, V.A., 2016. 150,000 Years of loess accumulation in central Alaska. *Quaternary Science Reviews* 135, 1–23.
- Jensen, B.J.L., Reyes, A.V., Froese, D.G., Stone, D.B., 2013. The Palisades is a key reference site for the middle Pleistocene

- of eastern Beringia: new evidence from paleomagnetism and regional tephrostratigraphy. *Quaternary Science Reviews* 63, 91–108.
- Jia, G., Rao, Z., Zhang, J., Li, Z., Chen, F., 2013. Tetraether biomarker records from a loess-paleosol sequence in the western Chinese Loess Plateau. *Frontiers in Microbiology* 4, 199. <http://dx.doi.org/10.3389/fmicb.2013.00199>
- Jiang, W., Cheng, Y., Yang, X., Yang, S., 2013. Chinese Loess Plateau vegetation since the Last Glacial Maximum and its implications for vegetation restoration. *Journal of Applied Ecology* 50, 440–448.
- Jiang, W., Yang, X., Cheng, Y., 2014. Spatial patterns of vegetation and climate on the Chinese Loess Plateau since the Last Glacial Maximum. *Quaternary International* 334–335, 52–60.
- Jipa, D.C., 2014. The conceptual sedimentary model of the Lower Danube loess basin: sedimentogenetic implications. *Quaternary International* 351, 14–24.
- Johnsen, S.J., Dahl-Jensen, D., Gundestrup, N., Steffensen, J.P., Clausen, H.B., Miller, H., Masson-Delmotte, V., Sveinbjörnsdóttir, A.E., White, J., 2001. Oxygen isotope and palaeotemperature records from six Greenland ice-core stations: Camp Century, Dye-3, GRIP, GISP2, Renland and NorthGRIP. *Journal of Quaternary Science* 16, 299–307.
- Johnson, W.C., Willey, K.L., 2000. Isotopic and rock magnetic expression of environmental change at the Pleistocene-Holocene transition in the central Great Plains. *Quaternary International* 67, 89–106.
- Johnson, W.C., Willey, K.L., Mason, J.A., May, D.W., 2007. Stratigraphy and environmental reconstruction at the middle Wisconsinan Gilman Canyon Formation type locality, Buzzard's Roost, southwestern Nebraska, USA. *Quaternary Research* 67, 474–486.
- Karrow, P.F., McAndrews, J.H., Miller, B.B., Morgan, A.V., Seymour, K.L., White, O.L., 2001. Illinoian to Late Wisconsinan stratigraphy at Woodbridge, Ontario. *Canadian Journal of Earth Sciences* 38, 921–942.
- Kasse, C., 1993. Periglacial environments and climate development during the Early Pleistocene Tiglian stage (Beerse Glacial) in northern Belgium. *Geologie en Mijnbouw* 72, 107–123.
- Kasse, C., 1997. Cold-climate aeolian sand-sheet formation in north-western Europe (c. 14–12.4 ka): a response to permafrost degradation and increased aridity. *Permafrost and Periglacial Processes* 8, 295–311.
- Kasse, C., 1999. Late Pleniglacial and Late Glacial aeolian phases in the Netherlands. In: Schirmer, W. (Ed.), *Dunes and Fossil Soils. GeoArchaeoRhein* 3. LIT Verlag, Münster, Germany, pp. 61–82.
- Kasse, C., 2002. Sandy aeolian deposits and environments and their relation to climate during the Last Glacial Maximum and Lateglacial in northwest and central Europe. *Progress in Physical Geography* 26, 507–532.
- Kasse, C., Vandenberghe, D., De Corte, F., Van den Haute, P., 2007. Late Weichselian fluvio-aeolian sands and coversands of the type locality Grubbenvorst (southern Netherlands): sedimentary environments, climate record and age. *Journal of Quaternary Science* 22, 695–708.
- Kaufman, D.S., Manley, W.F., 1998. A new procedure for determining D/L amino acid ratios in fossils using reverse phase liquid chromatography. *Quaternary Science Reviews* 17, 987–1000.
- Kaufman, D.S., Manley, W.F., Ager, T.A., Axford, Y., Balascio, N.L., Begét, J.E., Brigham-Grette, J., et al., 2004. Pleistocene maximum and late Wisconsinan glacier extents across Alaska, U.S.A. In: Ehlers, J., Gibbard, P.L., eds., *Quaternary Glaciations – Extent and Chronology, Part II: North America. Developments in Quaternary Sciences*, Vol. 2. Elsevier, Amsterdam, pp. 9–27.
- Kehl, M., Sahvati, R., Ahmadi, H., Frechen, M., Skowronek, A., 2005. Loess paleosol-sequences along a climatic gradient in northern Iran. *Eiszeitalter und Gegenwart* 55, 149–173.
- Kehrwald, N.M., McCoy, W.D., Thibeault, J., Burns, S.J., Oches, E.A., 2010. Paleoclimatic implications of the spatial patterns of modern and LGM European land-snail shell $\delta^{18}\text{O}$. *Quaternary Research* 74, 166–176.
- Kleiss, H.J., 1973. Loess distribution along the Illinois soil-development sequence. *Soil Science* 115, 194–198.
- Koloszar, L., 2010. The thickest and the most complete loess sequence in the Carpathian basin: the borehole Udvari-2A. *Open Geosciences* 2, 165–174.
- Koppes, M., Gillespie, A.R., Burke, R.M., Thompson, S.C., Stone, J., 2008. Late Quaternary glaciation in the Kyrgyz Tien Shan. *Quaternary Science Reviews* 27, 846–866.
- Kosnik, M.A., Kaufman, D.S., Hua, Q., 2008. Identifying outliers and assessing the accuracy of amino acid racemization measurements for geochronology: I. Age calibration curves. *Quaternary Geochronology* 3, 308–327.
- Koster, E., 1988. Ancient and modern cold-climate aeolian sand deposition. *Journal of Quaternary Science* 3, 69–83.
- Kozarski, S., 1990. Pleniglacial and Late Vistulian aeolian phenomena in Poland: new occurrences, palaeoenvironmental and stratigraphic interpretations. *Acta Geographica Debrecina 1987–1988*, 26–27, 31–45.
- Kruk, J., Alexadrowicz, S., Milisauskas, S., Śnieszko, Z., 1996. *Environmental Changes and Settlement on the Loess Uplands*. [In Polish.] Polish Academy of Sciences, Kraków, Poland.
- Kruk, J., Milisauskas, S., 1999. *The Rise and Fall of Neolithic Societies*. [In Polish.] Polish Academy of Sciences, Kraków, Poland.
- Kukla, G.J., 1975. Loess stratigraphy of central Europe. In: Butzer, K.W., Isaac, L.I. (Eds.), *After the Australopithecines*. Mouton, The Hague, the Netherlands, pp. 99–187.
- Kukla, G., 1977. Pleistocene land-sea correlations. 1. Europe. *Earth-Science Reviews* 13, 307–374.
- Kukla, G., 1987. Loess stratigraphy in central China. *Quaternary Science Reviews* 6, 191–219.
- Kukla, G., An, Z., 1989. Loess stratigraphy in central China. *Palaeogeography, Palaeoclimatology, Palaeoecology* 72, 203–225.
- Kukla, G., Heller, F., Liu, X., Xu, T., Liu, T., An, Z., 1988. Pleistocene climates in China dated by magnetic susceptibility. *Geology* 16, 811–814.
- Kutzbach, J.E., 1987. Model simulations of the climatic patterns during the deglaciation of North America. In: Ruddiman, W.F., Wright, H.E. (Eds.), *North America and Adjacent Oceans during the Last Deglaciation - The Geology of North America*. The Geological Society of America, Boulder, pp. 425–446.
- LaGarry, H.E., 1998. Lithostratigraphic revision and redescription of the Brule Formation (White River Group) of northwestern Nebraska. In: Terry, D.O. Jr., LaGarry, H.E., Hunt, R.M. Jr. (Eds.), *Depositional Environments, Lithostratigraphy, and Biostratigraphy of the White River and Arikaree Groups (Late Eocene-Early Miocene, North America)*. Geological Society of America, Special Paper 325. Geological Society of America, Boulder, CO, pp. 63–91.
- Lagroix, F., Banerjee, S.K., 2004. The regional and temporal significance of primary aeolian magnetic fabrics preserved in Alaskan loess. *Earth and Planetary Science Letters* 225, 379–395.

- Lambert, F., Delmonte, B., Petit, J.R., Bigler, M., Kaufmann, P.R., Hutterli, M.A., Stocker, T.F., Ruth, U., Steffensen, J.P., Maggi, V., 2008. Dust-climate couplings over the past 800,000 years from the EPICA Dome C ice core. *Nature* 452, 616–619.
- Lang, A., Hatté, C., Rousseau, D.D., Antoine, P., Fontugne, M., Zöller, L., Hambach, U., 2003. High-resolution chronologies for loess: comparing AMS¹⁴C and optical dating results. *Quaternary Science Reviews* 22, 953–959.
- Laskar, J., Robutel, P., Joutel, F., Gastineau, M., Correia, A.C.M., Levrard, B., 2004. A long-term numerical solution for the insolation quantities of the Earth. *Astronomy Astrophysics* 428, 261–285.
- Lautridou, J.-P., 1981. Lithostratigraphie et chronostratigraphie des loess de Haute Normandie. In: Pécsi, M. (Ed.), *Studies on Loess. Acta Geologica Academiae Scientiarum Hungaricae* 22. Akadémiai Kiadó, Budapest, pp. 125–132.
- Lautridou, J.-P., Sommé, J., 1981. L'extension des niveaux repères périglaciaires et grandes fentes de gel de la stratigraphie du Pleistocène Récent de la France du Nord-Ouest. *Biuletyn Peryglacjalny* 28, 179–185.
- Lautridou, J.P., Sommé, J., Jamagne, M., 1984. Sedimentological, mineralogical and geochemical characteristics of the loess of north-western France. In: Pécsi, M. (Ed.), *Lithology and Stratigraphy of Loess and Paleosols*. Geographical Research Institute of the Hungarian Academy of Science, Budapest, pp. 121–132.
- Lea, P.D., 1990. Pleistocene periglacial eolian deposits in south-western Alaska: sedimentary facies and depositional processes. *Journal of Sedimentary Petrology* 60, 582–591.
- Lea, P.D., Waythomas, C.F., 1990. Late-Pleistocene eolian sand sheets in Alaska. *Quaternary Research* 34, 269–281.
- Lehmkuhl, F., Haselein, F., 2000. Quaternary paleoenvironmental change on the Tibetan Plateau and adjacent areas (western China and western Mongolia). *Quaternary International* 65, 121–145.
- Lehmkuhl, F., Hilgers, A., Fries, S., Hülle, D., Schlütz, F., Shumilovskikh, L., Felauer, T., Protze, J., 2011. Holocene geomorphological processes and soil development as indicator for environmental change around Karakorum, Upper Orkhon Valley (central Mongolia). *Catena* 87, 31–44.
- Lehmkuhl, F., Schulte, P., Zhao, H., Hülle, D., Protze, J., Stauch, G., 2014. Timing and spatial distribution of loess and loess-like sediments in the mountain areas of the northeastern Tibetan Plateau. *Catena* 117, 23–33.
- Lehmkuhl, F., Zens, J., Krauß, L., Schulte, P., Kels, H., 2016. Loess-paleosol sequences at the northern European loess-belt in Germany: distribution, geomorphology and stratigraphy. *Quaternary Science Reviews* 153, 11–30.
- Leigh, D.S., 1994. Roxana Silt of the Upper Mississippi Valley: lithology, source, and paleoenvironment. *Geological Society of America Bulletin* 106, 430–442.
- Leigh, D.S., Knox, J.C., 1994. Loess of the Upper Mississippi Valley Driftless Area. *Quaternary Research* 42, 30–40.
- Leonard, A.B., Frye, J.C., 1960. *Wisconsinan Molluscan Faunas of the Illinois Valley Region*. Illinois Geological Survey Circular 304. Illinois Geological Survey, Urbana, IL.
- Li, B., Li, S.-H., 2012. Luminescence dating of Chinese loess beyond 130 ka using the non-fading signal from K-feldspar. *Quaternary Geochronology* 10, 24–31.
- Li, F., Wu, N., Pei, Y., Hao, Q., Rousseau, D.-D., 2006. Wind-blown origin of Dongwan late Miocene–Pliocene dust sequence documented by land snail record in western Chinese Loess Plateau. *Geology* 34, 405–408.
- Li, Y., Song, Y., Chen, X., Li, J., Mamadjanov, Y., Aminov, J., 2016a. Geochemical composition of Tajikistan loess and its provenance implications. *Palaogeography, Palaeoclimatology, Palaeoecology* 446, 186–194.
- Li, Y., Yang, S., Wang, X., Hu, J., Cui, L., Huang, X., Jiang, W., 2016b. Leaf wax n-alkane distributions in Chinese loess since the Last Glacial Maximum and implications for paleoclimate. *Quaternary International* 399, 190–197.
- Liang, Y., Yang, T.B., Velichko, A.A., Zeng, B., Shi, P.H., Wang, L.D., Chen, Y., 2016. Paleoclimatic record from Chumbur-Kosa section in Sea of Azov region since Marine Isotope Stage 11. *Journal of Mountain Science* 13, 985–999.
- Licht, A., Pullen, A., Kapp, P., Abell, J., Gieser, N., 2016. Eolian cannibalism: reworked loess and fluvial sediment as the main sources of the Chinese Loess Plateau. *Geological Society of America Bulletin* 128, 944–956.
- Lisiecki, L.E., Raymo, M.E., 2005. A Pliocene–Pleistocene stack of 57 globally distributed benthic $\delta^{18}\text{O}$ records. *Paleoceanography* 20, PA1003.
- Litaor, M.I., 1987. The influence of eolian dust on the genesis of alpine soils in the Front Range, Colorado. *Soil Science Society of America Journal* 51, 142–147.
- Liu, C.-Q., Masuda, A., Okada, A., Yabuki, S., Zhang, J., Fan, Z.-L., 1993. A geochemical study of loess and desert sand in northern China: implications for continental crust weathering and composition. *Chemical Geology* 106, 359–374.
- Liu, J., Murray, A.S., Buylaert, J.-P., Jain, M., Chen, J., Lu, Y., 2016. Stability of fine-grained TT-OSL and post-IR IRSL signals from a c. 1 Ma sequence of aeolian and lacustrine deposits from the Nihewan Basin (northern China). *Boreas* 45, 703–714.
- Liu, Q.S., Roberts, A.P., Larrasoana, J.C., Banerjee, S.K., Guyodo, Y., Tauxe, L., Oldfield, F., 2012. Environmental magnetism: principles and applications. *Reviews of Geophysics* 50, RG4002.
- Liu, T., Ding, Z., 1998. Chinese loess and the paleomonsoon. *Annual Review of Earth and Planetary Sciences* 26, 111–145.
- Liu, T.S., 1966. *Composition and Texture of Loess*. Science Press, Beijing.
- Liu, T.S., 1985. *Loess and Environment*. China Ocean Press, Beijing.
- Liu, W., Huang, Y., 2005. Compound specific D/H ratios and molecular distributions of higher plant leaf waxes as novel paleoenvironmental indicators in the Chinese Loess Plateau. *Organic Geochemistry* 36, 851–860.
- Liu, W., Huang, Y., An, Z., Clemens, S.C., Li, L., Prell, W.L., Ning, Y., 2005. Summer monsoon intensity controls C₄/C₃ plant abundance during the last 35 ka in the Chinese Loess Plateau: carbon isotope evidence from bulk organic matter and individual leaf waxes. *Palaogeography, Palaeoclimatology, Palaeoecology* 220, 243–254.
- Liu, W., Sun, J., 2012. High-resolution anisotropy of magnetic susceptibility record in the central Chinese Loess Plateau and its paleoenvironment implications. *Science China Earth Science* 55, 488–494.
- Liu, W., Yang, H., Sun, Y., Wang, X., 2011. $\delta^{13}\text{C}$ values of loess total carbonate: a sensitive proxy for Asian summer monsoon in arid northwestern margin of the Chinese loess plateau. *Chemical Geology* 284, 317–322.
- Liu, X., 2010. *The Silk Road in World History*. Oxford University Press, New York.
- Lorenzo, F., Mehl, A., Zárate, M., 2017. Dinámica fluvial y sedimentología del humedal Bañados del Atuel, provincia de La Pampa, Argentina. ACTAS XX Congreso Geológico Argentino, San Miguel de Tucumán, pp. 91–93.

- Lu, H., An, Z., 1998. Paleoclimatic significance of grain size of loess-palaeosol deposit in Chinese Loess Plateau. *Science in China* 41D, 626–631.
- Lu, H., Stevens, T., Yi, S., Sun, X., 2006. An erosional hiatus in Chinese loess sequences revealed by closely spaced optical dating. *Chinese Science Bulletin* 51, 2253–2259.
- Lu, H.Y., Wu, N.Q., Liu, K.B., Jiang, H., Liu, T.S., 2007. Phytoliths as quantitative indicators for the reconstruction of past environmental conditions in China II: palaeoenvironmental reconstruction in the Loess Plateau. *Quaternary Science Reviews* 26, 759–772.
- Luehmann, M.D., Peter, B., Connallon, C.B., Schaetzl, R.J., Smidt, S.J., Liu, W., Kincare, K., Walkowiak, T.A., Thorlund, E., Holler, M.S., 2016. Loamy, two-storied soils on the outwash plains of southwestern Lower Michigan: pedoturbation of loess with the underlying sand. *Annals of the Association of American Geographers* 106, 551–571.
- Luehmann, M.D., Schaetzl, R.J., Miller, B.A., Bigsby, M., 2013. Thin, pedoturbated and locally sourced loess in the western Upper Peninsula of Michigan. *Aeolian Research* 8, 85–100.
- Maat, P.B., Johnson, W.C., 1996. Thermoluminescence and new C-14 age estimates for late Quaternary loesses in southwestern Nebraska. *Geomorphology* 17, 115–128.
- Machalett, B., Oches, E.A., Frechen, M., Zöller, L., Hambach, U., Mavlyanova, N.G., Markovic, S.B., Endlicher, W., 2008. Aeolian dust dynamics in central Asia during the Pleistocene: driven by the long-term migration, seasonality and permanency of the Asiatic polar front. *Geophysics, Geochemistry, Geosystems* 9, Q08Q09. <http://dx.doi.org/10.1029/2007GC001938>.
- Maher, B.A., 2011. The magnetic properties of Quaternary aeolian dusts and sediments, and their palaeoclimatic significance. *Aeolian Research* 3, 87–144.
- Maher, B.A., 2016. Palaeoclimatic records of the loess/palaeosol sequences of the Chinese Loess Plateau. *Quaternary Science Reviews* 154, 23–84.
- Maher, B.A., Thompson, R., 1992. Paleoclimatic significance of the mineral magnetic record of the Chinese loess and paleosols. *Quaternary Research* 37, 155–170.
- Mahowald, N.M., Muhs, D.R., Levis, S., Rasch, P.J., Yoshioka, M., Zender, C.S., Luo, C., 2006. Change in atmospheric mineral aerosols in response to climate: Last glacial period, pre-industrial, modern, and doubled carbon dioxide climates. *Journal of Geophysical Research*, 111. doi: <http://dx.doi.org/10.1029/2005JD006653>
- Mancini, M.V., Paez, M.M., Prieto, A.R., Stutz, S., Tonello, M., Vilanova, I., 2005. Mid-Holocene climatic variability reconstruction from pollen records (32°–52°S, Argentina). *Quaternary International* 132, 47–59.
- Manikowska, B., 1994. Etat des études des processus éoliens dans la région de Lodz (Pologne centrale). *Biuletyn Peryglacjalny* 33, 107–131.
- Markewich, H.W., Wysocki, D.A., Pavich, M.J., Rutledge, E.M., Millard, H.T., Rich, F.J., Maat, P.B., Rubin, M., McGeehin, J.P., 1998. Paleopedology plus TL, ¹⁰Be, and ¹⁴C dating as tools in stratigraphic and paleoclimatic investigations, Mississippi River Valley, U.S.A. *Quaternary International* 51–2, 143–167.
- Marković, S.B., Bokhorst, M., Vandenberghe, J., Oches, E.A., Zöller, L., McCoy, W.D., Gaudenyi, T., Jovanović, M., Hambach, U., Machalett, B., 2008. Late Pleistocene loess-palaeosol sequences in the Vojvodina region, North Serbia. *Journal of Quaternary Science* 23, 73–84.
- Marković, S.B., Fitzsimmons, K.E., Sprafke, T., Gavrilovic, D., Smalley, I.J., Jovic, V., Svirčev, Z., Gavrilov, M.B., Bešlin, M., 2016. The history of Danube loess research. *Quaternary International* 399, 86–99.
- Marković, S.B., Hambach, U., Catto, N., Jovanović, M., Buggle, B., Machalett, B., Zöller, L., Glaser, B., Frechen, M., 2009. Middle and Late Pleistocene loess sequences at Batajnica, Vojvodina, Serbia. *Quaternary International* 198, 255–266.
- Marković, S.B., Hambach, U., Stevens, T., Kukla, G.J., Heller, F., McCoy, W.D., Oches, E.A., Buggle, B., Zöller, L., 2011. The last million years recorded at the Stari Slankamen loess-palaeosol sequence: revised chronostratigraphy and long-term environmental trends. *Quaternary Science Reviews* 30, 1142–1154.
- Marković, S.B., Oches, E.A., McCoy, W.D., Gaudenyi, T., Frechen, M., 2007. Malacological and sedimentological evidence for “warm” climate from the Irig loess sequence (Vojvodina, Serbia). *Geophysics, Geochemistry, Geosystems* 8, Q09008.
- Marković, S.B., Oches, E.A., Sümegei, P., Jovanovic, M., Gaudenyi, T., 2006. An introduction to the Middle and Upper Pleistocene loess-palaeosol sequence at Ruma brickyard, Vojvodina, Serbia. *Quaternary International* 149, 80–86.
- Marković, S.B., Stevens, T., Kukla, G.J., Hambach, U., Fitzsimmons, K.E., Gibbard, P., Buggle, B., et al., 2015. Danube loess stratigraphy – towards a pan-European loess stratigraphic model. *Earth-Science Reviews* 148, 228–258.
- Marshak, B.I., 2003. The Archaeology of Sogdiana. *The Silk Road* 1, 2–8.
- Martignier, L., Nussbaumer, M., Adatte, T., Gobat, J.-M., Verrecchia, E.P., 2015. Assessment of a locally-sourced loess system in Europe: the Swiss Jura Mountains. *Aeolian Research* 18, 11–21.
- Mason, J.A., Jacobs, P.M., Hanson, P.R., Miao, X.D., Goble, R.J., 2003. Sources and paleoclimatic significance of Holocene Bignell Loess, central Great Plains, USA. *Quaternary Research* 60, 330–339.
- Mason, J.A., Joeckel, R.M., Bettis, E.A. III, 2007. Middle to Late Pleistocene loess record in eastern Nebraska, USA, and implications for the unique nature of Oxygen Isotope Stage 2. *Quaternary Science Reviews* 26, 773–792.
- Mason, J.A., Miao, X.D., Hanson, P.R., Johnson, W.C., Jacobs, P. M., Goble, R.J., 2008. Loess record of the Pleistocene-Holocene transition on the northern and central Great Plains, USA. *Quaternary Science Reviews* 27, 1772–1783.
- Masson-Delmotte, V., Schulz, M., Abe-Ouchi, A., Beer, J., Ganopolski, A., González Rouco, J.F., Jansen, E., Lambeck, K., Luterbacher, J., Naish, T., Osborn, T., Otto-Bliesner, B., Quinn, T., Ramesh, R., Rojas, M., Shao, X., Timmermann, A., 2013. Information from Paleoclimate Archives. In: Stocker, T.F., Qin, G.-K. Plattner, M. Tignor, S.K. Allen, J. Boschung, A. Nauels, Y. Xia, V. Bex, P.M. Midgley (Eds.), *Climate Change 2013: The Physical Science Basis. Contribution of Working Group I to the Fifth Assessment Report of the Intergovernmental Panel on Climate Change*. Cambridge University Press, Cambridge, pp. 383–464.
- Matasova, G., Petrovský, E., Jordanova, N., Zykina, V., Kapika, A., 2001. Magnetic study of Late Pleistocene loess/palaeosol sections from Siberia: palaeoenvironmental implications. *Geophysical Journal International* 147, 367–380.
- Matthews, N.E., Vasquez, J.A., Calvert, A.T., 2015. Age of the Lava Creek supereruption and magma chamber assembly at Yellowstone based on ⁴⁰Ar/³⁹Ar and U-Pb dating of sanidine and zircon crystals. *Geochemistry, Geophysics, Geosystems* 16, 2508–2528.
- McLennan, S.M., 2001. Relationships between the trace element composition of sedimentary rocks and upper continental crust. *Geochemistry, Geophysics, Geosystems* 2, 1021. <http://dx.doi.org/10.1029/2000GC000109>.

- McTainsh, G., 1987. Desert loess in northern Nigeria. *Zeitschrift für Geomorphologie N.F.* 31, 145–165.
- Mesner, S., Kreutzer, S., Fuchs, M., Faust, D., 2014. Identifying depositional and pedogenetic controls of Late Pleistocene loess-palaeosol sequences (Saxony, Germany) by combined grain size and microscopic analyses. *Zeitschrift für Geomorphologie, Supplementary. Issues* 58, 63–90.
- Miao, X.D., Mason, J.A., Johnson, W.C., Wang, H., 2007. High-resolution proxy record of Holocene climate from a loess section in southwestern Nebraska, USA. *Palaeogeography, Palaeoclimatology, Palaeoecology* 245, 368–381.
- Miller, B.B., Graham, R.W., Morgan, A.V., Norton, G.M., McCoy, W.D., Palmer, D.F., Smith, A.J., Pilny, J.J., 1994. A biota associated with Matuyama-age sediments in west-central Illinois. *Quaternary Research* 41, 350–365.
- Moine, O., 2014. Weichselian Upper Pleniglacial environmental variability in north-western Europe reconstructed from terrestrial mollusc faunas and its relationship with the presence/absence of human settlements. *Quaternary International* 337, 90–113.
- Moine, O., Antoine, P., Hatté, C., Landais, A., Mathieu, J.C., Prud'homme, C., Rousseau, D., 2017. The impact of Last Glacial climate variability in west-European loess revealed by radiocarbon dating of fossil earthworm granules. *Proceedings of the National Academy of Sciences of the United States of America* 114, 6209–6214.
- Moine, O., Rousseau, D.-D., Jolly, D., Vianey-Liaud, M., 2002. Paleoclimatic reconstruction using mutual climatic range on terrestrial mollusks. *Quaternary Research* 57, 162–172.
- Moine, O., Rousseau, D.D., Antoine, P., 2008. The impact of Dansgaard-Oeschger cycles on the loessic environment and malacofauna of Nussloch (Germany) during the Upper Weichselian. *Quaternary Research* 70, 91–104.
- Mücher, H., Vreeken, W., 1981. (Re)deposition of loess in southern Limburg, The Netherlands. II. Micromorphology of the lower silt loam complex and comparison with deposits produced under laboratory conditions. *Earth Surface Processes and Landforms* 6, 355–363.
- Muhs, D.R., 2013a. The geologic records of dust in the Quaternary. *Aeolian Research* 9, 3–48.
- Muhs, D.R., 2013b. Loess and its geomorphic, stratigraphic, and paleoclimatic significance in the Quaternary. In: Shroder, J.F. (Ed.), *Treatise on Geomorphology*. Academic Press, San Diego, CA, pp. 149–183.
- Muhs, D.R., Ager, T.A., Been, J., Bradbury, J.P., Dean, W.E., 2003a. A late Quaternary record of eolian silt deposition in a maar lake, St. Michael Island, western Alaska. *Quaternary Research* 60, 110–122.
- Muhs, D.R., Ager, T.A., Bettis, E.A., III, McGeehin, J., Been, J.M., Begét, J.E., Pavich, M.J., Stafford, T.W. Jr., Stevens, D.S.P., 2003b. Stratigraphy and paleoclimatic significance of late Quaternary loess-palaeosol sequences of the last interglacial-glacial cycle in central Alaska. *Quaternary Science Reviews* 22, 1947–1986.
- Muhs, D.R., Ager, T.A., Skipp, G., Beann, J., Budahn, J.R., McGeehin, J.P., 2008a. Paleoclimatic significance of chemical weathering in loess-derived paleosols of subarctic central Alaska. *Arctic, Antarctic, and Alpine Research* 40, 396–411.
- Muhs, D.R., Bettis, E.A. III, 2000. Geochemical variations in Peoria Loess of western Iowa indicate paleowinds of midcontinental North America during last glaciation. *Quaternary Research* 53, 49–61.
- Muhs, D.R., Bettis, E.A. III, 2003. Quaternary loess-palaeosol sequences as examples of climate-driven sedimentary extremes. *Geological Society of America Special Paper* 370, 53–74.
- Muhs, D.R., Bettis, E.A. III, Aleinikoff, J.N., McGeehin, J.P., Beann, J., Skipp, G., Marshall, B.D., Roberts, H.M., Johnson, W.C., Benton, R., 2008b. Origin and paleoclimatic significance of late Quaternary loess in Nebraska: evidence from stratigraphy, chronology, sedimentology, and geochemistry. *Geological Society of America Bulletin* 120, 1378–1407.
- Muhs, D.R., Bettis, E.A. III, Been, J., McGeehin, J., 2001. Impact of climate and parent material on chemical weathering in loess-derived soils of the Mississippi River Valley. *Soil Science Society of America Journal* 65, 1761–1777.
- Muhs, D.R., Bettis, E.A. III, Roberts, H.M., Harlan, S.S., Paces, J.B., Reynolds, R.L., 2013a. Chronology and provenance of last-glacial (Peoria) loess in western Iowa and paleoclimatic implications. *Quaternary Science Reviews* 80, 468–481.
- Muhs, D.R., Budahn, J.R., 2006. Geochemical evidence for the origin of late Quaternary loess in central Alaska. *Canadian Journal of Earth Sciences* 43, 323–337.
- Muhs, D.R., Budahn, J., Johnson, D.L., Rehis, M., Beann, J., Skipp, G., Fisher, E., Jones, J.A., 2008c. Geochemical evidence for airborne dust additions to soils in Channel Islands National Park, California. *Geological Society of America Bulletin* 120, 106–126.
- Muhs, D.R., Budahn, J.R., McGeehin, J.P., Bettis, E.A. III, Skipp, G., Paces, J.B., Wheeler, E.A., 2013b. Loess origin, transport, and deposition over the past 10,000 years, Wrangell-St. Elias National Park, Alaska. *Aeolian Research* 11, 85–99.
- Muhs, D.R., Budahn, J., Reheis, M., Beann, J., Skipp, G., Fisher, E., 2007. Airborne dust transport to the eastern Pacific Ocean off southern California: evidence from San Clemente Island. *Journal of Geophysical Research* 112, D13203. <http://dx.doi.org/10.1029/2006JD007577>.
- Muhs, D.R., Budahn, J.R., Skipp, G.L., McGeehin, J.P., 2016. Geochemical evidence for seasonal controls on the transportation of Holocene loess, Matanuska Valley, southern Alaska, USA. *Aeolian Research* 21, 61–73.
- Muhs, D.R., McGeehin, J.P., Beann, J., Fisher, E., 2004. Holocene loess deposition and soil formation as competing processes, Matanuska Valley, southern Alaska. *Quaternary Research* 61, 265–276.
- Muhs, D.R., Pigati, J.S., Budahn, J.R., Skipp, G.L., Bettis, E.A. III, Jensen, B., 2018. Origin of last-glacial loess in the western Yukon-Tanana Upland, central Alaska, USA. *Quaternary Research* (in press).
- Muhs, D.R., Roskin, J., Tsoar, H., Skipp, G., Budahn, J.R., Sneh, A., Porat, N., Stanley, J.-D., Katra, I., Blumberg, D.G., 2013c. Origin of the Sinai-Negev erg, Egypt and Israel: mineralogical and geochemical evidence for the importance of the Nile and sea level history. *Quaternary Science Reviews* 69, 28–48.
- Munroe, J.S., Attwood, E.C., O'Keefe, S.S., Quackenbush, P.J.M., 2015. Eolian deposition in the alpine zone of the Uinta Mountains, Utah, USA. *Catena* 124, 119–129.
- Nagashima, K., Tada, R., Tani, A., Toyoda, S., Sun, Y., Isozaki, Y., 2007. Contribution of aeolian dust in Japan Sea sediments estimated from ESR signal intensity and crystallinity of quartz. *Geochemistry Geophysics Geosystems*, 8. doi: 10.1029/2006GC001364.
- Nagashima, K., Tada, R., Tani, A., Sun, Y., Isozaki, Y., Toyoda, S., Hasegawa, H., 2011. Millennial-scale oscillations of the westerly jet path during the last glacial period. *Journal of Asian Earth Sciences* 40, 1214–1220.
- Nash, T.A., Conroy, J.L., Grimley, D.A., Guenther, W.R., Curry, B.B., 2017. Episodic deposition of Illinois Valley Peoria Silt in

- association with Lake Michigan Lobe fluctuations during the last glacial maximum. *Quaternary Research* (in press). <https://doi.org/10.1017/qua.2017.66>.
- Nawrocki, J., Polechonska, O., Boguckij, A., Lanczont, M., 2006. Palaeowind directions recorded in the youngest loess in Poland and western Ukraine as derived from anisotropy of magnetic susceptibility measurements. *Boreas* 35, 266–271.
- Necula, C., Dimofte, D., Panaiotu, C., 2015. Rock magnetism of a loess-palaeosol sequence from the western Black Sea shore (Romania). *Geophysical Journal International* 202, 1733–1748.
- Nekola, J.C., Coles, B.F., 2010. Pupillid land snails of eastern North America. *American Malacological Bulletin* 28, 29–57.
- Nelson, M.S., Rittenour, T.M., 2015. Using grain-size characteristics to model soil water content: application to dose-rate calculation for luminescence dating. *Radiation Measurements* 81, 142–149.
- Nie, J., Song, Y., Möller, A., Stockli, D.F., Peng, W., Stevens, T., Bird, A., Oalman, J., Liu, S., Horton, B.K., Fang, X., 2014. Provenance of the upper Miocene–Pliocene Red Clay deposits of the Chinese loess plateau. *Earth and Planetary Science Letters* 407, 35–47.
- Nie, J., Stevens, T., Rittner, M., Stockli, D., Garzanti, E., Limonta, M., Bird, A., et al., 2015. Loess Plateau storage of northeastern Tibetan Plateau-derived Yellow River sediment. *Nature Communications* 6, 8511. <http://dx.doi.org/10.1038/ncomms9511>.
- North Greenland Ice Core Project Members, Andersen, K.K., Azuma, N., Barnola, J.-M., Bigler, M., Biscaye, P., Caillon, N., et al., 2004. High-resolution record of Northern Hemisphere climate extending into the last interglacial period. *Nature* 431, 147–151.
- Nottebaum, V., Stauch, G., Hartmann, K., Zhang, J., Lehmkuhl, F., 2015. Unmixed loess grain size populations along the northern Qilian Shan (China): relationships between geomorphologic, sedimentologic and climatic controls. *Quaternary International* 372, 151–166.
- Novothy, A., Frechen, M., Horváth, E., Wacha, L., Rolf, C., 2011. Investigating the penultimate and last glacial cycles of the Süttő loess section (Hungary) using luminescence dating, high-resolution grain size, and magnetic susceptibility data. *Quaternary International* 234, 75–85.
- Nowaczyk, B., 1986. *The Age of Dunes, Their Textural and Structural Properties against Atmospheric Circulation Pattern of Poland during the Late Vistulian and Holocene*. *Seria Geografia* 28. Adam Mickiewicz University Press, Poznań, Poland.
- Nugteren, G., Vandenberghe, J., 2004. Spatial climatic variability on the Central Loess Plateau (China) as recorded by grain size for the last 250 kyr. *Global and Planetary Change* 41, 185–206.
- Nyland, K.E., Schaetzl, R.J., Ignatov, A., Miller, B.A., 2017. A new depositional model for sand-rich loess on the Buckley Flats outwash plain, northwestern Lower Michigan. *Aeolian Research* (in press). <https://doi.org/10.1016/j.aeolia.2017.05.005>.
- Obrecht, I., Buggle, B., Catto, N., Marković, S.B., Bösel, S., Vandenberghe, D.A.G., Hambach, U., et al., 2014. The Late Pleistocene Belotinac section (southern Serbia) at the southern limit of the European loess belt: environmental and climate reconstruction using grain size and stable C and N isotopes. *Quaternary International* 334–335, 10–19.
- Obrecht, I., Hambach, U., Veres, D., Zeeden, C., Böskén, J., Stevens, T., Marković, S.B., et al., 2017. Shift of large-scale atmospheric systems over Europe during late MIS 3 and implications for Modern Human dispersal. *Scientific Reports* 7, 5848. <http://dx.doi.org/10.1038/s41598-017-06285-x>.
- Obrecht, I., Zeeden, C., Hambach, U., Veres, D., Marković, S.B., Böskén, J., Svirčev, Z., Bačević, N., Gavrilov, M.B., Lehmkuhl, F., 2016. Tracing the influence of Mediterranean climate on southeastern Europe during the past 350,000 years. *Scientific Reports* 6, 36334. <http://dx.doi.org/10.1038/srep36334>.
- Obrecht, I., Zeeden, C., Schulte, P., Hambach, U., Eckmeier, E., Timar-Gabor, A., Lehmkuhl, F., 2015. Aeolian dynamics at the Orlovat loess–paleosol sequence, northern Serbia, based on detailed textural and geochemical evidence. *Aeolian Research* 18, 69–81.
- Oches, E.A., Banerjee, S.K., Solheid, P.A., Frechen, M., 1998. High resolution proxies of climate variability in the Alaskan loess record. In: Busacca, A.J. (Ed.), *Dust Aerosols, Loess Soils and Global Change*. *Miscellaneous Publication No. MISC0190*. Washington State University, College of Agriculture and Home Economics, Pullman, pp. 167–170.
- Oches, E.A., McCoy, W.D., 2001. Historical developments and recent advances in amino acid geochronology applied to loess research: examples from North America, Europe, and China. *Earth-Science Reviews* 54, 173–192.
- Owczarek, P., Opała-Owczarek, M., Rahmonov, O., Razzokov, A., Jary, Z., Niedźwiedź, T., 2017. Relationships between loess and the Silk Road reflected by environmental change and its implications for human societies in the area of ancient Panjikent, Central Asia. *Quaternary Research* (in press). <https://doi.org/10.1017/qua.2017.69>.
- Owen, L.A., Dortch, J.M., 2014. Nature and timing of Quaternary glaciation in the Himalayan–Tibetan orogen. *Quaternary Science Reviews* 88, 14–54.
- Paepe, R., 1966. Comparative stratigraphy of Würm loess deposits in Belgium and Austria. *Bulletin de la Société Belgique de Géologie* 75, 203–216.
- Paepe, R., Sommé, J., 1970. Les loess et la stratigraphie du Pleistocène récent dans le nord de la France et en Belgique. *Annales Société Géologique du Nord* 90, 191–201.
- Palmer, A.S., Pillans, B.J., 1996. Record of climatic fluctuations from ca. 500 ka loess deposits and paleosols near Wanganui, New Zealand. *Quaternary International* 34–36, 155–162.
- Parés, J.M., 2015. Sixty years of anisotropy of magnetic susceptibility in deformed sedimentary rocks. *Frontiers in Earth Science* 3, 4. <https://doi.org/10.3389/feart.2015.00004>.
- Patton, H., Hubbard, A., Andreassen, K., Winsborrow, M., Stroeven, A.P., 2016. The build-up, configuration, and dynamical sensitivity of the Eurasian ice-sheet complex to Late Weichselian climatic and oceanic forcing. *Quaternary Science Reviews* 153, 97–121.
- Pécsi, M., 1966. Löss und lössartige Sedimente im Karpatenbecken und ihre lithostratigraphischen Gliederung. *Petermanns Geographische Mitteilungen* 110, 176–189, 241–252.
- Pécsi, M., 1985. Chronostratigraphy of Hungarian loesses and the underlying subaerial formation. In: Pécsi, M. (Ed.), *Loess and the Quaternary: Chinese and Hungarian Case Studies*. *Studies in Geography in Hungary* 18. Akadémiai Kiadó, Budapest, pp. 33–49.
- Peterse, F., Martínez-García, A., Zhou, B., Beets, C.J., Prins, M.A., Zheng, H., Eglinton, T.I., 2014. Molecular records of continental air temperature and monsoon precipitation variability in East Asia spanning the past 130,000 years. *Quaternary Science Reviews* 83, 76–82.
- Péwé, T.L., 1955. Origin of the upland silt near Fairbanks, Alaska. *Geological Society of America Bulletin* 66, 699–724.
- Péwé, T.L., 1975. *Quaternary Geology of Alaska*. *U.S. Geological Survey Professional Paper 835*. U.S. Government Printing Office, Washington, DC.

- Péwé, T.L., Berger, G.W., Westgate, J.A., Brown, P.M., Leavitt, S.W., 1997. Eva Interglaciation Forest Bed, Unglaciated East-Central Alaska: Global Warming 125,000 Years Ago. *Geological Society of America Special Paper* 319. Geological Society of America, Boulder, CO.
- Pfannenstiel, M., 1950. *Die Quartärsgeschichte des Donaudeltas*. Bonner Geographische Abhandlungen, Bonn, Germany.
- Pickering, R., Jacobs, Z., Herries, A.I.R., Karkanias, P., Bar-Matthews, M., Woodhead, J.D., Kappen, P., Fisher, E., Marean, C.W., 2013. Paleoanthropologically significant South African sea caves dated to 1.1–1.0 million years using a combination of U–Pb, TT-OSL and palaeomagnetism. *Quaternary Science Reviews* 65, 39–52.
- Pigati, J.S., McGeehin, J.P., Muhs, D.R., Bettis, E.A., 2013. Radiocarbon dating late Quaternary loess deposits using small terrestrial gastropod shells. *Quaternary Science Reviews* 76, 114–128.
- Pigati, J.S., McGeehin, J.P., Muhs, D.R., Grimley, D.A., Nekola, J.C., 2015. Radiocarbon dating loess deposits in the Mississippi Valley using terrestrial gastropod shells (Polygyridae, Heliciniidae, and Discidae). *Aeolian Research* 16, 25–33.
- Pigati, J.S., Rech, J.A., Nekola, J.C., 2010. Radiocarbon dating of small terrestrial gastropod shells in North America. *Quaternary Geochronology* 5, 519–532.
- Porter, D., Bishop, S., 1990. Soil and lithostratigraphy below the Loveland/Sicily Island silt, Crowley's Ridge, Arkansas. *Proceedings of the Arkansas Academy of Science* 44, 86–90.
- Porter, S.C., An, Z.S., 1995. Correlation between climate events in the North Atlantic and China during the last glaciation. *Nature* 375, 305–308.
- Prasad, A.K., Poolton, N.R.J., Kook, M., Jain, M., 2017. Optical dating in a new light: a direct, non-destructive probe of trapped electrons. *Scientific Reports* 7, 12097. <http://dx.doi.org/10.1038/s41598-017-10174-8>.
- Preece, S.J., Westgate, J.A., Stemper, B.A., Péwé, T.L., 1999. Tephrochronology of late Cenozoic loess at Fairbanks, central Alaska. *Geological Society of America Bulletin* 111, 71–90.
- Prins, M.A., Vriend, M., Nugteren, G., Vandenberghe, J., Lu, H., Zheng, H., Weltje, G.J., 2007. Late Quaternary aeolian dust input variability on the Chinese Loess Plateau: inferences from unmixing of loess grain-size records. *Quaternary Science Reviews* 26, 230–242.
- Prud'Homme, C., Antoine, P., Moine, O., Turpin, E., Huguenard, L., Robert, V., Degeai, J.-P., 2015. Earthworm calcite granules: a new tracker of millennial-timescale environmental changes in Last Glacial loess deposits. *Journal of Quaternary Science* 30, 529–536.
- Prud'homme, C., Lecuyer, C., Antoine, P., Moine, O., Hatté, C., Fourel, F., Martineau, F., Rousseau, D.-D., 2016. Palaeotemperature reconstruction during the Last Glacial from dO18 of earthworm calcite granules from Nussloch loess sequence, Germany. *Earth and Planetary Science Letters* 442, 13–20.
- Prud'homme, C., 2017. Les granules de calcite de vers de terre, un support innovant pour la reconstitution du paléoclimat du Dernier Glaciaire en milieu loessique européen: Application à l'étude des interactions Homme-Environnement au Paléolithique, Ecole doctorale: Géographie paris. *Université Paris 1 Panthéon Sorbonne, Paris*. p. 270.
- Pullen, A., Ibáñez-Mejía, M., Gehrels, G.E., Ibáñez-Mejía, J.C., Pecha, M., 2014. What happens when $n = 1000$? Creating large- n geochronological datasets with LA-ICP-MS for geological investigations. *Journal of Analytical Atomic Spectrometry* 29, 971–980.
- Pullen, A., Kapp, P., McCallister, A.T., Chang, H., Gehrels, G.E., Garzzone, C.N., Heermance, R.V., Ding, L., 2011. Qaidam Basin and northern Tibetan Plateau as dust sources for the Chinese Loess Plateau and paleoclimatic implications. *Geology* 39, 1031–1034.
- Pye, K., 1995. The nature, origin and accumulation of loess. *Quaternary Science Reviews* 14, 653–667.
- Pye, K., Johnson, R., 1988. Stratigraphy, geochemistry, and thermoluminescence ages of Lower Mississippi valley loess. *Earth Surface Processes and Landforms* 13, 103–124.
- Pye, K., Zhou, L.P., 1989. Late Pleistocene and Holocene aeolian dust deposition in north China and the northwest Pacific Ocean. *Palaeogeography, Palaeoclimatology, Palaeoecology* 73, 11–23.
- Rech, J.A., Nekola, J.C., Pigati, J.S., 2012. Radiocarbon ages of terrestrial gastropods extend duration of ice-free conditions at the Two Creeks forest bed, Wisconsin, USA. *Quaternary Research* 77, 289–292.
- Reger, R.D., Pinney, D.S., Burke, R.M., Wiltse, M.A., 1996. Catalog and Initial Analyses of Geologic Data Related to Middle to Late Quaternary Deposits, Cook Inlet Region, Alaska. Report of Investigations 95-6. State of Alaska, Department of Natural Resources, Division of Geological and Geophysical Surveys, Fairbanks, AK.
- Renssen, H., Kasse, C., Vandenberghe, J., Lorenz, S.J., 2007. Weichselian Late Pleniglacial surface winds over northwest and central Europe: a model-data comparison. *Journal of Quaternary Science* 22, 281–293.
- Rex, R.W., Syers, J.K., Jackson, M.L., Clayton, R.N., 1969. Eolian origin of quartz in soils of the Hawaiian Islands and in Pacific pelagic sediments. *Science* 163, 277–279.
- Roberts, H.M., 2008. The development and application of luminescence dating to loess deposits: a perspective on the past, present and future. *Boreas* 37, 483–507.
- Roberts, H.M., Muhs, D.R., Wintle, A.G., Duller, G.A.T., Bettis, E.A. III, 2003. Unprecedented last-glacial mass accumulation rates determined by luminescence dating of loess from western Nebraska. *Quaternary Research* 59, 411–419.
- Rodbell, D.T., Forman, S.L., Pierson, J., Lynn, W.C., 1997. Stratigraphy and chronology of Mississippi Valley loess in western Tennessee. *Geological Society of America Bulletin* 109, 1134–1148.
- Roering, J.J., Almond, P., Tonkin, P., McKean, J., 2002. Soil transport driven by biological processes over millennial time scales. *Geology* 30, 1115–1118.
- Rossignol, J., Moine, O., Rousseau, D.D., 2004. The Buzzard's Roost and Eustis mollusc sequences: comparison between the paleoenvironments of two sites in the Wisconsinian loess of Nebraska, USA. *Boreas* 33, 145–154.
- Rousseau, D.D., 1987. Paleoclimatology of the Achenheim series (middle and upper Pleistocene, Alsace, France). A malacological analysis. *Palaeogeography, Palaeoclimatology, Palaeoecology* 59, 293–314.
- Rousseau, D.D., 1991. Climatic transfer function from Quaternary molluscs in European loess deposits. *Quaternary Research* 36, 195–209.
- Rousseau, D.D., 2001. Loess biostratigraphy: new advances and approaches in mollusc studies. *Earth-Science Reviews* 54, 157–171.
- Rousseau, D.D., Antoine, P., Hatté, C., Lang, A., Zöller, L., Fontugne, M., Othman, D.B., et al., 2002. Abrupt millennial climatic changes from Nussloch (Germany) Upper Weichselian eolian records during the Last Glaciation. *Quaternary Science Reviews* 21, 1577–1582.

- Rousseau, D.D., Antoine, P., Gerasimenko, N., Sima, A., Fuchs, M., Hatte, C., Moine, O., Zoeller, L., 2011. North Atlantic abrupt climatic events of the last glacial period recorded in Ukrainian loess deposits. *Climate of the Past* 7, 221–234.
- Rousseau, D.D., Boers, N., Sima, A., Svensson, A., Bigler, M., Lagroix, F., Taylor, S., Antoine, P., 2017a. (MIS3 & 2) millennial oscillations in Greenland dust and Eurasian aeolian records – a paleosol perspective. *Quaternary Science Reviews* 169, 99–113.
- Rousseau, D.-D., Chauvel, C., Sima, A., Hatte, C., Lagroix, F., Antoine, P., Balkanski, Y., et al., 2014. European glacial dust deposits: geochemical constraints on atmospheric dust cycle modeling. *Geophysical Research Letters* 41, 7666–7674.
- Rousseau, D.-D., Derbyshire, E., Antoine, P., Hatté, C., 2013. Loess records – Europe. In: Elias, S.A., Mock, C.J. (Ed.), *Encyclopedia of Quaternary Science*. 2nd ed. Elsevier, Amsterdam, pp. 606–619.
- Rousseau, D.D., Gerasimaenko, N., Matvviishina, Z., Kukla, G.J., 2001. Late Pleistocene environments of central Ukraine. *Quaternary Research* 56, 349–356.
- Rousseau, D.-D., Kukla, G., 1994. Late Pleistocene climate record in the Eustis loess section, Nebraska, based on land snail assemblages and magnetic susceptibility. *Quaternary Research* 42, 176–187.
- Rousseau, D.-D., Sima, A., Antoine, P., Hatté, C., Lang, A., Zöller, L., 2007. Link between European and North Atlantic abrupt climate changes over the last glaciation. *Geophysical Research Letters* 34, L22713. <http://dx.doi.org/10.1029/2007GL031716>.
- Rousseau, D.-D., Svensson, A., Bigler, M., Sima, A., Steffensen, J. P., Boers, N., 2017b. Eurasian contribution to the last glacial dust cycle: how are loess sequences built? *Climate of the Past* 13, 1181–1197.
- Rousseau, D.D., Wu, N., Guo, Z.T., 2000. The terrestrial mollusks as new indices of the Asian paleomonsoons in the Chinese loess plateau. *Global and Planetary Change* 26, 199–206.
- Rousseau, D.D., Wu, N., Pei, Y., Li, F., 2009. Three exceptionally strong East-Asian summer monsoon events during glacial times in the past 470 kyr. *Climate of the Past* 5, 157–169.
- Roxby, P.M., 1938. The terrain of early Chinese civilization. *Geography* 23, 225–236.
- Rozanski, K., Araguás-Araguás, L., Gonfiantini, R., 1993. Isotopic patterns in modern global precipitation. In: Swart, P.K., Lohmann, K.C., Mckenzie, J., Savin, S. (Eds.), *Climate Change in Continental Isotopic Records. Geophysical Monograph* 78. American Geophysical Union, Washington, DC, pp. 1–36.
- Ruegg, G.H.J., 1983. Periglacial eolian evenly laminated sandy deposits in the Late Pleistocene of N.W. Europe, a facies unrecorded in modern sedimentological handbooks. In: Brookfield, M.E., Ahlbrandt, T.S. (Eds.), *Eolian Sediments and Processes*. Elsevier, Amsterdam, pp. 455–482.
- Ruhe, R.V., 1954. Relations of the properties of Wisconsin loess to topography in western Iowa. *American Journal of Science* 252, 663–672.
- Ruhe, R.V., 1973. Background of model for loess-derived soils in the upper Mississippi River basin. *Soil Science* 115, 250–253.
- Ruocco, M., 1989. A 3 Ma paleomagnetic record of coastal continental deposits in Argentina. *Palaeoecology, Palaeogeography, Palaeoclimatology* 72, 105–113.
- Rutledge, E.M., Guccione, M.J., Markewich, H.W., Wysocki, D.A., Ward, L.B., 1996. Loess stratigraphy of the Lower Mississippi Valley. *Engineering Geology* 45, 167–183.
- Rutledge, E.M., Holowaychuk, N., Hall, G.F., Wilding, L.P., 1975. Loess in Ohio in relation to several possible source areas: I. Physical and chemical properties. *Soil Science Society of America Journal* 39, 1125–1132.
- Rutter, N.W., Ding, Z.L., 1993. Paleoclimates and monsoon variations interpreted from micromorphogenic features of the Baoji paleosols, China. *Quaternary Science Reviews* 12, 853–862.
- Rutter, N.W., Ding, Z.L., Evans, M.E., Liu, T.S., 1991. Baoji-type pedostratigraphic section, Loess Plateau, north-central China. *Quaternary Science Reviews* 10, 1–22.
- Sanborn, P.T., Smith, C.A.S., Froese, D.G., Zazula, G.D., Westgate, J.A., 2006. Full-glacial paleosols in perennially frozen loess sequences, Klondike goldfields, Yukon Territory, Canada. *Quaternary Research* 66, 147–157.
- Sarianidi, V., 1992. Food-producing and other Neolithic communities in Khorasan and Transoxania: eastern Iran, Soviet Central Asia and Afghanistan. In: Dani, A.H., Masson, V.M. (Eds.), *History of Civilizations of Central Asia*. Vol. 1, The Dawn of Civilization: Earliest Times to 700 B.C. UNESCO, Paris, pp. 105–122.
- Sarnthein, M., Tetzlaff, G., Koopmann, B., Wolter, K., Pflaumann, U., 1981. Glacial and interglacial wind regimes over the eastern subtropical Atlantic and North-West Africa. *Nature (London)* 293, 193–196.
- Sayago, J.M., 1983. Geología de la Sierra de Ancasti-16. Geomorfología de la Sierra de Ancasti (Argentina). *Münstersche Forschungszur Geologie und Paläontologie* 59, 265–284.
- Schaetzl, R.J., 1998. Lithologic discontinuities in some soils on drumlins: theory, detection, and application. *Soil Science* 163, 570–590.
- Schaetzl, R.J., 2008. The distribution of silty soils in the Grayling Fingers region of Michigan: evidence for loess deposition onto frozen ground. *Geomorphology* 102, 287–296.
- Schaetzl, R.J., Attig, J.W., 2013. The loess cover of northeastern Wisconsin. *Quaternary Research* 79, 199–214.
- Schaetzl, R.J., Hook, J., 2008. Characterizing the silty sediments of the Buckley Flats outwash plain: evidence for loess in NW Lower Michigan. *Physical Geography* 29, 1–18.
- Schaetzl, R.J., Larson, P.H., Faulkner, D.J., Running, G.L., Jol, H. M., Rittenour, T.M., 2017. Eolian sand and loess deposits indicate west-northwest paleowinds during the Late Pleistocene in western Wisconsin, USA. *Quaternary Research* (in press). <https://doi.org/10.1017/qua.2017.88>.
- Schaetzl, R.J., Loope, W.L., 2008. Evidence for an eolian origin for the silt-enriched soil mantles on the glaciated uplands of eastern Upper Michigan, USA. *Geomorphology* 100, 285–295.
- Schaetzl, R.J., Luehmann, M.D., 2013. Coarse-textured basal zones in thin loess deposits: products of sediment mixing and/or paleoenvironmental change? *Geoderma* 192, 277–285.
- Schaetzl, R.J., Weisenborn, B.N., 2004. The Grayling Fingers geomorphic region of Michigan: soils, sedimentology, stratigraphy and geomorphic development. *Geomorphology* 61, 251–274.
- Schäfer, I., Bliedtner, M., Wolf, D., Faust, D., Zech, R., 2016a. Evidence for humid conditions during the last glacial from leaf wax patterns in the loess-paleosol sequence El Paraíso, central Spain. *Quaternary International* 407A, 64–73.
- Schäfer, I., Lanny, V., Franke, J., Eglinton, T., Zech, M., Vysloužilová, B., Zech, R., 2016b. Leaf waxes in litter and topsoils along a European transect. *Soil* 2, 551–564.
- Schatz, A.-K., Qi, Y., Siebel, W., Wu, J., Zöller, L., 2015. Tracking potential source areas of central European loess: examples from Tokaj (HU), Nussloch (D) and Grub (AT). *Open Geoscience* 7, 678–720.

- Schatz, A.-K., Zech, M., Buggle, B., Gulyas, S., Hambach, U., Markovic, S., Sümege, P., Scholten, T., 2011. The late Quaternary loess record of Tokaj, Hungary: reconstructing palaeoenvironment, vegetation and climate using stable C and N isotopes and biomarkers. *Quaternary International* 240, 52–61.
- Scheib, A.J., Birke, M., Dinelli, E., 2013. Geochemical evidence of aeolian deposits in European soils. *Boreas* 43, 175–192.
- Schirmer, W., 2016. Late Pleistocene loess of the lower Rhine. *Quaternary International* 411, 44–61.
- Schreuder, L., Beets, C., Prins, M., Hatté, C., Peterese, F., 2016. Late Pleistocene climate evolution in southeastern Europe recorded by soil bacterial membrane lipids in Serbian loess. *Palaeogeography, Palaeoclimatology, Palaeoecology* 449, 141–148.
- Schwan, J., 1988. The structure and genesis of Weichselian to Early Holocene aeolian sand sheets in western Europe. *Sedimentary Geology* 55, 197–232.
- Schwan, J., 1991. Palaeowetness indicators in a Weichselian Late Glacial to Holocene aeolian succession in the southwestern Netherlands. *Zeitschrift für Geomorphologie, Supplementband* 90, 155–169.
- Scull, P., Schaetzl, R.J., 2011. Using PCA to characterize and differentiate the character of loess deposits in Wisconsin and Upper Michigan, USA. *Geomorphology* 127, 143–155.
- Shackleton, N.J., An, Z., Dodonov, A.E., Gavin, J., Kukla, G.J., Ranov, V.A., Zhou, L.P., 1995. Accumulation rate of loess in Tajikistan and China: relationship with global ice volume cycles. *Quaternary Proceedings* 4, 1–6.
- Shang, Y., Beets, C.J., Tang, H., Prins, M., Lahaye, Y., van Elsas, R., Sukselainen, L., Kaakinen, A., 2016. Variations in the provenance of the late Neogene Red Clay deposits in northern China. *Earth and Planetary Science Letters* 439, 88–100.
- Shimek, B., 1899. The distribution of loess fossils. *Journal of Geology* 7, 122–140.
- Sima, A., Kageyama, M., Rousseau, D.D., Ramstein, G., Balkanski, Y., Antoine, P., Hatté, C., 2013. Modeling dust emission response to North Atlantic millennial-scale climate variations from the perspective of East European MIS3 loess deposits. *Climate of the Past* 9, 1385–1402.
- Sima, A., Rousseau, D.D., Kageyama, M., Ramstein, G., Schulz, M., Balkanski, Y., Antoine, P., Dulac, F., Hatté, C., 2009. Imprint of North-Atlantic abrupt climate changes on western European loess deposits as viewed in a dust emission model. *Quaternary Science Reviews* 28, 2851–2866.
- Simmons, A.H., 2011. *The Neolithic Revolution in the Near East*. University of Arizona Press, Tucson.
- Simonson, R.W., 1995. Airborne dust and its significance to soils. *Geoderma* 65, 1–43.
- Sitzia, L., Bertran, P., Bahain, J.-J., Bateman, M.D., Hernandez, M., Garon, H., de Lafontaine, G., et al., 2015. The Quaternary coversands of southwest France. *Quaternary Science Reviews* 124, 84–105.
- Sláma, J., Košla, J., 2012. Effects of sampling and mineral separation on accuracy of detrital zircon studies. *Geochemistry, Geophysics, Geosystems* 13, Q05007. <http://dx.doi.org/10.1029/2012GC004106>.
- Smalley, I., 1995. Making the material: the formation of silt sized primary mineral particles for loess deposits. *Quaternary Science Reviews* 14, 645–651.
- Smalley, I., O'Hara-Dhand, K., Kwong, J., 2014. China: materials for a loess landscape. *Catena* 117, 100–107.
- Smalley, I., O'Hara-Dhand, K., Wint, J., Machalet, B., Jary, Z., Jefferson, I., 2009. Rivers and loess: the significance of long river transportation in the complex event-sequence approach to loess deposit formation. *Quaternary International* 198, 7–18.
- Smalley, I.J., 1968. The loess deposits and Neolithic culture of northern China. *Man (new series)* 3, 224–241.
- Smalley, I.J., Krinsley, D.H., 1978. Loess deposits associated with deserts. *Catena* 5, 53–66.
- Smalley, I.J., Leach, J.A., 1978. The origin and distribution of the loess in the Danube basin and associated regions of east-central Europe—a review. *Sedimentary Geology* 21, 1–26.
- Smalley, I.J., Marković, S.B., O'Hara-Dhand, K., 2010. The INQUA Loess Commission as a central European enterprise. *Central European Journal of Geosciences* 2, 3–8.
- Smalley, I.J., Mavlyanova, N.G., Rakhmatullayev, K.L., Shermatov, M.S., Machalet, B., O'Hara-Dhand, K., Jefferson, I.F., 2006. The formation of loess deposits in the Tashkent region and parts of central Asia; and problems with irrigation, hydrocollapse and soil erosion. *Quaternary International* 152–153, 59–69.
- Smith, B.J., Wright, J.S., Whalley, W.B., 2002. Sources of non-glacial, loess-size quartz silt and the origins of “desert loess.” *Earth-Science Reviews* 59, 1–26.
- Smith, G.D., 1942. *Illinois Loess: Variations in Its Properties and Distribution*. University of Illinois Agricultural Experiment Station Bulletin 490. University of Illinois, Urbana.
- Song, Y., Guo, Z., Marković, S., Hambach, U., Deng, C., Chang, L., Wu, J., Hao, Q., 2018. Magnetic stratigraphy of the Danube loess: a composite Titel-Stari Slankamen loess section over the last one million years in Vojvodina, Serbia. *Journal of Asian Earth Sciences* 155, 68–80.
- Song, Y., Hao, Q.Z., Ge, J.Y., Zhao, D.A., Zhang, Y., Li, Q., Zuo, X.X., Lü, Y.W., Wang, P., 2014. Quantitative relationships between magnetic enhancement of modern soils and climatic variables over the Chinese Loess Plateau. *Quaternary International* 334, 119–131.
- Song, Y., Lai, Z., Li, Y., Chen, T., Wang, Y., 2015. Comparison between luminescence and radiocarbon dating of late Quaternary loess from the Ili Basin in central Asia. *Quaternary Geochronology* 30, 405–410.
- Sprafke, T., Obrecht, I., 2016. Loess: rock, sediment or soil – what is missing for its definition? *Quaternary International* 399, 198–207.
- Stanley, K.E., Schaetzl, R.J., 2011. Characteristics and paleo-environmental significance of a thin, dual-sourced loess sheet, north-central Wisconsin. *Aeolian Research* 2, 241–251.
- Stevens, T., Adamiec, G., Bird, A.F., Lu, H., 2013a. An abrupt shift in dust source on the Chinese Loess Plateau revealed through high sampling resolution OSL dating. *Quaternary Science Reviews* 82, 121–132.
- Stevens, T., Armitage, S.J., Lu, H., Thomas, D.S.G., 2006. Sedimentation and diagenesis of Chinese loess: Implications for the preservation of continuous high-resolution climate records. *Geology* 34, 849–852.
- Stevens, T., Buylaert, J.-P., Lu, H., Thiel, C., Murray, A., Frechen, M., Yi, S., Zeng, L., 2016. Mass accumulation rate and monsoon records from Xifeng, Chinese Loess Plateau, based on a luminescence age model. *Journal of Quaternary Science* 31, 391–405.
- Stevens, T., Carter, A., Watson, T.P., Vermeesch, P., Andò, S., Bird, A.F., Lu, H., Garzanti, E., Cottam, M.A., Sevastjanova, I., 2013b. Genetic linkage between the Yellow River, the Mu Us desert and the Chinese Loess Plateau. *Quaternary Science Reviews* 78, 355–368.
- Stevens, T., Lu, H., Thomas, D.S.G., Armitage, S.J., 2008. Optical dating of abrupt shifts in the Late Pleistocene East Asian monsoon. *Geology* 36, 415–418.

- Stevens, T., Palk, C., Carter, A., Lu, H.Y., Clift, P.D., 2010. Assessing the provenance of loess and desert sediments in northern China using U-Pb dating and morphology of detrital zircons. *Geological Society of America Bulletin* 122, 1331–1344.
- Stiglitz, B.C., Banerjee, S.K., Gourlan, A., Oches, E., 2006. A multiproxy study of Argentina loess: marine oxygen isotope stage 4 and 5 environmental record from pedogenic hematite. *Palaeogeography, Palaeoclimatology, Palaeoecology* 239, 45–62.
- Stott, L.D., 2002. The influence of diet on the $\delta^{13}\text{C}$ of shell carbon in the pulmonate snail *Helix aspersa*. *Earth and Planetary Science Letters* 195, 249–259.
- Stuut, J.-B., Smalley, I., O'Hara-Dhand, K., 2009. Aeolian dust in Europe: African sources and European deposits. *Quaternary International* 198, 234–345.
- Sun, D., Bloemendal, J., Rea, D.K., Vandenberghe, J., Jiang, F., An, Z., Su, R., 2002. Grain-size distribution function of polymodal sediments in hydraulic and aeolian environments, and numerical partitioning of sedimentary components. *Sedimentary Geology* 152, 262–277.
- Sun, J., 2002a. Provenance of loess material and formation of loess deposits on the Chinese Loess Plateau. *Earth and Planetary Science Letters* 203, 845–859.
- Sun, J., 2002b. Source regions and formation of the loess sediments on the high mountain regions of northwestern China. *Quaternary Research* 58, 341–351.
- Sun, J.M., Liu, T.S., 2000. Stratigraphic evidence for the uplift of the Tibetan Plateau between ~1.1 and ~0.9 Myr ago. *Quaternary Science Reviews* 54, 309–320.
- Sun, Y., An, Z., 2005. Late-Pliocene-Pleistocene changes in mass accumulation rates of eolian deposits on the central Chinese Loess Plateau. *Journal of Geophysical Research: Atmospheres* 110, D23101. <http://dx.doi.org/10.1029/2005JD006064>.
- Sun, Y., Clemens, S.C., An, Z., Yu, Z., 2006. Astronomic timescale and palaeoclimatic implication of stacked 3.6-Myr monsoon records from the Chinese Loess Plateau. *Quaternary Science Reviews* 25, 33–48.
- Sun, Y., Clemens, S.C., Morrill, C., Lin, X., Wang, X., An, Z., 2012. Influence of Atlantic meridional overturning circulation on the East Asian winter monsoon. *Nature Geoscience* 5, 46–49.
- Sun, Y.B., Qiang, X.K., Liu, Q.S., Bloemendal, J., Wang, X.L., 2013. Timing and lock-in effect of the Laschamp geomagnetic excursion in Chinese loess. *Geochemistry, Geophysics, Geosystems* 14, 4952–4961.
- Svirčev, Z., Marković, S.B., Stevens, T., Codd, G., Smalley, I., Simeunović, J., Obreht, I., Dulić, T., Pantelić, D., Hambach, U., 2013. Importance of biological loess crusts for loess formation in semi-arid environments. *Quaternary International* 296, 206–215.
- Sweeney, M.R., Mason, J.A., 2013. Mechanisms of dust emission from Pleistocene loess deposits, Nebraska, U.S.A. *Journal of Geophysical Research-Earth Surface* 118, 1–12.
- Swinehart, J.B., Souders, V.L., De Graw, H.M., Diffendal, R.F. Jr., 1985. Cenozoic paleogeography of western Nebraska. In: Flores, R. M., Kaplan, S.S. (Eds.), *Cenozoic Paleogeography of West-Central United States*. Rocky Mountain Section. Society of Economic Paleontologists and Mineralogists, Denver, CO, pp. 209–229.
- Taber, S., 1943. Perennially frozen ground in Alaska: its origin and history. *Geological Society of America Bulletin* 54, 1433–1548.
- Taber, S., 1953. Origin of Alaska silts. *American Journal of Science* 251, 321–336.
- Taber, S., 1958. Complex origin of silts in the vicinity of Fairbanks, Alaska. *Geological Society of America Bulletin* 69, 131–136.
- Tanner, S., Katra, I., Haim, A., Zaady, E., 2016. Short-term soil loss by eolian erosion in response to different rain-fed agricultural practices. *Soil and Tillage Research* 155, 149–156.
- Tarling, D.H., Hrouda, F., 1993. *The Magnetic Anisotropy of Rocks*. Chapman and Hall, London.
- Taylor, S.N., Lagroix, F., 2015. Magnetic anisotropy reveals the depositional and postdepositional history of a loess-paleosol sequence at Nussloch (Germany). *Journal of Geophysical Research: Solid Earth* 120, 2859–2876.
- Taylor, S.N., Lagroix, F., Rousseau, D.D., Antoine, P., 2014. Mineral magnetic characterization of the Upper Pleniglacial Nussloch loess sequence (Germany): an insight into local environmental processes. *Geophysical Journal International* 199, 1463–1480.
- Taylor, S.R., McLennan, S.M., 1985. *The continental crust: its composition and evolution*. Blackwell Scientific Publication, Carlton, 312 p.
- Taylor, S.R., McLennan, S.M., McCulloch, M.T., 1983. Geochemistry of loess, continental crustal composition and crustal modal ages. *Geochimica et Cosmochimica Acta* 47, 1897–1905.
- Terhorst, B., Thiel, C., Peticzka, R., Sprafke, T., Frechen, M., Fladerer, F.A., Roetzel, R., Neugebauer-Maresch, C., 2011. Casting new light on the chronology of the loess/paleosol sequences in Lower Austria. *E&G – Quaternary Science Journal* 60, 270–277.
- Thomas, E.K., Clemens, S.C., Sun, Y., Prell, W.L., Huang, Y., Gao, L., Loomis, S., Chen, G., Liu, Z., 2016. Heterodynes dominate precipitation isotopes in the East Asian monsoon region, reflecting interaction of multiple climate factors. *Earth and Planetary Science Letters* 455, 196–206.
- Thorpe, J., Smith, H.T.U., 1952. *Pleistocene Eolian Deposits of the United States, Alaska, and Parts of Canada*. National Research Council Committee for the Study of Eolian Deposits, Geological Society of America, 1:2,500,000 scale map. Geological Society of America, New York.
- Timar-Gabor, A., Vandenberghe, D.A.G., Vasiliniuc, S., Panaoiu, C.E., Panaoiu, C.G., Dimofte, D., Cosma, C., 2011. Optical dating of Romanian loess: a comparison between silt-sized and sand-sized quartz. *Quaternary International* 240, 62–70.
- Tissoux, H., Valladas, H., Voinchet, P., Reyss, J.L., Mercier, N., Falgueres, C., Bahain, J.J., Zoeller, L., Antoine, P., 2010. OSL and ESR studies of Aeolian quartz from the Upper Pleistocene loess sequence of Nussloch (Germany). *Quaternary Geochronology* 5, 131–136.
- Trask, P.D., 1932. *Origin and Environment of Source Sediments of Petroleum*. Gulf, Houston, TX.
- Tripaldi, A., Zárate, M., 2017. *Geoformas eólicas de la cuenca del río Salado-Chadileuví, provincia de la Pampa Argentina*. Actas XX Congreso Geológico Argentino, San Miguel de Tucumán, pp. 183–185.
- Tsatskin, A., Heller, F., Hailwood, E.A., Gendler, T.S., Hus, J., Montgomery, P., Sartori, M., Virina, E.I., 1998. Pedosedimentary division, rock magnetism and chronology of the loess/paleosol sequence at Rozany (Ukraine). *Palaeogeography, Palaeoclimatology, Palaeoecology* 143, 111–133.
- Tsoar, H., Pye, K., 1987. Dust transport and the question of desert loess formation. *Sedimentology* 34, 139–153.
- Tuthorn, M., Zech, R., Ruppenthal, M., Oelmann, Y., Kahmen, A., del Valle, H., Eglinton, T., Rozanski, K., Zech, M., 2015. Coupling $\delta^2\text{H}$ and $\delta^{18}\text{O}$ biomarker results yields information on relative humidity and isotopic composition of precipitation. *Biogeosciences* 12, 3913–3924.

- Tuthorn, M., Zech, M., Ruppenthal, M., Oelmann, Y., Kahmen, A., del Valle, H.F., Wilcke, W., Glaser, B., 2014. Oxygen isotope ratios ($^{18}\text{O}/^{16}\text{O}$) of hemicellulose-derived sugar biomarkers in plants, soils and sediments as paleoclimate proxy II: insight from a climate transect study. *Geochimica et Cosmochimica Acta* 126, 624–634.
- Újvári, G., Klötzli, U., 2015. U-Pb ages and Hf composition of zircons in Austrian last glacial loess: constraints on heavy mineral sources and sediment transport pathways. *International Journal of Earth Sciences* 104, 1365–1385.
- Újvári, G., Klötzli, U., Kiraly, F., Ntaflou, T., 2013. Towards identifying the origin of metamorphic components in Austrian loess: insights from detrital rutile chemistry, thermometry and U-Pb geochronology. *Quaternary Science Reviews* 75, 132–142.
- Újvári, G., Kovacs, J., Varga, G., Raucsik, B., Markovic, S.B., 2010. Dust flux estimates for the Last Glacial Period in East Central Europe based on terrestrial records of loess deposits a review. *Quaternary Science Reviews* 29, 3157–3166.
- Újvári, G., Varga, A., Balogh-Brunstad, Z., 2008. Origin, weathering and geochemical composition of loess in southwestern Hungary. *Quaternary Research* 69, 421–437.
- Újvári, G., Varga, A., Ramos, F.C., Kovács, J., Németh, T., Stevens, T., 2012. Evaluating the use of clay mineralogy, Sr–Nd isotopes and zircon U–Pb ages in tracking dust provenance: an example from loess of the Carpathian Basin. *Chemical Geology* 304, 83–96.
- Vandenberghe, D.A.G., Dereese, C., Kasse, C., Van den haute, P., 2013. Late Weichselian (fluvio-) aeolian sediments and Holocene drift-sands of the classic type locality in Twente (E Netherlands): a high-resolution dating study using optically stimulated luminescence. *Quaternary Science Reviews* 68, 96–113.
- Vandenberghe, J., 1985. Palaeoenvironment and stratigraphy during the last glacial in the Belgian–Dutch border region. *Quaternary Research* 24, 23–38.
- Vandenberghe, J., 1991. Changing conditions of aeolian sand deposition during the last deglaciation period. *Zeitschrift für Geomorphologie, Supplementband* 90, 193–207.
- Vandenberghe, J., 2003. Climate forcing of fluvial system development: an evolution of ideas. *Quaternary Science Reviews* 22, 2053–2060.
- Vandenberghe, J., 2013. Grain size of fine-grained windblown sediment: a powerful proxy for process identification. *Earth Science Reviews* 121, 18–30.
- Vandenberghe, J., An, Z.S., Nugteren, G., Lu, H.Y., Van Huissteden, K., 1997. New absolute time scale for the Quaternary climate in the Chinese loess region by grain-size analysis. *Geology* 25, 35–38.
- Vandenberghe, J., French, H.M., Gorbunov, A., Marchenko, S., Velichko, A.A., Jin, H., Cui, Z., Zhang, T., Wan, X., 2014a. The Last Permafrost Maximum (LPM) map of the Northern Hemisphere: permafrost extent and mean annual air temperatures, 25–17 ka BP. *Boreas* 43, 652–666.
- Vandenberghe, J., Kasse, C., 2008. Les formations sableuses en milieux périglaciaires: sables de couverture et sables dunaires. In: Dewolf, Y., Bourrié, G. (Eds.), *Les formations superficiales*. Ellipses, Paris, pp. 317–321.
- Vandenberghe, J., Krook, L., 1981. Stratigraphy and genesis of Pleistocene deposits at Alphen (southern Netherlands). *Geologie en Mijnbouw* 60, 417–426.
- Vandenberghe, J., Krook, L., 1985. La stratigraphie et la genèse de dépôts Pleistocènes à Goirle (Pays-Bas). *Bulletin Association Française d' études Quaternaires* 1985/4, 239–247.
- Vandenberghe, J., Markovic, S., Jovanovic, M., Hambach, U., 2014b. Site-specific variability of loess and palaeosols (Ruma, Vojvodina, northern Serbia). *Quaternary International* 334–335, 86–93.
- Vandenberghe, J., Renssen, H., Roche, D.M., Goosse, H., Velichko, A.A., Gorbunov, A., Levvasseur, G., 2012. Eurasian permafrost instability constrained by reduced sea-ice cover. *Quaternary Science Reviews* 34, 16–23.
- Vandenberghe, J., Renssen, H., van Huissteden, K., Nugteren, G., Konert, M., Lu, H., Dodonov, A., Buylaert, J.-P., 2006. Penetration of Atlantic westerly winds into central and East Asia. *Quaternary Science Reviews* 25, 2380–2389.
- Vandenberghe, J., Sun, Y., Wang, X., Abels, H.A., Liu, X., 2018. Grain-size characterization of reworked fine-grained aeolian deposits. *Earth-Science Reviews* 177, 43–52.
- Vandenberghe, J., Van Huissteden, J., 1988. Fluvio-aeolian interaction in a region of continuous permafrost. Proceedings 5th International Permafrost Conference, Trondheim, Norway, pp. 876–881.
- Van der Hammen, T., Maarleveld, G.C., Vogel, J., Zagwijn, W.H., 1967. Stratigraphy, climatic succession and radiocarbon dating of the last glacial in the Netherlands. *Geologie en Mijnbouw* 46, 79–95.
- Van Huissteden, J., 1990. Tundra rivers of the last glacial: sedimentation and geomorphological processes during the Middle Pleniglacial in Twente, eastern Netherlands. *Mededelingen Rijks Geologische Dienst* 44, 1–138.
- Van Huissteden, J., Vandenberghe, J., Van der Hammen, T., Laan, W., 2000. Fluvial and eolian interaction under permafrost conditions: Weichselian Late Pleniglacial, Twente, eastern Netherlands. *Catena* 40, 307–321.
- Varga, G., 2011. Similarities among the Plio-Pleistocene terrestrial aeolian dust deposits in the World and in Hungary. *Quaternary International* 234, 98–108.
- Velichko, A.A., 1990. Loess–paleosol formation on the Russian Plain. *Quaternary International* 7/8, 103–114.
- Velichko, A.A., Catto, N.R., Kononov, M.Y., Morozova, T.D., Novenko, E.Y., Panin, P.G., Ryskov, G.Y., et al., 2009. Progressively cooler, drier interglacials in southern Russia through the Quaternary: evidence from the Sea of Azov region. *Quaternary International* 198, 204–219.
- Veres, D., Lane, C.S., Timar-Gabor, A., Hambach, U., Constantin, D., Szakács, A., Onac, B.P., 2013. The Campanian Ignimbrite/Y5 tephra layer – a regional stratigraphic marker for Isotope Stage 3 deposits in the Lower Danube region, Romania. *Quaternary International* 293, 22–33.
- Vermeesch, P., 2004. How many grains are needed for a provenance study? *Earth and Planetary Science Letters* 224, 441–451.
- Vermeesch, P., 2012. On the visualisation of detrital age distributions. *Chemical Geology* 312–313, 190–194.
- Vermeesch, P., 2013. Multi-sample comparison of detrital age distributions. *Chemical Geology* 341, 140–146.
- Vermeesch, P., Garzanti, E., 2015. Making geological sense of ‘Big Data’ in sedimentary provenance analysis. *Chemical Geology* 409, 20–27.
- Vlaminck, S., Kehl, M., Lauer, T., Shahriari, A., Sharifi, J., Eckmeier, E., Lehndorff, E., Khormali, F., Frechen, M., 2016. Loess-soil sequence at Toshan (northern Iran): insights into late Pleistocene climate change. *Quaternary International* 399, 122–135.
- Vriend, M., Prins, M.A., Buylaert, J.P., Vandenberghe, J., Lu, H., 2011. Contrasting dust supply patterns across the north-western

- Chinese Loess Plateau during the last glacial–interglacial cycle. *Quaternary International* 240, 167–180.
- Wacha, L., Rolf, C., Hambach, U., Frechen, M., Galović, L., Duchoslav, M., 2017. The Last Glacial aeolian record of the Island of Susak (Croatia) as seen from a high-resolution grain-size and rock magnetic analysis. *Quaternary International* (in press). <https://doi.org/10.1016/j.quaint.2017.08.016>.
- Wang, X., Wei, H., Taheri, M., Khormali, F., Danukalova, G., Chen, F., 2016. Early Pleistocene climate in western arid central Asia inferred from loess-palaeosol sequences. *Scientific Reports* 6, 20560. <http://dx.doi.org/10.1038/srep20560>.
- Wang, X.L., Lu, Y.C., Wintle, A.G., 2006. Recuperated OSL dating of fine-grained quartz in Chinese loess. *Quaternary Geochronology* 1, 89–100.
- Wang, Z., Zhao, H., Dong, G., Zhou, A., Liu, J., Zhang, D., 2014. Reliability of radiocarbon dating on various fractions of loess-soil sequence for Dadiwan section in the western Chinese Loess Plateau. *Frontiers of Earth Science* 8, 540–546.
- Waroszewski, J., Sprafke, T., Kabala, C., Muszyfaga, Elżbieta, Labaz, Beata, Woźniczka, P., 2017. Aeolian silt contribution to soils on mountain slopes (Mt. Ślęza, southwest Poland). *Quaternary Research*, 1–16. doi: 10.1017/qua.2017.76.
- Watson, W., 1966. *Early Civilization in China*. Thames and Hudson, London.
- Westgate, J.A., Stemper, B.A., Péwé, T.L., 1990. A 3 m.y. record of Pliocene-Pleistocene loess in interior Alaska. *Geology* 18, 858–861.
- Wiesenberg, G.L.B., Gocke, M., 2013. Reconstruction of the late Quaternary paleoenvironments of the Nussloch loess paleosol sequence—comment to the paper published by Zech et al., *Quaternary Research* 78 (2012), 226–235. *Quaternary Research* 79, 304–305.
- Wilding, L.P., Odell, R.T., Fehrenbacher, J.B., Beavers, A.H., 1963. Source and distribution of sodium in Solonchic soils in Illinois. *Soil Science Society of America Proceedings* 27, 432–438.
- Williams, J.R., 1962. *Geologic Reconnaissance of the Yukon Flats District, Alaska*. U.S. Geological Survey Bulletin 1111-H. U.S. Government Printing Office, Washington, DC.
- Willmes, C., 2015. *LGM Sea Level Change (HiRes)*. CRC 806 Database. Collaborative Research Centre 806, Department of Geography, University of Cologne, Cologne, Germany.
- Wintle, A.G., Adamiec, G., 2017. Optically stimulated luminescence signals from quartz: a review. *Radiation Measurements* 98, 10–33.
- Wright, J.S., 2001. “Desert” loess versus “glacial” loess: quartz silt formation, source areas and sediment pathways in the formation of loess deposits. *Geomorphology* 36, 231–256.
- Wu, B., Wu, N.Q., 2011. Terrestrial mollusk records from Xifeng and Luochuan L9 loess strata and their implications for paleoclimatic evolution in the Chinese Loess Plateau during Marine Oxygen Isotope Stages 24–22. *Climate of the Past* 7, 349–359.
- Wünnemann, B., Mischke, S., Chen, F.H., 2006. A Holocene sedimentary record from Bosten Lake, China. *Palaeogeography, Palaeoclimatology, Palaeoecology* 234, 223–238.
- Xiao, G., Zong, K., Li, G., Hu, Z., Dupont-Nivet, G., Peng, S., Zhang, K., 2012. Spatial and glacial-interglacial variations in provenance of the Chinese Loess Plateau. *Geophysical Research Letters* 39, L20715. <http://dx.doi.org/10.1029/2012GL053304>.
- Yaalon, D.H., 1969. Origin of desert loess. In: Ters, M. (Ed.), *Etudes sur le Quaternaire dans le Monde*, Vol. 2. Association Française pour l’Etude du Quaternaire, Paris, France, p. 755.
- Yaalon, D.H., Dan, J., 1974. Accumulation and distribution of loess-derived deposits in the semi-desert and desert fringe areas of Israel. *Zeitschrift für Geomorphologie, Supplementband* 20, 91–105.
- Yaalon, D.H., Ganor, E., 1973. The influence of dust on soils during the Quaternary. *Soil Science* 116, 146–155.
- Yaalon, D.H., Ganor, E., 1979. East Mediterranean trajectories of dust-carrying storms from the Sahara and Sinai. In: Morales, C. (Ed.), *Saharan Dust*. John Wiley and Sons, Chichester, UK, pp. 187–193.
- Yanes, Y., 2015. Stable isotope ecology of land snails from a high-latitude site near Fairbanks, interior Alaska, USA. *Quaternary Research* 83, 588–595.
- Yanes, Y., Gutierrez-Zugasti, I., Delgado, A., 2012. Late-glacial to Holocene transition in northern Spain deduced from land-snail shelly accumulations. *Quaternary Research* 78, 373–385.
- Yang, B., Wang, J., Bräuning, A., Dong, Z., Esper, J., 2009. Late Holocene climatic and environmental changes in arid central Asia. *Quaternary International* 194, 68–78.
- Yang, S., Ding, Z., 2006. Winter–spring precipitation as the principal control on predominance of C₃ plants in central Asia over the past 1.77 Myr: evidence from $\delta^{13}\text{C}$ of loess organic matter in Tajikistan. *Palaeogeography, Palaeoclimatology, Palaeoecology* 235, 330–339.
- Yang, S., Ding, Z., 2008. Advance-retreat history of the East-Asian summer monsoon rainfall belt over northern China during the last two glacial-interglacial cycles. *Earth and Planetary Science Letters* 274, 499–510.
- Yang, S., Ding, Z., 2010. Drastic climatic shift at ~2.8 Ma as recorded in eolian deposits of China and its implications for redefining the Pliocene-Pleistocene boundary. *Quaternary International* 219, 37–44.
- Yang, S., Ding, Z., 2014. A 249 kyr stack of eight loess grain size records from northern China documenting millennial-scale climate variability. *Geochemistry, Geophysics, Geosystems* 15, 798–814.
- Yang, S., Ding, F., Ding, Z., 2006. Pleistocene chemical weathering history of Asian arid and semi-arid regions recorded in loess deposits of China and Tajikistan. *Geochimica et Cosmochimica Acta* 70, 1695–1709.
- Yang, S., Ding, Z., Li, Y., Wang, X., Jiang, W., Huang, X., 2015. Warming-induced northwestward migration of the East Asian monsoon rain belt from the Last Glacial Maximum to the mid-Holocene. *Proceedings of the National Academy of Sciences of the United States of America* 112, 13178–13183.
- Yang, S., Ding, Z., Wang, X., Tang, Z., Gu, Z., 2012. Negative $\delta^{18}\text{O}$ – $\delta^{13}\text{C}$ relationship of pedogenic carbonate from northern China indicates a strong response of C₃/C₄ biomass to the seasonality of Asian monsoon precipitation. *Palaeogeography, Palaeoclimatology, Palaeoecology* 317–318, 32–40.
- Yang, Y., Mason, J.A., Zhang, H., Lu, H., Ji, J., Chen, J., Liu, L., 2017. Provenance of loess in the central Great Plains, U.S.A., based on Nd–Sr isotopic composition, and paleoenvironmental implications. *Quaternary Science Reviews* 173, 114–123.
- Yapp, C.J., 1979. Oxygen and carbon isotope measurements of land snail shell carbonate. *Geochimica et Cosmochimica Acta* 43, 629–635.
- Yin, J., Su, Y., Fang, X., 2016. Climate change and social vicissitudes in China over the past two millennia. *Quaternary Research* 86, 133–143.
- Yong, M., Sun, Y., 1994. The western regions under the Hsiung–Nu and the Han. In: Harmatta, J., Puri, B.N., Etemadi, G.F. (Eds.), *History of Civilizations of Central Asia*. Vol. 2, The Development

- of Sedentary and Nomadic Civilizations: 700 B.C. to A.D. 250. UNESCO, Paris, pp. 219–238.
- Youn, J.H., Seong, Y.B., Choi, J.H., Abdrakhmatov, K., Ormukov, C., 2014. Loess deposits in the northern Kyrgyz Tien Shan: implications for the paleoclimate reconstruction during the Late Quaternary. *Catena* 117, 81–93.
- Zagwijn, W.H., Paepe, R., 1968. Die Stratigraphie der weichselzeitlichen Ablagerungen der Niederlande und Belgiens. *Eiszeitalter und Gegenwart* 19, 129–146.
- Zárate, M., 2003. Loess of southern South America. *Quaternary Science Reviews* 22, 1987–2006.
- Zárate, M., Blasi, A., 1993. Late Pleistocene–Holocene eolian deposits of the southern Buenos Aires Province, Argentina: a preliminary model. *Quaternary International* 17, 15–20.
- Zárate, M., Tripaldi, A., 2012. The aeolian system of central Argentina. *Aeolian Research* 3, 401–417.
- Zech, M., Buggle, B., Leiber, K., Markovic, S., Glaser, B., Hambach, U., Huwe, B., et al., 2009. Reconstructing Quaternary vegetation history in the Carpathian Basin, SE Europe, using n-alkane biomarkers as molecular fossils: problems and possible solutions, potential and limitations. *E&G – Quaternary Science Journal* 85, 150–157.
- Zech, M., Glaser, B., 2009. Compound-specific $\delta^{18}\text{O}$ analyses of neutral sugars in soils using GC-Py-IRMS: problems, possible solutions and a first application. *Rapid Communications in Mass Spectrometry* 23, 3522–3532.
- Zech, M., Krause, T., Meszner, S., Faust, D., 2013a. Incorrect when uncorrected: reconstructing vegetation history using n-alkane biomarkers in loess-paleosol sequences – a case study from the Saxonian loess region, Germany. *Quaternary International* 296, 108–116.
- Zech, M., Kreutzer, S., Zech, R., Goslar, T., Meszner, S., McIntyre, C., Häggi, C., Eglinton, T., Faust, D., Fuchs, M., 2017. Comparative ^{14}C and OSL dating of loess-paleosol sequences to evaluate post-depositional contamination of n-alkane biomarkers. *Quaternary Research* 87, 180–189.
- Zech, M., Rass, S., Buggle, B., Löscher, M., Zöller, L., 2012a. Reconstruction of the late Quaternary paleoenvironment of the Nussloch loess paleosol sequence, Germany, using n-alkane biomarkers. *Quaternary Research* 78, 326–335.
- Zech, M., Rass, S., Buggle, B., Löscher, M., Zöller, L., 2013b. Reconstruction of the late Quaternary paleoenvironments of the Nussloch loess paleosol – response to the comments by G. Wiesenberg and M. Gocke. *Quaternary Research* 79, 306–307.
- Zech, M., Tuthorn, M., Detsch, F., Rozanski, K., Zech, R., Zöller, L., Zech, W., Glaser, B., 2013c. A 220 ka terrestrial $\delta^{18}\text{O}$ and deuterium excess biomarker record from an eolian permafrost paleosol sequence, NE-Siberia. *Chemical Geology* 360–361, 220–230.
- Zech, M., Tuthorn, M., Zech, R., Schlütz, F., Zech, W., Glaser, B., 2014. A 16-ka $\delta^{18}\text{O}$ record of lacustrine sugar biomarkers from the High Himalaya reflects Indian Summer Monsoon variability. *Journal of Paleolimnology* 51, 241–251.
- Zech, M., Zech, R., Buggle, B., Zöller, L., 2011. Novel methodological approaches in loess research – interrogating biomarkers and compound-specific stable isotopes. *E&G – Quaternary Science Journal* 60, 170–187.
- Zech, M., Zech, R., Glaser, B., 2007. A 240,000-year stable carbon and nitrogen isotope record from a loess-like palaeosol sequence in the Tumara Valley, northeast Siberia. *Chemical Geology* 242, 307–318.
- Zech, M., Zech, R., Rozanski, K., Gleixner, G., Zech, W., 2015. Do n-alkane biomarkers in soils/sediments reflect the $\delta^2\text{H}$ isotopic composition of precipitation? A case study from Mt. Kilimanjaro and implications for paleoaltimetry and paleoclimate research. *Isotopes in Environmental and Health Studies* 51, 508–524.
- Zech, R., Gao, L., Tarozo, R., Huang, Y., 2012b. Branched glycerol dialkyl glycerol tetraethers in Pleistocene loess-paleosol sequences: three case studies. *Organic Geochemistry* 53, 38–44.
- Zech, R., Zech, M., Marković, S., Hambach, U., Huang, Y., 2013d. Humid glacials, arid interglacials? Critical thoughts on pedogenesis and paleoclimate based on multi-proxy analyses of the loess-paleosol sequence Crvenka, northern Serbia. *Palaeogeography, Palaeoclimatology, Palaeoecology* 387, 165–175.
- Zeeberg, J.J., 1998. The European sand belt in eastern Europe – a comparison of Late Glacial dune orientation with GCM simulation results. *Boreas* 27, 127–139.
- Zeeden, C., Hambach, U., Händel, M., 2015. Loess magnetic fabric of the Krems-Wachtberg archaeological site. *Quaternary International* 372, 188–194.
- Zeeden, C., Hambach, U., Veres, D., Fitzsimmons, K., Obrecht, I., Böskén, J., Lehmkuhl, F., 2016a. Millennial scale climate oscillations recorded in the Lower Danube loess over the last glacial period. *Palaeogeography, Palaeoclimatology, Palaeoecology* (in press). <https://doi.org/10.1016/j.palaeo.2016.12.029>.
- Zeeden, C., Kels, H., Hambach, U., Schulte, P., Protze, J., Eckmeier, E., Marković, S.B., Klasen, N., Lehmkuhl, F., 2016b. Three climatic cycles recorded in a loess-paleosol sequence at Semlac (Romania) – implications for dust accumulation in south-eastern Europe. *Quaternary Science Reviews* 154, 130–154.
- Zhang, H., Lu, H., Xu, X., Liu, X., Yang, T., Stevens, T., Bird, A., et al., 2016. Quantitative estimation of the contribution of dust sources to Chinese loess using detrital zircon U-Pb age patterns. *Journal of Geophysical Research: Earth Surface* 121, 2085–2099.
- Zhang, N., Yamada, K., Suzuki, N., Yoshida, N., 2014. Factors controlling shell carbon isotopic composition of land snail *Acusta despecta sieboldiana* estimated from laboratory culturing experiment. *Biogeosciences* 11, 5335–5348.
- Zhang, X.Y., Arimoto, R., An, Z., 1999. Glacial and interglacial patterns for Asian dust transport. *Quaternary Science Reviews* 18, 811–819.
- Zhang, Z., Zhao, M., Eglinton, G., Lu, H., Huang, C., 2006. Leaf wax lipids as paleovegetational and paleoenvironmental proxies for the Chinese Loess Plateau over the last 170 kyr. *Quaternary Science Reviews* 20, 575–594.
- Zhao, H., Qiang, X., Sun, Y., 2014. Apparent timing and duration of the Matuyama-Brunhes geomagnetic reversal in Chinese loess. *Geochemistry, Geophysics, Geosystems* 15, 4468–4480.
- Zheng, H., Chen, H., Cao, J., 2002. Palaeoenvironmental implication of the Plio-Pleistocene loess deposits in southern Tarim Basin. *Chinese Science Bulletin* 47, 700–704.
- Zheng, H., Powell, C.M., Butcher, K., Cao, J., 2003. Late Neogene loess deposition in southern Tarim Basin: tectonic and palaeoenvironmental implications. *Tectonophysics* 375, 49–59.
- Zhou, L.P., Shackleton, N.J., 1999. Misleading positions of geomagnetic reversal boundaries in Eurasian loess and implications for correlation between continental and marine sedimentary sequences. *Earth and Planetary Science Letters* 168, 117–130.

- Zhu, R., Liu, Q., Jackson, M.J., 2004. Paleoenvironmental significance of the magnetic fabrics in Chinese loess-paleosols since the last interglacial (<130 ka). *Earth and Planetary Science Letters* 221, 55–69.
- Zöller, L., Semmel, A., 2001. 175 Years of loess research in Germany – long records and “unconformities. *Earth-Science Reviews* 54, 19–28.
- Zykin, V.S., Zykina, V.S., 2015. The Middle and Late Pleistocene loess-soil record in the Iskitim area of Novosibirsk Priobie, south-eastern West Siberia. *Quaternary International* 365, 15–25.
- Zykina, V., Zykin, V., 2012. *Loess-Soil Sequence and Environment and Climate Evolution of West Siberia in Pleistocene*. [In Russian.] Academic Publishing House “Geo,” Novosibirsk, Russia.